Report DSO-2014-05

Large-Scale Filter Performance Tests

Results of "Crack-Box" Testing

Dam Safety Technology Development Program
U.S. Army Corps of Engineers Risk Management Center

U.S. Department of the Interior
Bureau of Reclamation
Technical Service Center
Denver, Colorado

US Army Corps of Engineers®
Risk Management Center
Denver, Colorado

July 2014

The public reporting burden for this collection of information is estimated to average 1 hour per response, including the time for reviewing instructions, searching existing data sources, gathering and maintaining the data needed, and completing and reviewing the collection of information. Send comments regarding this burden estimate or any other aspect of this collection of information, including suggestions for reducing the burden, to Department of Defense, Washington Headquarters Services, Directorate for Information Operations and Reports (0704-0188), 1215 Jefferson Davis Highway, Suite 1204, Arlington, VA 22202-4302. Respondents should be aware that notwithstanding any other provision of law, no person shall be subject to any penalty for failing to comply with a collection of information if it does not display a currently valid OMB control number.
PLEASE DO NOT RETURN YOUR FORM TO THE ABOVE ADDRESS.

1. REPORT DATE *(DD-MM-YYYY)*	2. REPORT TYPE	3. DATES COVERED (From - To)
30/07/2014	Research	n/a

4. TITLE AND SUBTITLE	5a. CONTRACT NUMBER
Large-Scale Filter Performance Tests	n/a
	5b. GRANT NUMBER n/a
	5c. PROGRAM ELEMENT NUMBER n/a
6. AUTHOR(S) Ted Howard, Caleb Rudkin, Peter Irey	5d. PROJECT NUMBER n/a
	5e. TASK NUMBER n/a
	5f. WORK UNIT NUMBER n/a

7. PERFORMING ORGANIZATION NAME(S) AND ADDRESS(ES)	8. PERFORMING ORGANIZATION REPORT NUMBER
U.S. Department of Interior Bureau of Reclamation Technical Service Center	n/a

9. SPONSORING/MONITORING AGENCY NAME(S) AND ADDRESS(ES)		10. SPONSOR/MONITOR'S ACRONYM(S) DSO and USACE RMC
U.S. Department of Interior Bureau of Reclamation Dam Safety Office	Department of Defense U.S. Army Corps of Engineers Risk Management Center	11. SPONSOR/MONITOR'S REPORT NUMBER(S) DSO-2014-05

12. DISTRIBUTION/AVAILABILITY STATEMENT

No restrictions

13. SUPPLEMENTARY NOTE n/a

14. ABSTRACT

The Bureau of Reclamation, in partnership with the U.S. Army Corps of Engineers, has been conducting large-scale filter testing for several years. These tests have been performed to gain a better understanding of the performance of filters subject to cracking. In particular, they explore how well a crack can form within a filter, how well a cracked filter subject to a concentrated leak can heal, and how effectively a filter can stop or control a concentrated leak. This paper discusses the construction of the testing apparatus, filter materials tested, test procedures used, results for 14 tests that have been performed, and lessons learned pertinent to the design engineer.

15. SUBJECT TERMS

Embankment dam filters, filter cracking

16. SECURITY CLASSIFICATION OF: None			17. LIMITATION OF ABSTRACT	18. NUMBER OF PAGES	19a. NAME OF RESPONSIBLE PERSON
a. REPORT n/a	b. ABSTRACT n/a	a. THIS PAGE n/a			Peter Irey
					19b. TELEPHONE NUMBER *(Include area code)* (303) 445-3033

Report DSO-2014-05

Large-Scale Filter Performance Tests

Results of "Crack-Box" Testing

Bureau of Reclamation
U.S. Army Corps of Engineers

Prepared by:

Ted Howard
Caleb Rudkin
Peter Irey

U.S. Department of the Interior
Bureau of Reclamation
Technical Service Center
Denver, Colorado

US Army Corps of Engineers®
Risk Management Center
Denver, Colorado

July 2014

MISSION STATEMENTS

The U.S. Department of the Interior protects America's natural resources and heritage, honors our cultures and tribal communities, and supplies the energy to power our future.

The mission of the Bureau of Reclamation is to manage, develop, and protect water and related resources in an environmentally and economically sound manner in the interest of the American public.

BUREAU OF RECLAMATION
Dam Safety Technology Development Program
Geotechnical Services Division, 85-831100

DSO- 2014-05

Large-Scale Filter Performance Tests

07/30/2014
Date

Prepared by: Ted Howard
Geotechnical Engineer, Geotechnical Engineering Group 4, 85-831400

07/30/2014
Date

Prepared by: Caleb Rudkin
Geotechnical Engineer, Geotechnical Engineering Group 4, 85-831400

07/30/2014
Date

Prepared by: Peter Irey
Geotechnical Engineer, Geotechnical Engineering Group 1, 85-831100

7/30/2014
Date

Checked by: Robert Rinehart, Ph.D., P.E.
Civil Engineer, Materials Engineering and Research Laboratory, 85-81800

7/30/2014
Date

Technical approval: Dennis Hanneman, P.E.
Geotechnical Engineer, Geotechnical Engineering Group 1, 85-831100

7/30/2014
Date

Peer review: William Engemoen, P.E.
Geotechnical Engineer, Geotechnical Services Division, 85-832200

8/7/2014
Date

Approved: Chuck Redlinger, P.E.
U.S. Army Corps of Engineers, Risk Management Center

REVISIONS					
Date	Description	Prepared	Checked	Technical approval	Peer review

ACRONYMS AND ABBREVIATIONS

ASTM	American Society for Testing of Materials
ft^3	cubic feet
gpm	gallons per minute
lb/ft^3	pounds per cubic foot
lbf/ft^3	pound-force per cubic foot
mm	millimeters
Reclamation	Bureau of Reclamation
USCS	United Soil Classification System

ACKNOWLEDGMENTS

The authors are grateful for the funding provided by the U.S. Army Corps of Engineers Risk Management Center and by the Bureau of Reclamation Dam Safety Technology Development Program. The authors also wish to express their gratitude for the valuable contributions made by Kristi Evans, Jonathan East, Patrick Maier, Bethany Jackson, and Brandon Poos, and for the thoughtful feedback and guidance provided by the reviewers.

CONTENTS

Page

Introduction 1
Testing Apparatus 2
Materials Tested 4
Typical Test Procedure 5
Testing Program 7
Data Collected 10
  Quantitative Data 10
  Qualitative 12
Results 13
  Phase I Testing: Single-stage Sand Filter 13
    Test 1 13
    Test 2 15
    Test 3 16
    Test 4 17
    Test 5 18
    Test 6 19
  Phase II Testing: Broadly Graded Filter 20
    Test 7 20
    Test 8 21
    Test 9 24
  Phase III Testing: Two-Stage Filter 25
    Test 10 25
    Test 11 26
  Phase IV Testing: 5-Foot Filter 27
    Test 12 27
  Phase V Testing: Nonplastic Silt with Single-Stage Filter 29
    Test 13 29
  Phase VI Testing: Slow Filling Reservoir Single-Stage Filter 30
    Test 14 30
Conclusions 33
  Phase I 33
  Phase II 33
  Phase III 34
  Phase IV 34
  Phase V 34
  Phase VI 34
  Overall 35
Bibliography 36

Appendices

Appendix

A Sand Physical Property Results

B Sand Castle Test Results

C Silt Physical Property Results

D Geophysics Paper

E Maximum Density Tests

Figures

Figure Page

1 (a) Material box looking downstream, (b) channel between material box and reservoir, (c) reservoir looking upstream, and (d) profile view of the testing apparatus with the reservoir on the right and the material box on the left, connect by the channel 2
2 Testing apparatus after the material box had been cracked open 3
3 Sand gradation 5
4 (a) Electric vibratory plate compactor, (b) pneumatic pogo tamper 6
5 Phase II broadly graded filter material gradations 8
6 Phase III two-stage filter gradations 9
7 Phase V silt and sand gradations 9
8 Overhead view of Test 1: 3 feet of sand compacted to 94.8% of maximum dry density at 5.8% moisture content 14
9 Overhead view of Test 2: 3 feet of sand compacted to 81.3% 15
10 Overhead view of Test 3: 3 feet of sand compacted to 95.7% 17
11 Overhead view of Test 4: 3 feet of sand compacted to 87.6% 18
12 Overhead view of Test 5: 3 feet of sand compacted to 90.6% 19
13 Overhead view of Test 6: 3 feet of sand compacted to 92.9% 20
14 Overhead view of Test 7: 3 feet of broadly graded material compacted to 94.9% 21
15 Overhead view of Test 8: 3 feet of broadly graded material compacted to 103.4% 22
16 Picture taken during excavation of test 8 material 23
17 Overhead view of Test 9: 3 feet of broadly graded material compacted to 92.5% 24
18 Overhead view of Test 10: 3 feet of sand compacted to 91.8% and 2 feet of compacted gravel 26

Figures (continued)

Figure Page

19 Overhead view of Test 11: 3 feet of sand compacted to 89.3% and 2 feet of compacted gravel. 27
20 Overhead view of Test 12: 5 feet of sand compacted to 92.9% 28
21 Overhead view of Test 13: 2 feet of silt compacted to 94.9% and 3 feet of sand compacted to 91.8% 30
22 Overhead view of Test 14: 3 feet of sand compacted to 91.3% 31
23 Test 14 reservoir timeline 32

Tables

Table Page

1 Filter scenarios for each phase 11
2 Material properties 11
3 Test 12 crack width timeline 28
4 Test 14 reservoir timeline 32

INTRODUCTION

Cracking of embankment dams is a significant dam safety concern because it can lead to internal erosion, which can ultimately result in dam failure. Cracking can be caused by several factors including differential settlement, desiccation, and earthquakes. In the current state-of-practice, granular filters are the best line of defense against failure modes associated with embankment cracking. Although cracking has been observed in numerous dams, there is significant uncertainty about filter performance when cracking has occurred. This research was intended to answer questions about filter performance, specifically:

- Can various granular filters sustain cracks?
- Can granular filters meeting American Society for Testing of Materials (ASTM) C 33 fine aggregate requirements, as well as more broadly graded filters, sustain cracks?
- What type of filter performs better when cracked (single-stage, two-stage, or broadly-graded)?
- How do material properties impact filter performance when filters are cracked (i.e., gradation and density)?

Some previous research has been conducted to investigate filter performance. Park et al. (2004) [1] investigated the crack-stopping ability of filters using a laboratory filter device. The device was relatively small in scale and allowed for controlled conditions. McCook proposed a variety of tests (sand castle tests, compression tests, sand equivalency test) to determine if filter materials have undesirable properties, such as the ability to hold a crack. Vaughan and Soares (1982) [2] evaluated the self-healing property of filter sands by submerging compacted samples in water. They postulated that a sample's ability to collapse when wetted is similar to its ability to self-heal.

The research project reported herein was a joint venture between the U.S. Army Corps of Engineers and the Bureau of Reclamation (Reclamation). Testing was proposed in 2007 and occurred between 2009 and 2013. The intention of this study was to simulate the conditions in the upper portions of embankment dams to help designers assess failure modes involving cracking and improve design practices. This was done by relating factors such as gradation, density, and moisture content to filter performance when filters were cracked and subjected to concentrated flow. Tests were performed at the Materials Engineering and Research Laboratory at Reclamation's Technical Service Center in Denver, Colorado.

TESTING APPARATUS

A filter apparatus was developed that would model a granular filter within an embankment that was subjected to a concentrated leak. This required simulating geometric conditions, seepage conditions (stemming from an upstream reservoir), and cracking conditions. The constructed full-scale model is significantly larger than models used in previous research. This allows for a variety of filter configurations and materials to be used in the box. Also, the box is large enough to allow filter material to be placed and compacted using hand-held vibratory methods similar to those that are used in the field for special compaction.

The testing apparatus had two main components: (1) the reservoir, and (2) the material box, as shown in figure 1. The reservoir had dimensions of approximately 4 feet by 4 feet by 4.5 feet (length, width, and height, respectively), providing approximately 72 cubic feet (ft^3) of storage. Downstream of the reservoir, a 9-foot-long channel connected the material box to the reservoir. The material box was 8 feet by 8 feet by 4 feet (length, width, and height, respectively). Within the material box was a temporary partition wall, which could be adjusted or removed to allow for different filter thicknesses.

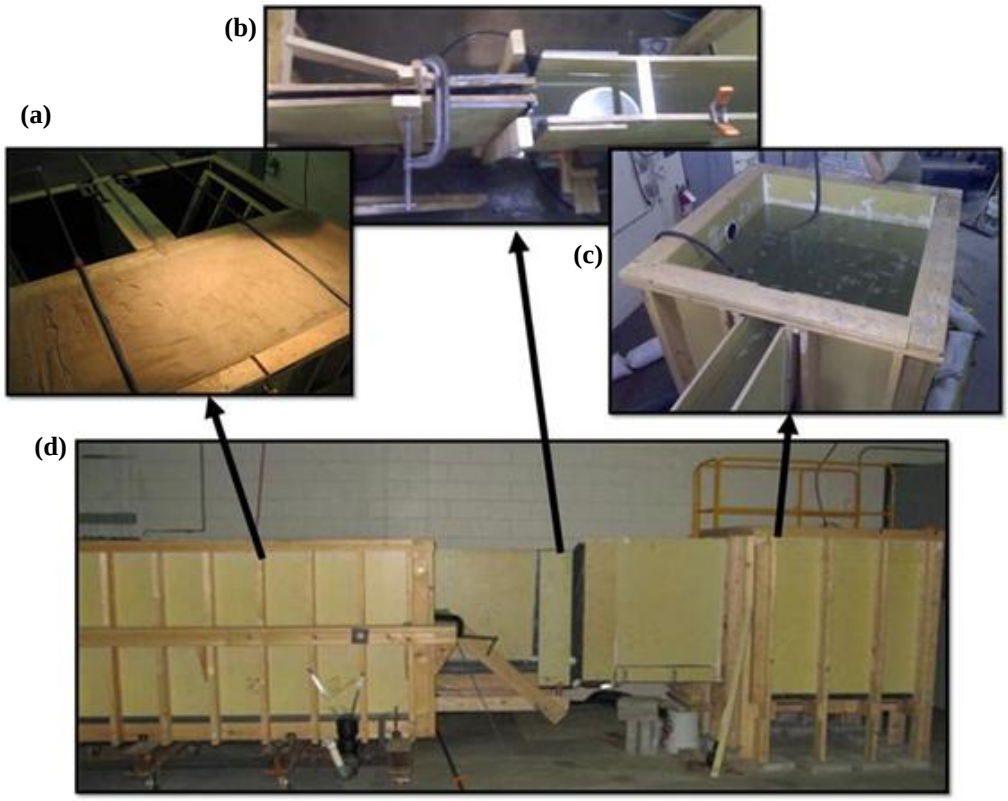

Figure 1.—(a) Material box looking downstream, (b) channel between material box and reservoir, (c) reservoir looking upstream, and (d) profile view of the testing apparatus with the reservoir on the right and the material box on the left, connect by the channel.

The material box consisted of two equally sized halves hinged together along the bottom of the box. This hinge allowed the material box to pivot about the bottom center, inducing a crack in the material within the box. The pivoting was initiated by lifting the center of the box (directly below the hinge) with hydraulic rams, as shown in figure 2. When the rams were raised, the weight of the material box and filter material kept the outer ends of the box stationary, causing the box to crack open down the center. The upstream and downstream channels were also hinged and would pivot open with the material box, allowing water from the reservoir to flow through the open cracks.

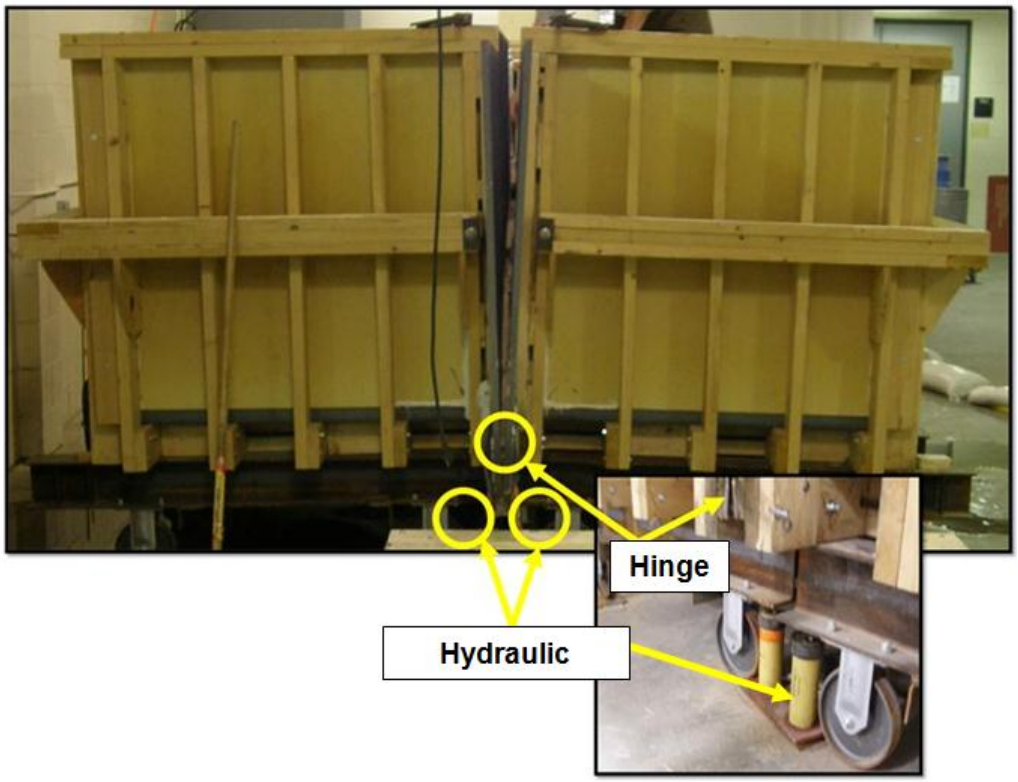

Figure 2.—Testing apparatus after the material box had been cracked open.

Crack formation within the compacted material depended on the material type, moisture content, and density. For some tests, open cracks were not sustained (likely due to self-healing of cohesionless sand) when the box was opened.

Coarse sandpaper was installed along the walls to provide friction between the filter material and box walls. This simulated the shear resistance provided by adjacent confining materials in an embankment dam. The sandpaper effectively prevented filter material from moving along the sides of the box and prevented the sides of the box from becoming a preferential flow path.

Drains were installed on the bottom of each side of the material box to allow drainage below the filter material. Allowing the filter material to drain simulated a larger chimney drain system that would be able to pass water vertically without becoming fully saturated. The drains could also be closed to prevent drainage, simulating a fully saturated filter. However, the box was not watertight, and a significant amount of water drained from the hinges and from other areas underneath the box, so simulating a fully saturated filter was never fully tested.

MATERIALS TESTED

Three granular filter/drain materials and one embankment (core) material were used over the course of the test program:

- ASTM C33 fine aggregate (sand)
- ASTM C33 coarse aggregate - size number 57 (57 stone)
- ASTM C33 coarse aggregate - size number 89 (89 stone)
- Nonplastic eolian silt, ML (silt)

Sand was used in a majority of the 14 tests. An initial gradation analysis found the sand contained 0.9 percent fines and was classified as a poorly graded sand (SP) in accordance with the Unified Soil Classification System (USCS) (see figure 3. Sand was acquired from Albert Frei and Son's pit number four, which is located in Brighton, Colorado. Pit number four is an alluvial deposit that requires washing to remove fines; the sand material is not crushed to meet gradation requirements. The material satisfied ASTM C33 requirements for gradation, material soundness, and limiting deleterious substance content. Appendix A includes results from physical property tests performed by an independent lab on samples taken from pit number four in January 2012. The results include a detailed petrography analysis. Reclamation conducted sand castle tests [3] on samples taken before and after compaction to ensure that the sand did not exhibit signs of cementation. Results determined that cementation was unlikely with this material, and they are shown in appendix B. Maximum dry unit weight tests were also conducted on the material using the vibrating hammer test, according to ASTM D7382 (see appendix E). The average maximum dry unit weight for the sand was 118.5 pounds per cubic foot (lb/ft^3).

Gravel materials, both the ASTM 57 stone and ASTM 89 stone, were purchased from Albert Frei and Son's pit number 6, located in Idaho Springs, Colorado. The gravels were manufactured (crushed, graded, washed) at the quarry to meet the ASTM C33 coarse gravel gradation requirements and satisfy ASTM C33 deleterious content and soundness requirements. Gradations for these gravel materials are presented later in this report when the different blends of materials are discussed.

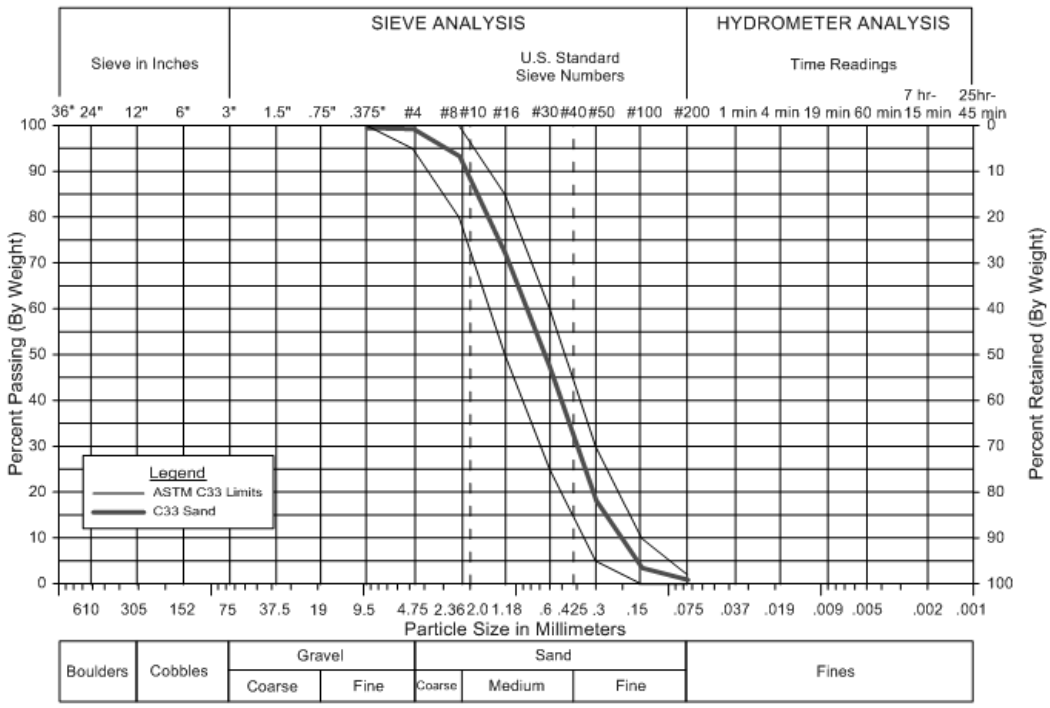

Figure 3.—Sand gradation.

Silt was acquired from near Bonny Dam in eastern Colorado. The material was taken from a borrow pit located near the dam's right abutment. Physical property testing was completed for the material and is included in appendix C. The material is nonplastic and classified as silt (ML) per USCS. The maximum dry density was determined to be 108.4 lb/ft^3 when compacted at 15.0% moisture content, as determined using USBR 5500 (which is similar to ASTM D698).

TYPICAL TEST PROCEDURE

Filter materials and configurations varied from test to test, but a general procedure was followed for all tests. The halves of the material box were hinged together, and potential areas of leakage were sealed. Material was then compacted in the material box using various types of equipment. Sand materials in tests 1-3 were compacted using a jumping jack. Granular (sand and gravel) materials for tests 4-13 were compacted using an electric vibrating plate compactor, as shown in figure 4. The silt in test 13 was compacted using the pneumatic tamper, which is also shown in figure 4.

Material was compacted in the material box at various moisture contents and lift heights to vary the percent compaction for each test. Trial tests were completed in a smaller box to determine which methods would produce the target percent

compaction. Different material densities were achieved when the lift height, moisture content, and compactive effort were varied.

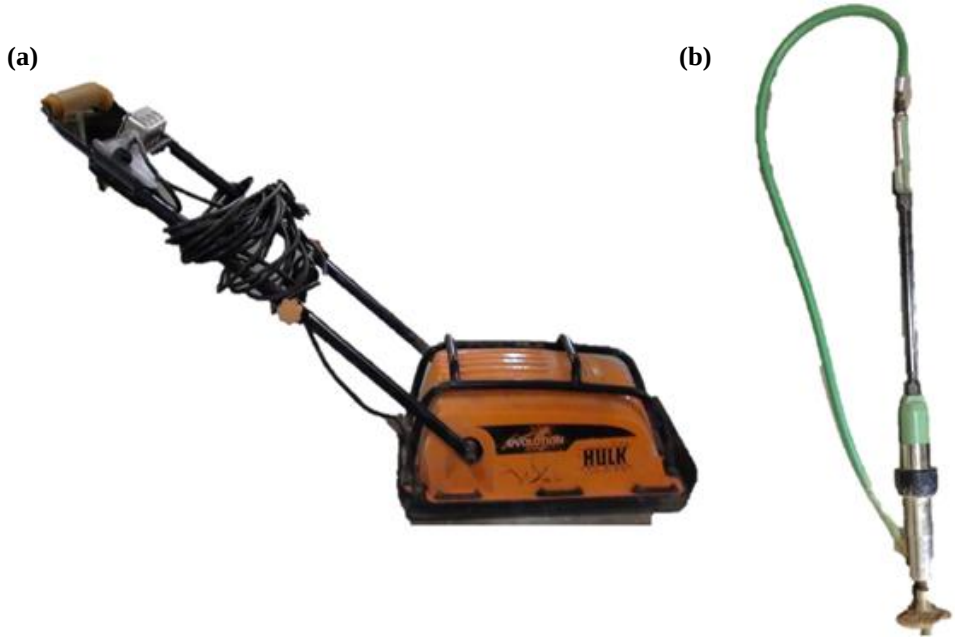

Figure 4.—(a) Electric vibratory plate compactor, (b) pneumatic pogo tamper.

Compaction methods were slightly altered when multiple materials were placed in the box. First, a 2-inch by 12-inch (8-foot-long) board was placed within the material box to separate the gravels (drain) from the sand (filter). The sand was dumped on the upstream side of the board. The gravel mix was then dumped downstream of the board. After placing and spreading the materials, the board was removed. The sand was compacted first, followed by the gravel. The board was then put back in place, and materials were once again added. This process continued until the materials reached a height of approximately 48 inches. The same process was used for placing silt embankment material upstream of the filter.

After filling the material box, the hydraulic rams lifted the box directly below the hinge, causing the box to open and potentially crack the compacted filter and embankment materials (if present). The crack width was based on the relative distance between the two halves of the material box, measured at the top of the box where the upstream channel aligned with the material box. It was assumed that the box was closed above the hinge. Typically, the crack was opened to a width of 1 inch before releasing the reservoir.

A bulkhead was used to contain water in the reservoir. Once the bulkhead was removed, the reservoir was released, and water was allowed to flow through or

into the material box. The reservoir level typically dropped several inches at this time.

The focal point of each test was observing the filter's performance immediately after the release of the reservoir. If filter material was able to slough (i.e., heal) enough to stop the concentrated leak, the reservoir level would rise back up to its original level as hoses continued to supply water (excess water flowed through an overflow valve within the reservoir). If the filter material did not slough enough to stop the concentrated leak, the hoses were generally unable to keep up with the outflow from the reservoir, and the reservoir level dropped.

TESTING PROGRAM

The temporary partition placed within the material box could be moved to accommodate different filter configurations. Filter material was placed in the material box in six different configurations, represented by each of the following phases:

- Phase I: single-stage sand filter (3 feet wide)
- Phase II: broadly graded filter (3 feet wide)
- Phase III: two-stage filter (3 feet of sand and 2 feet of gravel)
- Phase IV: single-stage sand filter (5 feet wide)
- Phase V: Nonplastic silt with single-stage sand filter (2 feet of silt and 3 feet of sand)
- Phase VI: Slow filling reservoir single-stage sand filter (3 feet wide)

Phase I testing (tests 1-6) examined the performance of single-stage sand filter material. For each test, the partition wall was located so that the sand filter would be 3 feet wide (upstream to downstream distance). The sand used in test 1 was reused in tests 2-6. After test 6, the sand was discarded, and additional sand was purchased. From this point on, sand was not reused.

Phase II testing (tests 7-9) examined the performance of broadly graded filter material. Broadly graded soils have an inherent risk of being unstable and can be subject to segregation of particles [4]. The broadly graded material was a mixture of sand, 89 stone, and 57 stone; these materials were described previously in the "Materials Tested" section. The respective proportions (by weight) were 35%, 40%, and 25%. A gradation for the broadly graded materials is shown in figure 5. These proportions were selected to maximize stability and minimize segregation, according to Sherard's internal stability criteria [4]. The materials were

thoroughly mixed in a 4-ft^3 concrete mixer and were carefully placed in the material box to reduce segregation. For each test, the partition wall was located so that the broadly graded filter would be 3 feet wide.

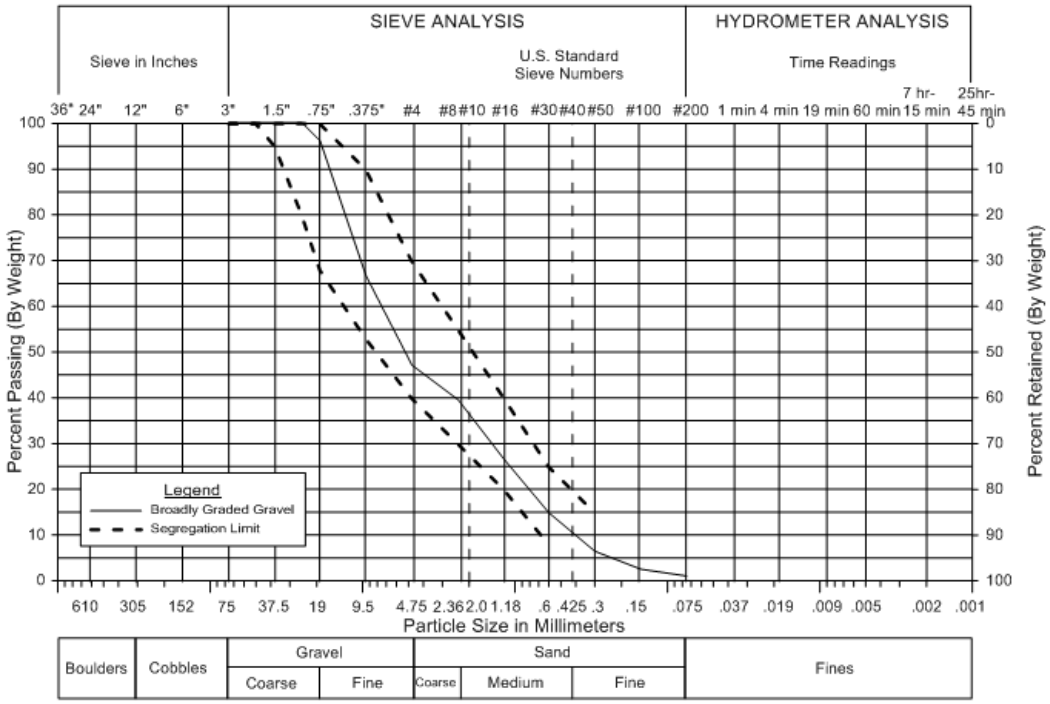

Figure 5.—Phase II broadly graded filter material gradations.

Phase III testing (tests 10 and 11) examined the performance of two-stage filters. For this test, a 3-foot-wide sand filter was placed upstream of a 2-foot-wide gravel filter. The sand had the same C33 fine aggregate gradation as previously discussed, and the gravel was an even mix (by weight) of 57 and 89 stone. Gradations of the sand and gravel material are shown in figure 6. Note that the gravel filter meets retention and permeability criteria for the sand filter [5].

Phase IV testing (test 12) examined the performance of a single-stage sand filter material, as was done in Phase I testing, except that the material box was modified to allow a filter width of 5 feet.

Phase V testing (test 13) examined the performance of a single-stage sand filter with an upstream embankment zone of nonplastic silt. For this test, a 2-foot-wide embankment zone was placed upstream of a 3-foot-wide sand filter. Note that the sand filter satisfies retention and permeability criteria for the embankment material [5]. Gradations of the silt and sand material are shown in figure 7.

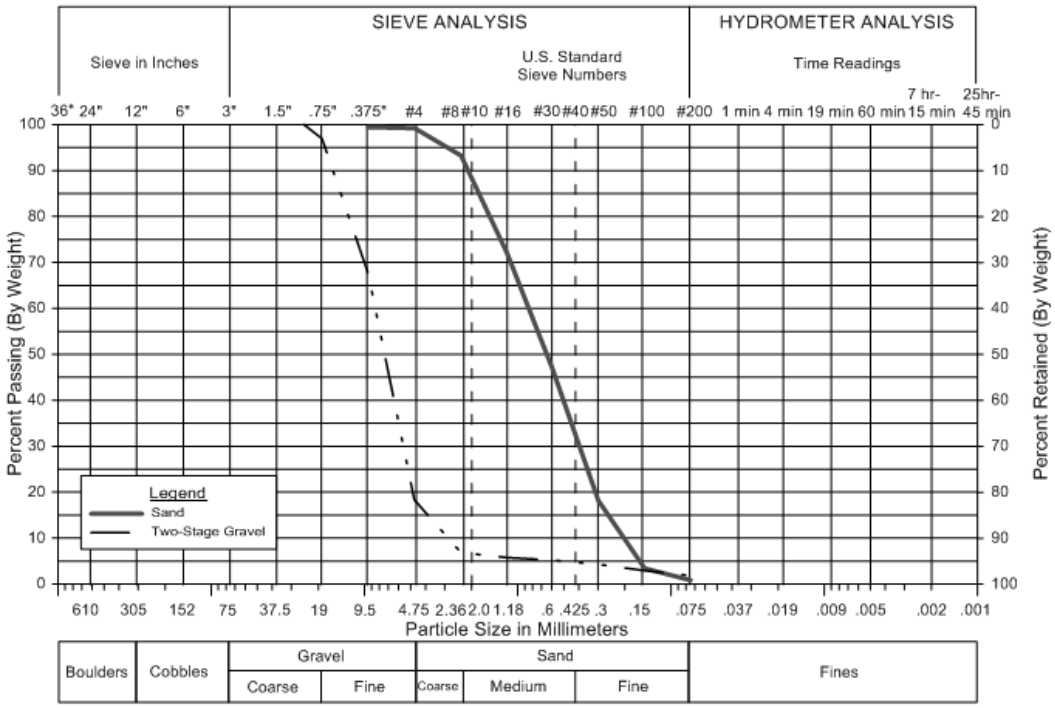

Figure 6.—Phase III two-stage filter gradations.

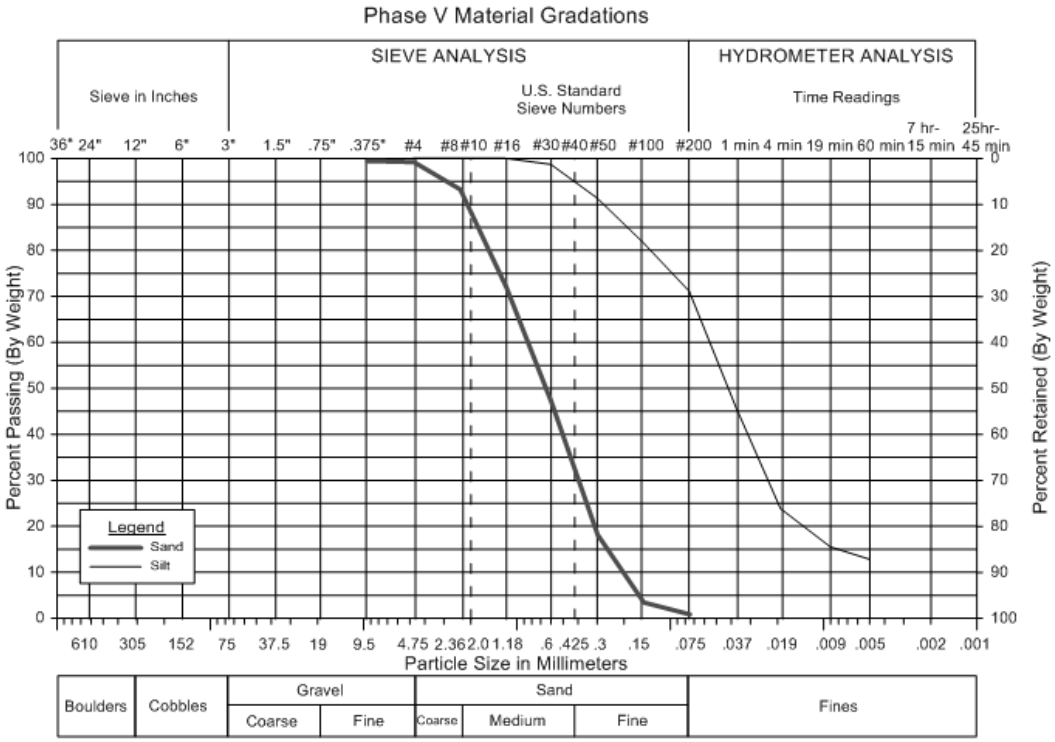

Figure 7.—Phase V silt and sand gradations.

Phase VI testing (test 14) examined the performance of a single-stage sand filter exposed to a slowly rising reservoir. For this test the sand filter was three feet wide. This phase was performed to observe the performance of a saturated sand filter and a slowly rising reservoir.

DATA COLLECTED

The test observations were divided into two categories: (1) quantitative, and (2) qualitative. This was done because there are events within the tests (such as sloughing, reservoir releases, how much the filter healed, or stopping a concentrated leak) that cannot be quantitatively measured. Pertinent soil properties were measured and recorded quantitatively whenever possible.

Quantitative Data

Several factors that influenced the filters' ability to sustain a crack and heal were observed. These factors were filter gradation, density, and moisture content (degree of saturation). These factors were measured to determine the extent of their influence on filter performance.

Gradation analyses were performed during each phase of testing, as previously explained. Compatibility between materials was analyzed using Reclamation design criteria [5]. For filter compatibility between adjacent zones, the $D_{85}B$ ($D_{85}B$ = particle size expressed in millimeters (mm), where 85 percent of the gradation is finer) and $D_{15}F$ ($D_{15}F$ = particle size expressed in mm, where 15 percent of the gradation is finer) are compared to determine if retention criteria is satisfied.

To determine if downstream material would be transported into the downstream channel, Reclamation's criteria for sizing pipe perforations [5] was used. To determine whether material would erode into the downstream channel, the $D_{50}B$ ($D_{50}B$ = particle size expressed in mm, where 50 percent of the gradation is finer) of the material in contact with the downstream channel was compared to the open channel width (typically 25.4 mm wide at the top and assumed to be 0.0 mm at the bottom). Table 1 shows that there are multiple scenarios for particle filtration.

For example, in Phase I, only sand particles at the bottom of the crack would not be transported downstream. In other cases, such as Phases II and III, the crack would keep the majority of the large gravel particles from transporting downstream. This is especially important for broadly graded material as discussed in Phase II testing.

Table 1. Filter scenarios for each phase

Phase	Upstream material	Downstream material or crack width
I	Sand: $D_{50}B$ = 0.65 mm	Crack width: 12.7 mm
II	Broadly graded filter: $D_{50}B$ = 5.0 mm	Crack width: 12.7 mm
III	Sand: $D_{15}B$ = 0.28 mm	Gravel: $D_{15}F$ = 4.0 mm
	Gravel: $D_{50}B$ = 7.2 mm	Crack width; 12.7 mm
IV	Sand: $D_{50}B$ = 0.65 mm	Crack width; 12.7 mm
V	Silt: $D_{15}B$ = 0.009	Sand: $D_{15}F$ = 0.28 mm
	Sand: $D_{50}B$ = 0.65 mm	Crack width: 12.7 mm
VI	Sand:$D_{50}B$ = 0.65 mm	Crack width: 12.7 mm

In-place unit weights of filter materials (except clean gravel mixes) were determined using sand cone tests (ASTM D1556). The maximum dry unit weight for the filter materials was determined using ASTM D7382. Percent compaction was calculated by comparing the in-place dry unit weight to the maximum dry unit weight. Moisture content of the filter material was determined during sand cone tests using the oven-dry method (USBR-5300).

Unit weight tests were not performed on gravel due to the inaccuracy of the sand cone test for these soils. Larger tests (i.e., water displacement test) could not be performed due to the lack of available area. Material properties for each test are listed in table 2.

Table 2. Material properties

Phase	Test	Box configuration	Average γ_{dry}[1] (lbf/ft^3)	Average compaction[2] (%)	Average moisture content (%)
I	1	3 feet of sand	111.6	94.8	5.8
	2	3 feet of sand	95.7	81.3	4.0
	3	3 feet of sand	112.6	95.7	4.4
	4	3 feet of sand	103.5	87.6	2.4
	5	3 feet of sand	107.1	90.6	3.1
	6	3 feet of sand	109.7	92.9	1.9
II	7	3 feet broadly graded	131.1	94.9	1.5
	8	3 feet broadly graded	142.9	103.4	5.8
	9	3 feet broadly graded	127.9	92.5	6.0
III	10	3 feet of sand	108.4	91.8	5.3
		2 feet of gravel	Not tested		
	11	3 feet of sand	107.8	89.3	5.7
		2 feet of gravel	Not tested		
IV	12	5 feet of sand	111.1	92.9	4.4

Table 2. Material properties

Phase	Test	Box configuration	Average γ_{dry}[1] (lbf/ft^3)	Average compaction[2] (%)	Average moisture content (%)
V	13	2 feet of silt	102.9	94.9	14.4
		3 feet of sand	109.8	91.8	3.0
VI	14	3 feet of sand, slow filling reservoir	109.2	91.3	4.9

[1] Dry unit weight and moisture content were calculated from sand cone samples.
[2] Percent compaction was calculated using the average dry unit weight and maximum dry unit weight (ASTM D 7382).
Note: lbf/ft^3 = pound-force per cubic foot.

As previously mentioned, sand castle tests were performed to determine if the filter materials exhibited cementing (see appendix B). Results from the sand castle tests showed that the material did not exhibit cementing behavior.

Flow rate from the downstream channel was recorded during Phase II testing only. The measurements were taken using a stop watch and graduated cylinder. The flow rate was measured to determine if fine-grained material placed in the upstream channel would reduce flow through the broadly graded filter. Flow measurements were not taken for other tests because material was not added into the upstream flows for any other tests.

Qualitative

Filter performance was judged qualitatively based on two observations made during each test:

1. Whether or not the filter material sustained a crack after the material box was cracked and before the reservoir was released.

2. Whether or not the filter healed under flow conditions (i.e., whether material sloughed into the crack sufficiently to stop the concentrated leak).

The first and second observations are affected by the strength of the material. Stronger materials (higher density or lower moisture content) tended to have larger, straighter cracks and slough in relatively larger volumes. Weaker materials (lower density or higher moisture content) tended to have numerous cracks, branching cracks, smaller cracks, and a tendency to slough in smaller pieces.

The second observation included two parts: (1) whether or not the filter sloughed, and (2) if the filter sloughed enough to stop the concentrated leak. The second

portion was difficult to determine due to fluctuations in the reservoir level. After the filter healed and the concentrated leak was stopped, the reservoir would begin rising and would overtop the healed material, allowing the water to flow uninhibited until the filter healed again. This cycle was due to the small size of the reservoir, the insufficient flow into the reservoir, and the lack of overlying material that would provide additional material to slough into the crack. If the reservoir had been larger, the reservoir elevation would fluctuate less, and this cycle would not happen. Also, if filter material had been placed a few feet above the maximum water surface, this cycle would not happen because material would likely be available to heal the crack and prevent filter overtopping.

This cycle can be seen clearly in Phase VI (test 14). In test 14, the filter stops any concentrated leaks until the reservoir is raised to within a few inches of the original height of the uncracked filter, and there is insufficient material above the water surface available to slough into and fill the crack.

Multiple video cameras were used to record filter performance. Cameras recorded the entire testing process, including the initial cracking of the box (pivoting of the hinge), releasing of the reservoir, and flow or seepage through the filter.

RESULTS

The qualitative results, as well as a description of the video, are presented for each test. Additionally, an overhead image is presented for each test to capture what the crack looked like prior to introducing flow from the reservoir. These images are oriented so that the upstream side (reservoir) is to the left of the material box. An explanation of the behavior from each test is also included in the summary section.

Phase I Testing: Single-Stage Sand Filter

Test 1

Average moisture content[1]	Average dry unit weight[1]	Average compaction (%)[1]
5.8%	111.6 lbf/ft^3	94.8%

[1] Results of sand cone tests performed on the filter before running the test.

Test Description

Sand was placed up to a height of 42 inches above the bottom of the box. The sand filter was 3 feet wide measured upstream to downstream. All of the figures show an overhead view of the material box and are oriented with the upstream side on the left side. Test 1 took place on September 29, 2009. The box was cracked approximately 0.5 inch (see figure 8). The crack walls appeared to be mostly vertical, and the path of the crack meandered about 1 inch in either direction, but was generally oriented upstream to downstream.

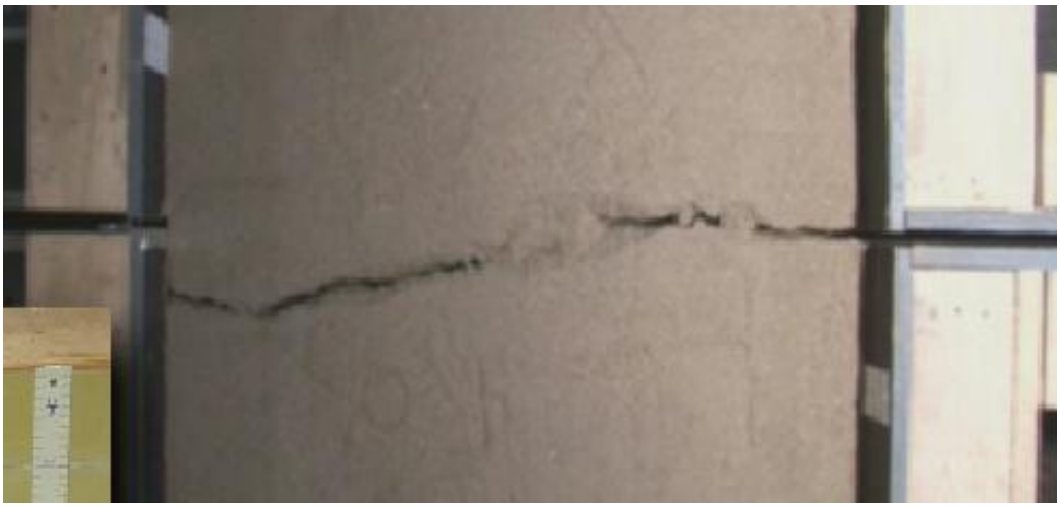

Figure 8.—Overhead view of Test 1: 3 feet of sand compacted to 94.8% of maximum dry density at 5.8% moisture content.

The reservoir was filled to a height of 41 inches and then released. The filter sloughed quickly after the reservoir was released. The concentrated leak was stopped, and water was unable to flow into the downstream channel. Small intermittent sloughing occurred, but the leak was stopped until the box was cracked wider, to approximately 1.5 inches. At this point, the crack sustained almost vertical walls, and water continued to flow into the downstream channel. The velocity of the flow was high enough to suspend sand particles and transport them downstream, outside of the box. This led to more water moving through the crack and eroding filter material. Additional larger sloughs occurred, but the leak was never fully stopped and continued to flow.

Summary

The filter material sustained a crack and initially healed enough to stop flow. Water flowed into the crack towards the downstream opening. The water did not suspend any particles, due to low velocities, and the opening at the downstream end of the crack was approximately 0.5 inch. Once the crack was opened to 1.5 inches, the water carried sand particles further downstream, increased water velocity, eroded the filter, and the concentrated leak continued to grow.

Test 2

Average moisture content[1]	Average dry unit weight[1]	Average compaction (%)[1]
4.0%	95.7 lbf/ft3	81.3%

[1] Results of sand cone tests performed on the filter before running the test.

Test Description

Sand was placed up to a height of 42 inches and was 3 feet wide. The filter material was not compacted during placement. Test 2 took place on November 24, 2009, and November 25, 2009. The box was cracked approximately1inch, but the filter did not sustain a large crack. Instead, the material settled, and small tension cracks appeared (see figure 9).

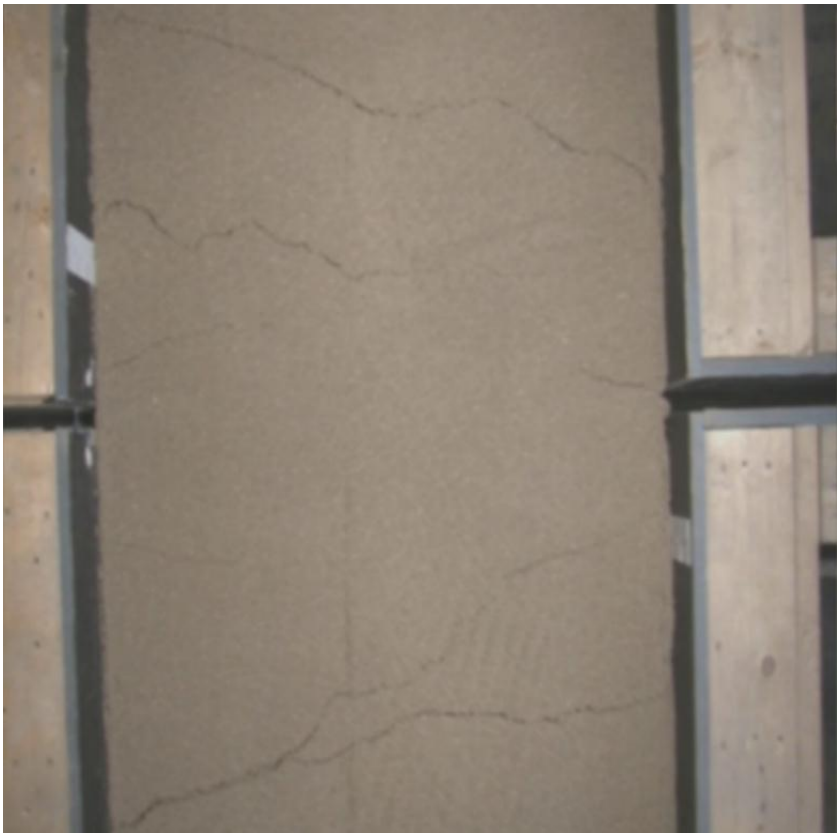

Figure 9.—Overhead view of Test 2: 3 feet of sand compacted to 81.3%.

The reservoir was filled to a height of 42 inches before being released. After releasing the reservoir, any concentrated leaks were stopped. The test was left in this state overnight, so that seepage could be observed. Side drains were closed

on November 25, 2009. Shortly after the drains were closed, water began to flow through the downstream channel. Filter material became saturated as the phreatic surface within the box rose. Saturation of the uncompacted filter sand caused additional settlement, and the reservoir slowly began to overtop the filter. Upon overtopping, the velocity of the flow was high enough to suspend sand particles and transport filter material into the downstream channel.

Summary

The filter material did not sustain a crack. The filter settled as it was saturated, and small tension cracks formed, running upstream to downstream. Eventually, enough settlement occurred, resulting in the filter being overtopped. Once overtopped, the uncompacted material was quickly transported downstream. Despite the flows eventually overtopping the filter, the filter material performed adequately at the lower density. The filter was overtopped due to settlement upon wetting and because the reservoir was set at the initial height of the filter. If the filter had been placed up to a height of 48 inches, and the reservoir filled to 42 inches, the filter would not have overtopped.

Test 3

Average moisture content[1]	Average dry unit weight[1]	Average compaction (%)[1]
4.5%	112.6 lbf/ft^3	95.7%

[1] Results of sand cone tests performed on the filter before running the test.

Test Description

Sand was placed up to a height of 48 inches and was 3 feet wide. Test 3 took place on April 13, 2010. The box was cracked approximately 0.875 inch (see figure 10). The crack walls appeared to be mostly vertical, and the crack meandered approximately 1 inch in either direction. Approximately 18 inches downstream of the box opening, the crack branched into two separate cracks, which then converged at the downstream opening, as shown in figure 10.

The reservoir was filled to an elevation of 44 inches and then released. The filter did not stop the concentrated leak. Sloughing started almost immediately, but the volume of the sloughed material was unable to permanently stop the leak. As the test progressed and the filter was significantly eroded, approximately 0.5 ft^3 of gravel was dumped at the downstream end of the filter. The addition of gravel slowed the flow of the water and prevented the transportation of sand downstream

Summary

Water was able to flow through the crack and transport material downstream unimpeded. The addition of gravel at the downstream end of the filter, once the

filter was significantly eroded, prevented sand particles from being transported downstream by retaining the sand particles and slowing the flow velocity.

Figure 10.—Overhead view of Test 3: 3 feet of sand compacted to 95.7%.

.

Test 4

Average moisture content[1]	Average dry unit weight[1]	Average compaction (%)[1]
2.4%	103.5 lbf/ft^3	87.6%

[1] Results of sand cone tests performed on the filter before running the test.

Test Description

Sand was placed up to a height of 47 inches and was 3 feet wide. Test 4 took place on December 16, 2010. The box was cracked approximately 1 inch, as shown in figure 11. The crack walls were not vertical, and the crack branched approximately 2 inches downstream. The branch caused two wedges to form for almost the entire length of the filter.

The reservoir was filled to a height of 42 inches and then released. The filter sloughed quickly after the reservoir was released and stopped the concentrated leak.

On January 12, 2011, efforts were made to initiate erosion through the sand; this was done using a wooden dowel to create a void at the entrance into the downstream channel. However, the material was able to quickly heal and fill the void, effectively stopping the concentrated leak.

Figure 11.—Overhead view of Test 4: 3 feet of sand compacted to 87.6%.

Summary

The filter material sustained multiple cracks but stopped any concentrated leaks. The multiple cracks provided multiple paths for the water to flow into, which produced a greater distribution of the wetting front, which then led to more sloughing.

Test 5

Average moisture content[1]	Average dry unit weight[1]	Average compaction (%)[1]
3.5%	107.2 lbf/ft^3	90.6%

[1] Results of sand cone tests performed on the filter before running the test

Test Description

Sand was placed up to a height of 48 inches, and the filter was 3 feet wide. Test 5 took place on February 15, 2011. The box was cracked approximately 1 inch (see figure 12). The crack walls appeared to be mostly vertical, and the crack meandered less than 1 inch in either direction. The crack also ran almost straight from upstream to downstream.

The reservoir was filled to a height of 43 inches, and the reservoir was released. Normal operations involve the bulkhead being removed entirely; in this test, the bulkhead was accidently left partially in place. Shortly after releasing, the bulkhead closed off flow from the reservoir. The bulkhead was then completely removed, fully releasing the reservoir. The filter sloughed significantly and stopped the concentrated leak. The reservoir was raised 2 inches the next day, to

a height of 45 inches, and the filter material was overtopped by the waterflow. Water velocities were sufficient to transport sand particles downstream.

Figure 12.—Overhead view of Test 5: 3 feet of sand compacted to 90.6%.

Summary

The filter sustained a crack, but the ability of the filter to stop the concentrated leak was masked by the fluctuations of the reservoir. If the reservoir level had been maintained, more sand may have been transported downstream, and the filter would have been unable to stop the leak. However, this is speculation. The filter stopped the leaks until the reservoir was raised to a height of 45 inches. Then, sloughed filter material in the crack was overtopped and eroded downstream.

Test 6

Average moisture content[1]	Average dry unit weight[1]	Average compaction (%)[1]
1.9%	109.2 lbf/ft^3	92.9%

[1] Results of sand cone tests performed on the filter before running the test.

Test Description

Sand was placed up to a height of 47 inches and was 3 feet wide. Test 6 took place on March 31, 2011. The box was cracked approximately 1 inch (see figure 13). The crack walls were mostly vertical, and the crack meandered less than 1 inch in either direction until about 24 inches downstream, where the crack branched into two separate cracks, creating small wedges of filter material.

The reservoir was filled to a height of 45 inches, and the bulkhead was slowly released. Filter material sloughed into the crack, and the filter initially stopped

the leaks. As the reservoir level rose, the sloughed filter material within the crack was not high enough to stop the leak. Once water was able to overtop the sloughed filter material in the crack, water velocities quickly increased and were able to transport particles downstream.

Figure 13.—Overhead view of Test 6: 3 feet of sand compacted to 92.9%.

Summary

The filter sustained a crack and was able to initially stop the leak. The relatively small amount of sloughed material was quickly transported downstream and out of the box once the filter was overtopped. As larger sloughs occurred, the flows through the crack were already large enough to transport the sloughed material downstream.

Phase II Testing: Broadly Graded Filter

Test 7

Average moisture content[1]	Average dry unit weight[1]	Average compaction (%)[1]
1.5%	131.1 lbf/ft^3	94.9%

[1] Results of sand cone tests performed on the filter before running the test.

Test Description

Broadly graded material was placed up to a height of 48 inches, and the filter was 3 feet wide. Test 7 took place on July 7, 2011. The box was cracked approximately 1 inch (see figure 14). The crack walls were mostly vertical, with

some sloughed particles in areas. Orientation of the crack was almost straight from upstream to downstream and meandered less than 1 inch in either direction.

Figure 14.—Overhead view of Test 7: 3 feet of broadly graded material compacted to 94.9%.

The reservoir was filled to a height of 46.5 inches and then released. The broadly graded material sloughed less than the sand filter. The leak was partially stopped by the filter; and as time progressed, more gravel material was caught at the downstream end of the filter, and the velocities slowed further. The following day, bentonite was added to the upstream channel. After 2 hours, the flow rate at the end of the downstream channel had dropped from 3.2 gallons per minute (gpm) to 3.0 gpm.

Summary

The filter sustained a crack but partially stopped the leak. Flow velocities were not high enough to move many sand or gravel particles out of the box, and the downstream channel opening retained the larger particle sizes, preventing them from being transported downstream. Bentonite was added to the upstream and did not significantly influence the flow rate coming out of the box. This may have been because the volume of bentonite was not high enough to influence the filter, the bentonite may have washed through the filter, or not enough time passed for the bentonite to infiltrate the filter and reduce the hydraulic conductivity.

Test 8

Average moisture content[1]	Average dry unit weight[1]	Average compaction (%)[1]
5.8%	142.9 lbf/ft^3	103.4%

[1] Results of sand cone tests performed on the filter before running the test.

Test Description

Broadly graded filter material was placed up to a height of 47 inches and was 3 feet wide. Test 8 took place on July 25, 2011. The box was cracked approximately 1 inch (see figure 15). The crack was not vertical and was branched in several locations. Large aggregate pieces extended into the crack, making the crack appear much narrower.

Figure 15.—Overhead view of Test 8: 3 feet of broadly graded material compacted to 103.4%.

The reservoir was filled to a height of 44 inches. Shortly after releasing the reservoir, water in the crack equalized with the reservoir at a height of 44 inches. The water surface did not drop until exiting the downstream face of the filter. No sloughing occurred during the test, and no material was transported downstream, even after allowing the test to continue for 50 hours.

Approximately 30 pounds of nonplastic silt was added to the upstream channel. Prior to adding this material, water flowed from the downstream channel at 9 gpm. Adding silt to the upstream channel reduced the downstream flow to 7 gpm.

Summary

The dense filter material sustained a crack, and the leak was partially stopped by the larger particles extending into the crack. Flow velocities were not high enough to move the larger sand or gravel particles out of the box, and the downstream channel retained the majority of the gravel sizes, preventing them from being transported downstream.

If the box had been cracked farther, there is a possibility the velocities would have increased, and the gravel would not have been retained on the downstream channel. This would likely have led to more filter material being transported downstream, eventually leading to sloughing and potentially healing of the filter.

During excavation of the broadly graded material, clean coarse sand was identified in the location of the crack, as shown in figure 16. The coarser sand is further evidence that the crack did not fully heal. As water flowed through the crack, finer sands were transported downstream, leaving behind the larger particles that were retained on the gravel. When silt was added to the upstream channel, flow through the filter did not reduce because the finer silt washed through the coarser sand and gravel.

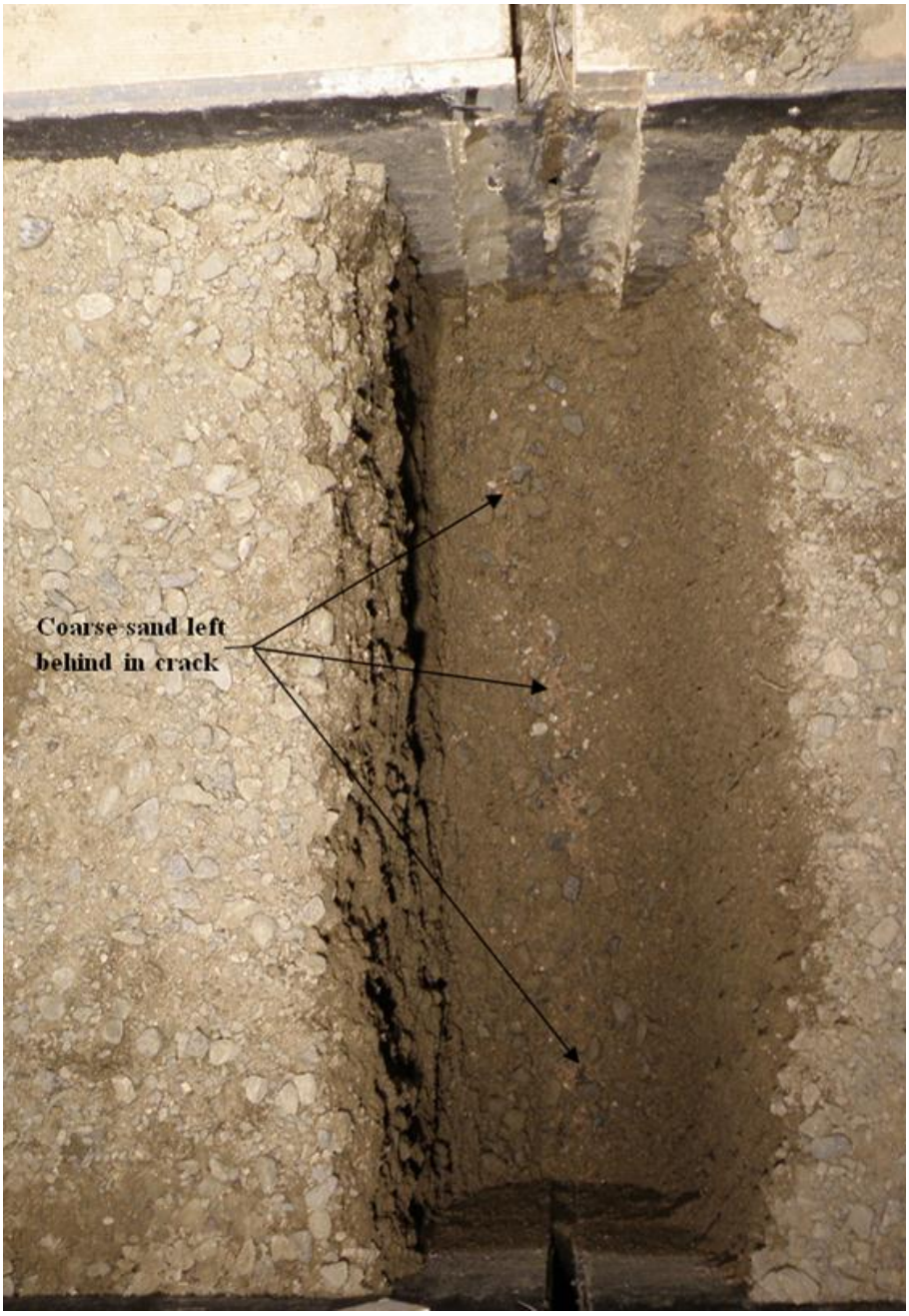

Figure 16.—Picture taken during excavation of test 8 material. The coarse sand (lighter in color) was evident throughout the entire excavation.

Test 9

Average moisture content[1]	Average dry unit weight[1]	Average compaction (%)[1]
6.0%	127.9 lbf/ft^3	92.5%

[1] Results of sand cone tests performed on the filter before running the test.

Test Description

Broadly graded material was placed up to a height of 48 inches, and the filter was 3 feet wide. Test 9 took place on August 15, 2011. The box was cracked approximately 1 inch, as seen in figure 17. The crack walls appeared to be mostly vertical, with some areas of sloughed particles. The crack orientated straight from upstream to downstream, and it meandered less than 1 inch in either direction. The crack branched about 8 inches from the downstream end of the filter.

Figure 17.—Overhead view of Test 9: 3 feet of broadly graded material compacted to 92.5%. (Note: the materials in tests 7, 8, and 9 are identical. The lighting in each photo affects the appearance of the material.)

The reservoir was filled to a height of 41 inches and then released. Some sloughing occurred, and the concentrated leak was stopped. As the test progressed, less water came through the downstream crack. Two days later, more water was flowing through the crack, but no material was being transported. Thirty pounds of silt were added to the upstream channel, and flow was reduced from 3.0 gpm 0.3 gpm after 1.5 hours.

Summary

The filter sustained a crack, but the leak was stopped. Flow velocities were not high enough to move many sand or gravel particles out of the box, and the

downstream channel opening retained the larger particle sizes. The silt added to the upstream channel showed that the broadly graded filter can still filter finer grained particles with a crack through the filter.

Tests 8 and 9 showed different trends in terms of filtering nonplastic silt that was added to the upstream channel. A major difference between tests 8 and 9 was the compaction effort (103.4% and 92.5% compaction, respectively). Material in Test 8 was noted as not sloughing. The material in Test 9 was noted as partially sloughing, which means that enough material sloughed into the crack to act as a filter for the silt added to the upstream channel.

Phase III Testing: Two-Stage Filter

Test 10

Average moisture content[1]	Average dry unit weight[1]	Average compaction (%)[1]
5.3%	108.4 lbf/ft^3	91.8%

[1] Results of sand cone tests performed on the sand filter only (not gravel) before running the test.

Test Description

The two-stage filter was placed up to a height of 48 inches and was configured as 3 feet of sand placed upstream of 2 feet of gravel. Test 10 took place on August 31, 2011. The box was cracked approximately 1 inch (see figure 18). Sand sustained a crack that was mostly vertical and meandered less than 1 inch in either direction. Gravel did not sustain a crack but settled by approximately 0.5 inch.

The reservoir was filled to a height of 45 inches and then released. Upon releasing the reservoir, the water level dropped approximately 2.5 inches. Filter material did not slough until the water level reached elevation 45; the sloughed material slumped into the upstream channel, rather than being transported downstream.

Although the test was allowed to run overnight, no water appeared in the downstream channel. At this point, a decision was made to widen the crack several more inches. This was done incrementally until reaching a maximum crack width of approximately 6.5 inches. Throughout the process, sand was observed to shift or slough into the crack. A flow path developed through the sand and into the gravel. While some sand was transported towards the gravel, the gravel effectively filtered the sand and minimized material transport.

Figure 18.—Overhead view of Test 10: 3 feet of sand compacted to 91.8% and 2 feet of compacted gravel.

Summary

Sand sustained a crack, but the gravel did not. Sand was not transported downstream because the gravel was filter compatible and because the velocity was not large enough to transport sand or gravel particles further downstream. As the crack width widened, flow was once again initiated. However, sand was never transported past the gravel. The gravel effectively drained water and filtered the sand.

Test 11

Average moisture content[1]	Average dry unit weight[1]	Average compaction (%)[1]
5.7%	107.8 lbf/ft^3	89.3%

[1] Results of sand cone tests performed on the sand filter only (not gravel) before running the test.

Test Description

Two-stage filter material was placed up to a height of 48 inches, with 3 feet of sand placed upstream of 2 feet of gravel. Test 11 took place on October 26, 2011. Geophysics instruments were added to the test, but they did not influence the outcome of the test. A report detailing the geophysics layout and data is located in appendix D. The box was cracked approximately 1 inch (see figure 19). The crack walls appeared to be mostly vertical in the sand, but the gravel did not sustain a crack. The crack in the sand filter branched immediately into two pieces

that meandered less than 1 inch in either direction. The two branches led into the gravel and were about 12 inches apart at that point.

Figure 19.—Overhead view of Test 11: 3 feet of sand compacted to 89.3% and 2 feet of compacted gravel.

The reservoir was filled to a height of 46 inches and then released. A very small amount of sloughing occurred in the sand filter, and no further sloughing of the gravel occurred. The concentrated leak was stopped. The box was cracked another 5.5 inches. Further sloughing of both materials occurred, but the leak was still stopped. Gravel material was then removed from the downstream side of the filter until the reservoir overtopped the two-stage filter. Flow velocities were high enough to transport sand and gravel downstream. The reservoir was at a height of 38 inches when the filter was overtopped. After the gravel material was removed, there was significant sloughing of both materials, but the filter could no longer stop the flow of water.

Summary

The sand sustained a crack, and the gravel did not. The two-stage filter system stopped any leaks despite large cracking. This filter material began to be transported downstream when gravel material was removed to the point where the filter could be overtopped.

Phase IV Testing: 5-Foot Filter

Test 12

Average moisture content[1]	Average unit weight[1]	Average compaction (%)[1]
4.4%	111.1 lbf/ft^3	92.9%

[1] Results of sand cone tests performed on the sand filter before running the test.

Test Description

Sand was placed up to a height of 48 inches, and the filter was 5 feet wide. Test 12 took place on January 17, 2012. Geophysics instrumentation was also included in this test. The geophysics equipment had no impact on the filter's performance, which is explained in detail in appendix D. The box was cracked approximately 1 inch (see figure 20). The crack walls were not vertical, and the crack branched at the upstream face. The branch caused a large wedge to form over the first 2.5 feet of the filter.

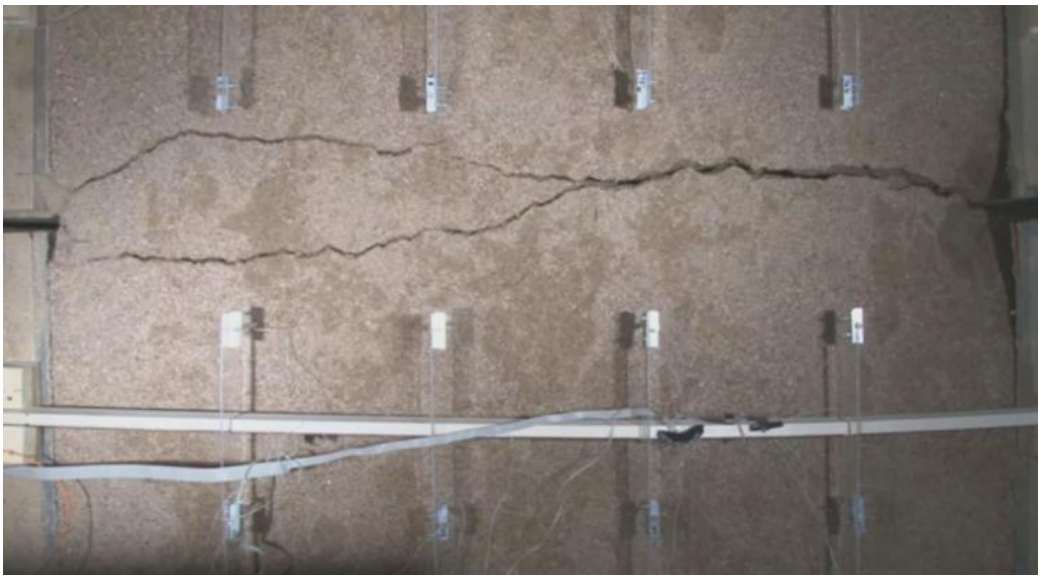

Figure 20.—Overhead view of Test 12: 5 feet of sand compacted to 92.9%.

The reservoir was filled to a height of 47 inches and released. As the filter material became saturated, it sloughed into the upstream channel. However, the flow velocities were not high enough to transport filter material downstream. The test continued for 2 days, and no water appeared in the downstream channel. At this point, a decision was made to expand the crack according to table 3.

Table 3. Test 12 crack width timeline

Crack width (in)	Time
1	11:10
1.5	11:14
2	11:19
2.5	11:24
3	11:30
3.5	11:36
4	11:43
4.5	11:51

As the box was cracked farther, more material was transported into the downstream channel. Also, the cracks within the box became wider, which allowed more water to flow towards the downstream end. At the downstream opening, the sand became liquefied and moved further downstream until the water drained out of the fluidized sand, at which time the sand became stable. Once the crack was opened to 4.5 inches, the upstream crack opening further, combined with more material moving downstream, caused a channel to fully open across the top of the crack.

Once the cycle mentioned above was in progress, portions of the filter fell into the channel and momentarily stopped flow, but the volume of sand was not significant enough to completely stop the flow.

Summary

Sand sustained a crack, but the additional width of the filter (2 feet) stopped the concentrated leaks. For larger crack widths, the 5-foot filter proved to be more robust and stopped any cracks from leaking for a longer period of time than did the 3-foot filter. However, the filter was unable to heal sufficiently after being opened 4.5 inches.

Phase V Testing: Nonplastic Silt with Single-Stage Filter

Test 13

Material	Average moisture content[1]	Average dry unit weight[1]	Average compaction (%)[1]
Sand	3.0%	109.8 lbf/ft^3	91.8%
Silt	14.4%	102.9 lbf/ft^3	94.9%

[1] Results of sand cone tests performed on the sand filter and silt before running the test.

Test Description

The filter and core materials were placed up to a height of 48 inches. The core was 2 feet wide, and the filter was 3 feet wide. Test 13 took place on March 16, 2013. The box was cracked approximately 1 inch (see figure 21). The crack walls appeared to be mostly vertical for both the silt and the sand. The crack ran almost straight from upstream to downstream and meandered less than 1 inch in either direction.

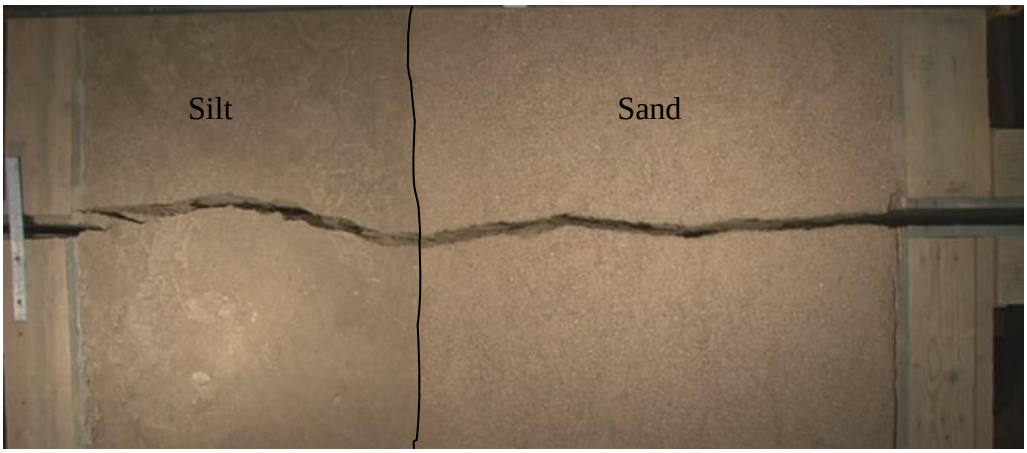

Figure 21.—Overhead view of Test 13: 2 feet of silt compacted to 94.9% and 3 feet of sand compacted to 91.8%.

The reservoir was filled to a height of 47 inches and then released. The filter and core material sloughed very little initially, and the concentrated leak was not stopped. When the filter did slough, it sloughed in large chunks that temporarily stopped the leaks until the reservoir level rose and the sloughed material was overtopped. The core material never sloughed, and there was little to no difference between Test 13 and Phase I tests. This implies that the inclusion of the core material did not influence the test.

Summary

The filter sustained a crack and was unable to stop the concentrated leak. The core material did not erode during the test and had little or no impact on the observed outcome. Little of the core material eroded. The core material was expected to have eroded significantly more than was observed given the material properties (nonplastic, eolian silt). If the core material had been fully saturated, it may have eroded significantly more than what was observed.

Phase VI Testing: Slow Filling Reservoir Single-Stage Filter

Test 14

Average moisture content[1]	Average dry unit weight[1]	Average compaction (%)[1]
4.9%	109.2 lbf/ft^3	91.3%

[1] Results of sand cone tests performed on the sand filter and silt before running the test.

Test Description

Sand was placed up to a height of 48 inches and was 3 feet wide. Test 14 took place on July 22, 2013.

Prior to testing, the reservoir was modified to maintain a constant elevation without continuous monitoring. This was done by installing outlet pipes every 12 inches.

The box was cracked approximately 1 inch (see figure 22). The sand sustained a crack that was mostly vertical and meandered less than 1 inch in either direction.

Figure 22.—Overhead view of Test 14: 3 feet of sand compacted to 91.3%.

The reservoir was filled incrementally as shown in table 4 and figure 23.

Summary

The filter material sustained a crack and was able to stop the leak at lower reservoir elevations. When the reservoir was at lower elevations, more material existed above the reservoir surface to slough into the crack and stop the leak. As the reservoir height increased, the volume of filter material above the water elevation decreased. Additionally, the crack was wider near the top. At higher reservoir elevations, the volume of material available to slough into the crack was reduced. It is concluded that if the filter material was extended several feet above the reservoir, enough material would have been able to slough into the crack to stop the concentrated leak when the reservoir reached 45 inches.

Table 4. Test 14 reservoir timeline

Reservoir height (in)	Time	Date	Hours since start
0	7:30 AM	7/22/2013	0.0
12	4:00 PM	7/22/2013	8.5
12	7:30 AM	7/23/2013	24.0
12	10:00 AM	7/24/2013	50.5
20.5	5:00 PM	7/24/2013	57.5
24	7:45 AM	7/25/2013	72.2
24	8:30 AM	7/26/2013	97.0
36	4:30 PM	7/26/2013	105.0
36	8:00 AM	7/29/2013	168.5
41	10:00 AM	7/29/2013	170.5
44	2:08 PM	7/29/2013	174.6
45	2:18 PM	7/29/2013	174.8
39	2:24 PM	7/29/2013	174.9

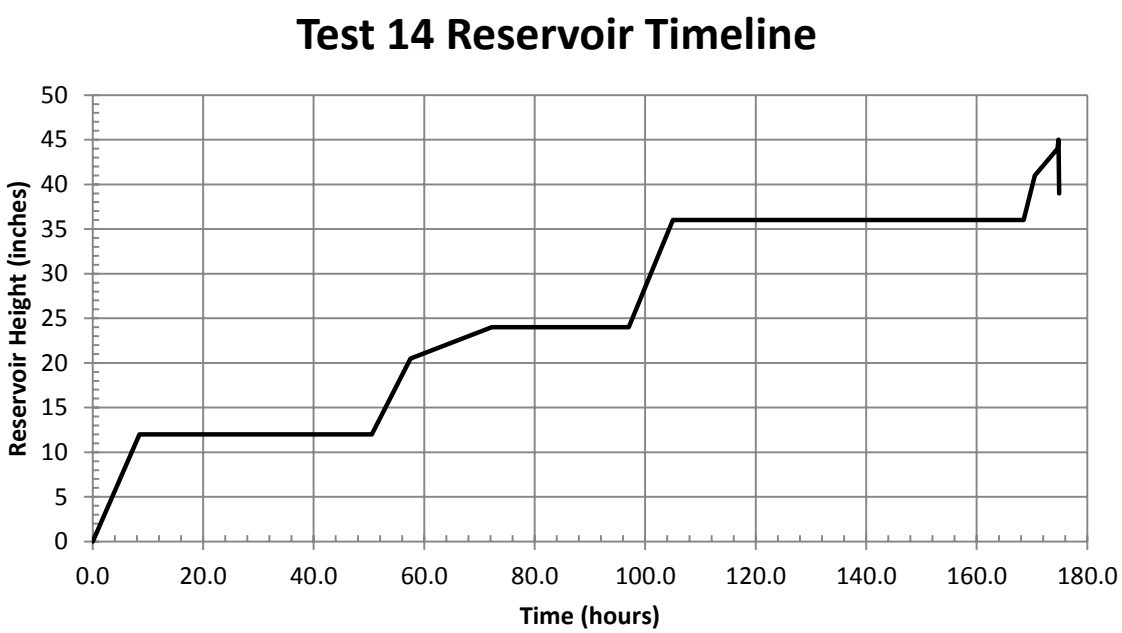

Figure 23.—Test 14 reservoir timeline.

CONCLUSIONS

Phase I

Nonplastic cohesionless materials that have low fines content are generally assumed to be unable to sustain a crack. Phase I shows that these types of materials can sustain a crack when there is little overlying material and the filter material is partially saturated. In particular, if these types of materials are dense, they can sustain a crack, not heal, and may eventually become unable to stop a concentrated leak.

Phase II

Broadly graded filters are also capable of sustaining cracks, despite consisting of cohesionless materials.

Tests with the broadly graded filter material generally exhibited visually lower flow velocities than tests with single-stage sand filters. During the Phase II tests, the material was resistant to downstream transport, which slowed erosion and led to lower flow velocities. Material resistance to downstream transport was twofold: (1) the aperture of the downstream channel opening stopped the larger gravel particles from being transported downstream, and (2) the larger particles of the broadly graded filter required higher flow velocities to be transported downstream. The erosion resistance resulted in a relatively open crack that allowed the water to flow freely at relatively low velocities from the upstream opening to the downstream end. Flow velocities remained low throughout the test due to the erosion resistance of the system, and velocities never grew to the point where the larger particles would be mobilized.

The satisfactory performance of the broadly graded filter may be credited to testing conditions. Filter particles were stopped by the aperture of the downstream channel opening. The opening acted as a secondary filter for the broadly graded material in a way similar to placing coarse gravel around a perforated toe drain pipe. Downstream flow velocities during the test were relatively constant as erosion and head cutting of the channel were stopped by the downstream channel opening size. The benefit of a reduced downstream aperture may not exist in field conditions, limiting the effectiveness of a broadly graded filter. The positive performance of the observed broadly graded filter could be carried into the field by placing a coarse geonet downstream of the filter so that the aperture of the geonet would act to retain the coarse filter particles.

Phase III

The two-stage filter was the most robust configuration tested. During the tests within this phase, the sand sustained an initial crack, while the gravel did not. Cracks did not form in the gravel because the gravels collapsed easily when no confining pressure existed. Filter compatibility of the gravel with the sand ensured that any sand particles transported by flows were retained by the gravel, which stopped transportation of filter material and the concentrated leak.

Phase IV

The 5-foot single-stage filter performed better than the 3-foot single-stage filter, but not as well as the two-stage filter. With only one test for Phase IV, test 12, conclusions are limited. One important aspect that makes it difficult to draw conclusions is the crack itself. The crack that formed was relatively small and branched almost immediately. This allowed for more sloughing and reduced flow to the downstream end of the box. The material was compacted to a similar density and moisture content as test 3, which formed a wide crack that ran straight for about 18 inches, and then branched into two cracks. Test 3 did not stop the concentrated leak. It is speculated that if the same crack had formed for test 12, it would have performed similarly to test 3 and would not have stopped the leak. Another possibility is that the 3-foot-wide filter arched over the smaller width, and the 5-foot filter was unable to interact with the upstream and downstream walls enough to arch and reduce sloughing. Intuitively, a filter that is 5 feet wide would perform better than a filter that is 3 feet wide, but the evidence is not conclusive in this phase.

Phase V

The single-stage 3-foot-wide filter with an upstream silt zone performed similarly to the single-stage filters in Phase I: the filter was dense and unable to slough sufficiently. The silt core material did not seem to influence the test. The well compacted core sustained a consistent crack throughout the test and did not slough or erode. The initial crack sustained in the sand was a continuation of the crack in the silt and allowed for a concentrated leak to flow freely from one end of the box to the other. High velocities associated with the open channel flows eroded the sand filter.

Phase VI

Phase VI tested a 3-foot-wide single-stage filter, and the reservoir level was slowly increased during the test. The filter material sustained a crack, but the filter stopped the concentrated leak until the reservoir was raised to a height similar to the tests in Phase I. The test did not fail until the reservoir heights were

higher because the filter sloughed sufficiently into the crack at lower reservoir levels, and there was sufficient volume of filter above the water in the crack to slough into the open crack.

Overall

The main purpose of a filter is to stop erosion of upstream soils. An ideal filter should also be able to function properly if compromised by a crack by healing to fill the crack and stopping the leak. This research suggests that a dense, poorly graded sand with nonplastic fines can, and will, sustain a crack. Additionally, that crack can allow the concentrated leak to transport sand particles downstream to the point that the filter would be compromised.

The lower parts of an embankment are more likely to be saturated and have much more overlying material, so a filter in this area is less likely to sustain a crack. The upper reaches of an embankment are more likely to sustain a crack because they are more likely to be partially saturated and have less overburden. There are three design considerations that can help ensure cracked filters do not lead to failure of an embankment.

One recommendation is to extend the filter to the crest of the dam (or as high as reasonably possible) so that the filter is above the maximum water surface. As discussed in the conclusions for Phase VI, when the reservoir reaches the upper limits of a filter there is not enough volume to slough, heal, and impede flow.

Another recommendation is to ensure an adequate width of single-stage filters. Benefits of a wider filter zone are discussed in the Phase IV conclusions. There is no recommendation on a minimum width, but designers should acknowledge the risk of contamination and the “Christmas Tree” effect, both of which can result in reducing the filter width to less than what is specified. Typically, Reclamation dams have a filter width of 8 feet. However, this may not be the case for smaller embankment dams where smaller equipment is used and project costs are lower.

The last recommendation is to design a two-stage filter. Including gravel downstream of the filter is the best way to ensure proper performance of sand filters. This is evident when two-stage filter test results are compared with single-stage filter tests (both 3 and 5 feet wide).

When designing a filter, these three recommendations should be considered to help ensure that filters are less likely to fail due to cracking. Design of single-stage filters with a narrow width makes the filter susceptible to cracking and reduces the ability of the filter to heal, stop a concentrated leak through the crack, and prevent erosion of upstream soils.

BIBLIOGRAPHY

[1] Park, Y., T.L. Brandon, and J.M. Duncan. 2004. DSO-04-06: "Investigation of the Ability of Filters to Stop Erosion through Cracks in Dams." Subcontract No. DEN33411..

[2] Vaughan, P., and H. Soares. 1982. "Design of Filters for Clay Cores of Dams," *Journal of the Geotechnical Engineering Division.* ASCE, Vol. 108, No. GT1, January 1982, pp. 17-31.

[3] Rinehart, R. 2012. "Development of a Test to Determine Cementation Potential of Embankment Dam Granular Filter Material – Results of Phase III Research." Bureau of Reclamation, Technical Service Center, Denver, Colorado.

[4] Sherard, J.L. 1979. "Sinkholes in Dams of Coarse, Broadly Graded Soils." Thirteenth Congress on Large Dams, Question 49, R2, New Delhi.

[5] Bureau of Reclamation. 2007. *Design Standards No. 13 - Embankment Dams*, Chapter 5, "Protective Filters."

APPENDICES

A Sand Physical Property Results

B Sand Castle Test Results

C Silt Physical Property Results

D Geophysics Paper

E Maximum Density Tests

APPENDIX A

Sand Physical Property Results

Kumar & Associates, Inc.
Geotechnical and Materials Engineers
and Environmental Scientists

ACEC
MEMBER

319 South 3rd Avenue
Frisco, CO 80443
phone: (970) 368-4779
fax: (970) 368-4978
email: kafrisco@kumarusa.com
www.kumarusa.com

Office Locations: Denver (HQ), Colorado Springs, Fort Collins, and Frisco, Colorado

January 31, 2012

Mr. Rick Foster
Albert Frei and Sons
P.O. Box 700
Henderson, Colorado 80640

Reference: Physical Properties Testing
Concrete Sand
Pit 4, Commerce City
Project No. 11-6-132

Dear Mr. Foster:

This letter presents results of physical properties testing performed on material picked up at your facility in December, 2011. Representative samples delivered were identified as Concrete Sand from Pit 4 in Commerce City, Colorado. Testing was performed to determine the materials compliance with ASTM, AASHTO, and City of Aurora specifications. The following testing was performed in general conformance with the applicable standards.

1) Sieve Analysis (Gradation) – ASTM C 136
2) Material Finer Than No. 200 Sieve by Washing – ASTM C 117
3) Specific Gravity & Absorption of Fine Aggregate – ASTM C 128
4) Organic Impurities – ASTM C 40
5) Clay Lumps & Friable Particles in Aggregate – ASTM C 142
6) Lightweight Particles 2.0 in Aggregate – ASTM C 123
7) Lightweight Particles 2.4 in Aggregate – ASTM C 123
8) Sodium Sulfate Soundness – ASTM C 88
9) Magnesium Sulfate Soundness – ASTM C 88
10) Rodded Unit Weight & Voids – ASTM C 29
11) Loose Unit Weight & Voids – ASTM C 29
12) Relative Density – ASTM D 4253 & ASTM D 4254
13) Moisture Content – ASTM D 2216
14) Potential Alkali Reactivity – ASTM C 1260
15) Petrographic Analysis – ASTM C 295
16) Sand Equivalency – ASTM D 2419
17) Atterberg Limits – ASTM D 4318

A summary of the aggregate test results is attached, followed by the complete test results. Based on the test results, the material tested meets the required specifications for Concrete Sand.

If you have any questions, please feel free to contact our office.

Sincerely,

KUMAR & ASSOCIATES, INC.

Matthew A. Best
Frisco Office Manager

Distribution: (1) Email rfoster@albertfreiandsons.com

KUMAR & ASSOCIATES

AGGREGATE SUMMARY SHEET

PROJECT INFORMATION

PROJECT NAME:	**2012 Aggregate Qualification**		
SAMPLE LOCATION:	**Pit 4, Commerce City, Colorado**		
MATERIAL TYPE:	**Concrete Sand**	K&A PROJECT NUMBER:	**11-6-132**

MECHANICAL SIEVE ANALYSIS (ASTM C 136 & ASTM C 117)

SIEVE SIZE US STD	SIEVE SIZE METRIC	PERCENT PASSING	ASTM C 33 SPEC	AASHTO (CDOT) (DIA) SPEC	City of Aurora Spec
1.5"	38	-	-	-	-
1"	25	-	-	-	-
3/4"	19	-	-	-	-
1/2"	12.5	-	-	-	-
3/8"	9.5	**100**	**100**	**100**	**100**
NO. 4	4.75	**100**	**95-100**	**95-100**	**95-100**
NO. 8	2.36	**90**	**80-100**	**80-100**	**80-100**
NO.10	2.00	**83**	-	-	-
NO.16	1.18	**64**	**50-85**	**50-85**	**50-85**
NO. 30	0.6	**37**	**25-60**	**25-60**	**25-60**
NO. 40	0.425	**23**	-	-	-
NO. 50	0.3	**12**	**10-30**	**10-30**	**10-30**
NO. 100	0.15	**3**	**0-10**	**2-10**	**0-10**
NO. 200	0.075	**0.5**	**3.0 Max**	**3.0 Max**	**3.0 Max**
Fineness Modulus		**2.94**			

*INDICATES OUT OF TOLERANCE

SPECIFIC GRAVITY AND ABSORPTION (ASTM C 128)

	RESULTS	SPECIFICATION	PASS/FAIL
Specific Gravity	**2.62**	**N/A**	**N/A**
Absorption (%)	**1.4%**	**N/A**	**N/A**

CLAY LUMPS AND FRIABLE PARTICLES (ASTM C 142)

	RESULTS	SPECIFICATION	PASS/FAIL
Weighted Particles	**0.2%**	**2.0% Max**	**Pass**

LIGHTWEIGHT PARTICLES (ASTM C 123)

	RESULTS	SPECIFICATION	PASS/FAIL
Specific Gravity 2.0	**< 0.1%**	**0.5% Max**	**Pass**
Specific Gravity 2.4	**< 0.1%**	**2.0% Max**	**Pass**
Sum of Deleterious Materials	**0.9%**	**3.0% Max**	**Pass**

SODIUM SULFATE SOUNDNESS (ASTM C 88)

	RESULTS	SPECIFICATION	PASS/FAIL
Weighted Loss (%)	**3%**	**12% Max**	**Pass**

MAGNESIUM SULFATE SOUNDNESS (ASTM C 88)

	RESULTS	SPECIFICATION	PASS/FAIL
Weighted Loss (%)	**5%**	**18% Max**	**Pass**

UNIT WEIGHT AND VOIDS IN AGGREGATE (ASTM C 29)

Rodded	RESULTS	SPECIFICATION	PASS/FAIL
Unit Weight (pcf)	**104**	**N/A**	**N/A**
Percent Voids	**35%**	**N/A**	**N/A**
Tons per cubic yard	**1.40**	**N/A**	**N/A**
Loose	RESULTS	SPECIFICATION	PASS/FAIL
Unit Weight (pcf)	**99**	**N/A**	**N/A**
Percent Voids	**39%**	**N/A**	**N/A**
Tons per cubic yard	**1.34**	**N/A**	**N/A**

SAND EQUIVALENCY (ASTM D 2419)

	RESULTS	SPECIFICATION	PASS/FAIL
Sand Equivalent	**90**	**80 Min**	**Pass**

POTENTIAL ALKALI REACTIVITY (ASTM C 1260)

14-Day Soak	RESULTS	SPECIFICATION	PASS/FAIL
Average Expansion	**0.06%**	**< 0.10%**	**Pass**
Classification	**Innocuous**		
Potential for Deleterious ASR	**Low Potential**		

MAXIMUM AND MINIMUM DENSITY USING RELATIVE DENSITY (ASTM D 4253 & D 4254)

	RESULTS	SPECIFICATION	PASS/FAIL
Minimum Density	**93.4**	**N/A**	**N/A**
Maximum Density	**129.8**	**N/A**	**N/A**

KUMAR & ASSOCIATES

AGGREGATE SUMMARY SHEET

PROJECT INFORMATION

PROJECT NAME:	**2012 Aggregate Qualification**		
SAMPLE LOCATION:	**Pit 4, Commerce City, Colorado**		
MATERIAL TYPE:	**Concrete Sand**	K&A PROJECT NUMBER:	**11-6-132**

DETERMINATION OF MOISTURE CONTENT OF SOIL AND ROCK (ASTM D 2216)			
	RESULTS	SPECIFICATION	PASS/FAIL
Concrete Sand	**3.3%**	**N/A**	**N/A**

ORGANIC IMPURITIES (ASTM C 40)			
	RESULTS	SPECIFICATION	PASS/FAIL
Concrete Sand	**Plate 1**	**< Plate 3**	**Pass**

DETERMINATION OF LIQUID LIMIT AND PLASTICITY INDEX (ASMT D 4318)			
	RESULTS	SPECIFICATION	PASS/FAIL
Liquid Limit	**Non-Liquid**	**N/A**	**N/A**
Plasticity Index	**Non-Plastic**	**N/A**	**N/A**

ATTACHMENT A

LABORATORY TEST RESULTS

KUMAR & ASSOCIATES

AGGREGATE RESULTS SHEET

PROJECT INFORMATION

PROJECT NAME:	**2012 Aggregate Qualification**		
SAMPLE LOCATION:	**Pit 4, Commerce City, Colorado**		
MATERIAL TYPE:	**Concrete Sand**	K&A PROJECT NUMBER:	**11-6-132**

Material Finer Than No. 200 Sieve (ASTM C 117)

Initial Dry Weight (g)	Final Dry Weight (g)	Passing No. 200 Sieve (%)
999.1	**994.5**	**0.5%**

SPECIFIC GRAVITY AND ABSORPTION (ASTM C 128)

Pycnometer & Water Weight (g)	SSD Soil Weight (g)	Pycnometer & Sample Weight (g)	Oven Dry Weight (g)	Bulk (SSD) Specific	Absorption (%)
660	**500.3**	**969.7**	**493.2**	**2.62**	**1.4%**

LIGHTWEIGHT PARTICLES (ASTM C 123)

	RESULTS	SPECIFICATION	PASS/FAIL
Specific Gravity 2.0	**< 0.1%**	**0.5% Max**	**Pass**
Specific Gravity 2.4	**< 0.1%**	**2.0% Max**	**Pass**

CLAY LUMPS AND FRIABLE PARTICLES (ASTM C 142)

Passing Sieve Size	Retained Sieve Size	Intial Weight (g)	Final Weight (g)	Percent Loss	Weighted Loss (%)
No. 4	No. 16	**41.3**	**41.2**	**0.2%**	**N/A**

ORGANIC IMPURITIES (ASTM C 40)

	RESULTS	SPECIFICATION	PASS/FAIL
Concrete Sand	**Plate 1**	**< Plate 3**	**Pass**

SAND EQUIVALENCY (ASTM D 2419)

Tube Number	Clay Reading	Sand Reading	Sand Equivalent
1	**4.3**	**3.8**	**89**
2	**4.3**	**3.9**	**91**
3	**4.4**	**3.9**	**89**
		Average Sand Equivalency	**90**

DETERMINATION OF MOISTURE CONTENT OF SOIL AND ROCK (ASTM D 2216)

Initial Weight (g)	Final Weight (g)	Moisture Content (%)
694.4	**672.5**	**3.3%**

UNIT WEIGHT AND VOIDS IN AGGREGATE (ASTM C 29)

Rodded	Sample Weight (lbs)	Bucket Volume (ft^3)	Unit Weight (pcf)
Sample 1	**26.05**	**0.2494**	**104.5**
Sample 2	**25.95**	**0.2494**	**104.1**
Sample 3	**26.07**	**0.2494**	**104.5**
		Average Unit Weight	**104**
Loose	Sample Weight (lbs)	Bucket Volume (ft^3)	Unit Weight (pcf)
Sample 1	**24.60**	**0.2494**	**98.6**
Sample 2	**24.64**	**0.2494**	**98.8**
Sample 3	**24.62**	**0.2494**	**98.7**
		Average Unit Weight	**99**

SODIUM SULFATE SOUNDNESS (ASTM C 88)

Retained Sieve Size	Percent Grading	Intial Weight (g)	Final Weight (g)	Percent Loss	Weighted Loss (%)
No. 8	**10**	**100.0**	**98.9**	**1.1%**	**0.1%**
No. 16	**26**	**100.0**	**97.1**	**2.9%**	**0.8%**
No. 30	**27**	**100.0**	**96.8**	**3.2%**	**0.9%**
No. 50	**25**	**100.0**	**96.0**	**4.0%**	**1.0%**
- No. 50	**12**	**-**	**-**	**-**	**-**
Total Grading		**100**	Total Weighted Loss		**3%**

MAGNESIUM SULFATE SOUNDNESS (ASTM C 88)

Retained Sieve Size	Percent Grading	Intial Weight (g)	Final Weight (g)	Percent Loss	Weighted Loss (%)
No. 8	**10**	**100.0**	**97.4**	**2.6%**	**0.3%**
No. 16	**26**	**100.0**	**93.4**	**6.6%**	**1.7%**
No. 30	**27**	**100.0**	**95.0**	**5.0%**	**1.4%**
No. 50	**25**	**100.0**	**92.3**	**7.7%**	**1.8%**
- No. 50	**12**	**-**	**-**	**-**	**-**
Total Grading		**100**	Total Weighted Loss		**5%**

DETERMINATION OF LIQUID LIMIT AND PLASTICITY INDEX (ASMT D 4318)

	RESULTS	SPECIFICATION	PASS/FAIL
Liquid Limit	**Non-Liquid**	**N/A**	**N/A**
Plasticity Index	**Non-Plastic**	**N/A**	**N/A**

KUMAR & ASSOCIATES

AGGREGATE RESULTS SHEET

PROJECT INFORMATION

PROJECT NAME:	**2012 Aggregate Qualification**		
SAMPLE LOCATION:	**Pit 4, Commerce City, Colorado**		
MATERIAL TYPE:	**Concrete Sand**	K&A PROJECT NUMBER:	**11-6-132**

Potential Alkali Reactivity of Aggregates, Mortar-Bar Method
ASTM C 1260

Cast Date: December 28, 2011

Cement: Holcim Type I/II - Portland

Cement Alkalies (Total Alkalies as Na2O): 0.75%

Cement Expansion (Autoclave): 0.02%

Cementitious Content: 440 g

Aggregate/Cement Ratio: 990g/440g

Water/Cement Ratio: 0.47

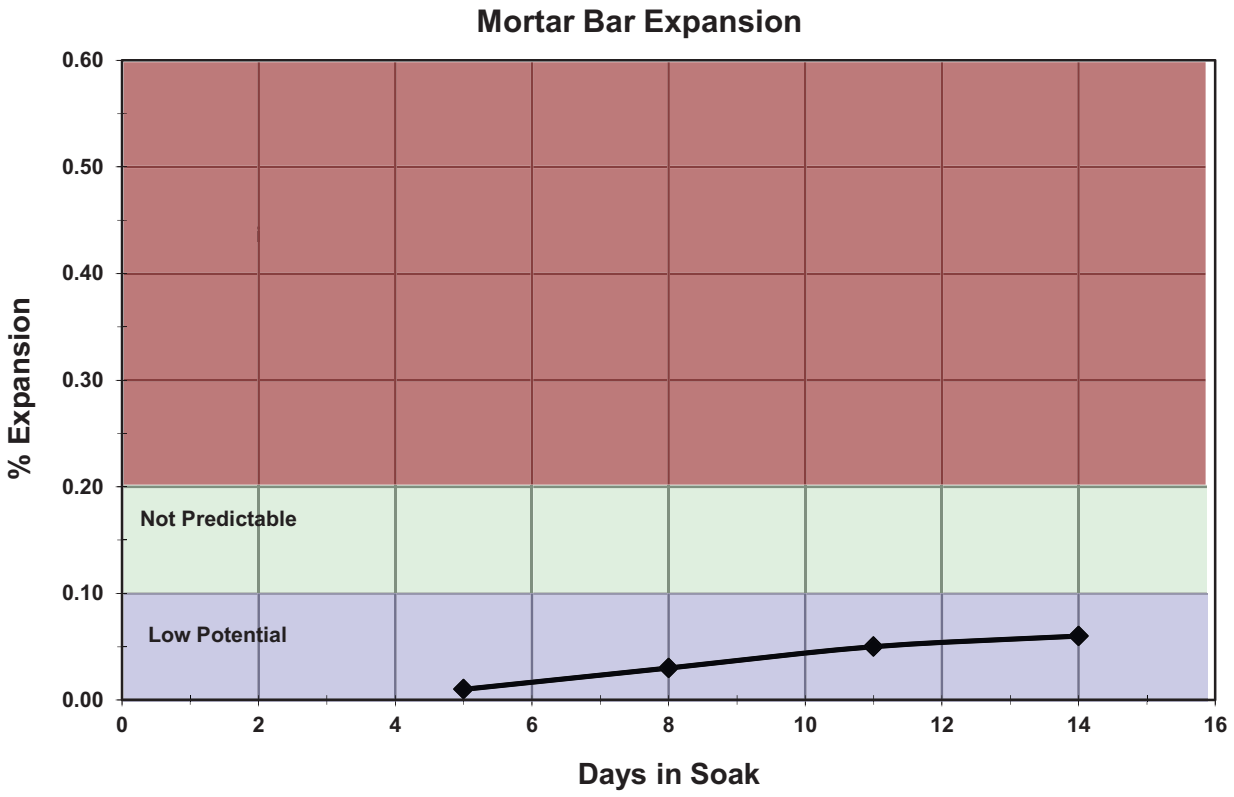

Date	Age (Days)	Expansion (%)			
		Sample ID			Average
		1	2	3	
1/3/12	5	0.005	0.022	0.009	**0.01**
1/6/12	8	0.026	0.032	0.028	**0.03**
1/9/12	11	0.059	0.049	0.047	**0.05**
1/11/12	14	0.065	0.058	0.053	**0.06**

KUMAR & ASSOCIATES

AGGREGATE RESULTS SHEET

PROJECT INFORMATION

PROJECT NAME:	**2012 Aggregate Qualification**		
SAMPLE LOCATION:	**Pit 4, Commerce City, Colorado**		
MATERIAL TYPE:	**Concrete Sand**	K&A PROJECT NUMBER:	**11-6-132**

RELATIVE DENSITY GRAPH

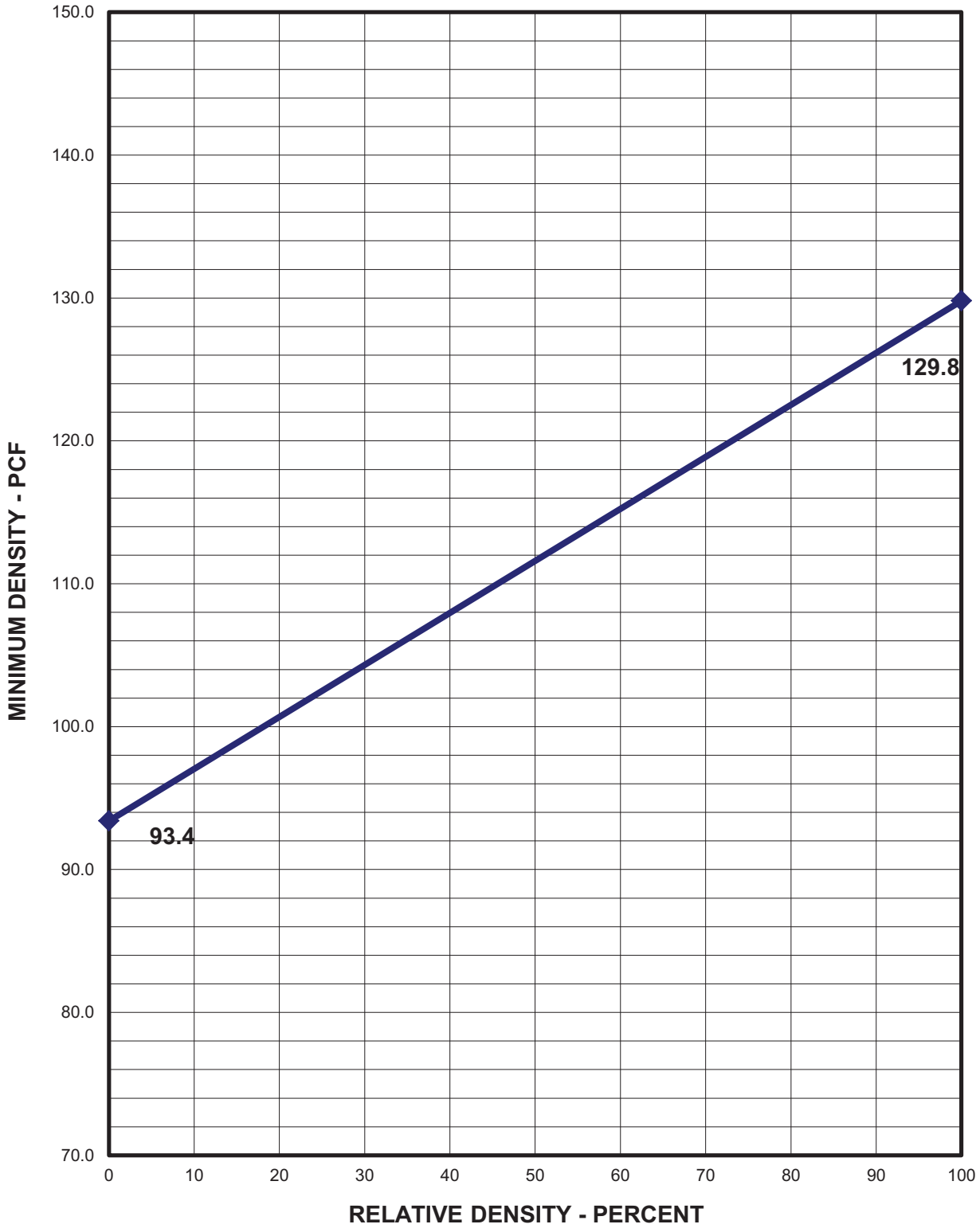

Figure A-4

Petrographic Investigation of Concrete Rock & Sand for Kumar & Associates, Inc. Project 11.6.132

Prepared for: Mr. Matthew Best
Kumar & Associates, Inc.
Frisco, Colorado

Prepared by: David Rothstein, Ph.D., P.G., FACI
Report No.: DRP12.929

27 JANUARY 2012

DRP Consulting, Inc. 3200 Carbon Place #104 Boulder, CO 80301
www.drpcinc.com

1.0 INTRODUCTION

Mr. Matthew Best of Kumar & Associates, Inc. (**K&A**) located in Frisco, Colorado requested DRP Consulting, Inc. (**DRP**) to conduct petrographic examinations of concrete rock and sand for **K&A** project 11.6.132. On 4 January 2012 **DRP** received three samples designated as #4 stone, #57/67 stone, and concrete sand. Each sample consisted of two (2) five-gallon buckets of material. The samples were assigned **DRP** sample numbers 16YD5216-16YD5218. Pursuant to the request of **K&A**, **DRP** combined the #4 stone sample with the #57/67 stone sample and designated this as #467 stone for the present analysis.

2.0 SCOPE OF WORK

The testing involved petrographic analysis of the stone and sand following methods outlined in ASTM C 295 [**1**]. This report summarizes the results of the analysis and provides photographs and micrographs of the sample. *Appendix A* contains the petrographic data from the stone analysis and *Appendix B* contains the petrographic data from the sand analysis.

3.0 PROCEDURES

The as-received samples were weighed, oven dried overnight at 105ºC and then weighed again to determine their moisture content. **Table 1** summarizes the moisture loss data. The samples were then quartered following procedures outlined in ASTM C702 [**2**]. Sieve analyses were performed on the dried fractions following ASTM C 136-06 [**3**] using a Ro-Tap® RX-30 sieve shaker. Multiple passes of materials were placed on sieves and agitated for five minutes per pass. **Figure 1** and **Figure 2** show photographs of the samples in their as-received condition and after sieving. The sieved fractions were then examined visually and petrographic analyses were performed on each sample following procedures outlined in ASTM C 295. A minimum of 150 particles were classified according to rock type for each sieve size; all particles were counted when there were less than 150 particles in the sieved fraction. A stereomicroscope with 3-180x magnification capability was used as the primary microscope for identifying the rock types for each sieve but petrographic thin sections were also used to facilitate the identification and description of the major rock types. The thin sections were prepared at **DRP** and examined using a petrographic microscope with 50-1000x magnification capability.

Table 1. Results of moisture content determination

Sample No.	As-received mass, kg (lbs)	Dry mass, kg (lbs)	Moisture Loss (%)
#467 Stone	52.23 (115.10)	52.13 (114.88)	0.19
Concrete Sand	25.81 (56.89)	25.52 (56.24)	1.14

1 *Guide for Petrographic Examination of Aggregates for Concrete.* Annual Book of ASTM Standards, v. 4.02. ASTM C295-03.
2 *Standard Practice for Reducing Samples of Aggregate to Testing Size.* Annual Book of ASTM Standards, v. 4.02. ASTM C702-98.
3 *Test Method for Sieve Analysis of Fine and Coarse Aggregates*, Annual Book of ASTM Standards, v. 4.02, ASTM C136-06.

4.0 FINDINGS

The findings of the examination relevant to the physical properties of the materials are as follows:

- The aggregate is from a natural river gravel source and is siliceous in composition. The aggregate consists primarily of granitic rocks with minor amounts of of granite, quartzite and limestone. The rocks are fresh, dense, and hard.

- The nominal top size of the stone is 38 mm (1 ½ in.) with 13.5% of the stone retained on this sieve. Only 0.3% of the stone passes the 4.75 mm (No. 4) sieve. **Table A1** contains the details of the sieve analysis. The nominal top size of the sand is 4.75 mm (#4 sieve) but this sieve retains only 0.1% of the sand. The fineness modulus of the sand is 2.97. **Table B1** contains the details of the sieve analysis.

- A light coating of dust that rinses off easily is present on both samples. No potentially deleterious materials identified in ASTM C33 such as coal, lignite, clay lumps or friable particles were observed in the stone; the sand contains traces of clay (0.2%). No deleterious coatings or incrustations were observed on the stone or sand particles.

- The particles are generally cuboidal (equant) to oblong in shape with well-rounded to sub-angular edges. Most of the fracture faces of the particles are fairly smooth. The stone and sand do not contain significant amounts of flattened particles.

The constituents of the stone and sand are summarized in **Table A2** and **Table B2**, respectively. **Table A3** and **Table B3** report the abundance of each component on a normalized weighted percentage basis.

The rock types observed in the samples include the following:

1. Granitic Rocks

Granitic rocks make up 85.5% of the stone and 96.9% of the sand. These rocks are hard and competent. The particles are typically sub-equant to oblong in shape with well-rounded to sub-angular edges. There are a variety of granitic rocks. In the stone these include red granitic rocks (53.6%), which are phaneritic and medium-grained with distinctive phenocrysts of red to pink alkali-feldspar (**Figure 3**). Phenocrysts of black biotite are commonly observed as well (**Figure 4**). Black granitic rocks make up 15.9% of the stone; these are also phaneritic and medium-grained with abundant phenocrysts of biotite and plagioclase feldspar. White to buff granitic rocks that are phaneritic with occasional phenocrysts of biotite make up 8.7% of the stone (**Figure 5**) and leucocratic granitic rocks, which are coarse-grained and consist of feldspar and quartz, make up 7.2% of the stone (**Figure 6**). In the sand granitic rocks include the red, black and white granitic rocks, which were counted as a single unit termed granite that makes up 42.3% of the sand, leucocratic granite (52.9%) and foliated granitic rocks (1.6%), which contain abundant biotite. Granitic rocks are potentially susceptible to alkali-silica reaction (ASR).

2. Quartzite

Quartzites make up 7.1% of the stone. These rocks are hard and competent and are sub-equant in shape with well-rounded to round edges. The rocks include quartz arenite, which consists almost entirely of quartz grains and arkosic quartzite, which consists of a mixture of different rock types that are mostly granitic. The quartz arenites are mostly white to buff in color and shows evidence of dynamic recrystallization and geological strain (**Figure 7**) The quartz arenite makes up 6.6% of the stone and is present in the sand in trace amounts (0.2%). The arkosic quartzites make up 0.6% of the stone. These rocks are dark red in color, which is imparted to them by a hematite cement (**Figure 8**). The arkosic quartzite consist of fragments of feldspar, quartz, granitic rocks and occasional fragments of diorite and siliceous volcanic rocks. These rocks are potentially susceptible to ASR.

3. Meta-graywacke

These rocks are metamorphic and make up 3.8% of the stone and were not observed in the sand. Metagraywackes are derived from sandstones that also contain abundant clay minerals. The rocks are mostly hard and competent and are tabular in shape with sub-round to sub-angular edges. Some of the rocks are moderately friable because they contain abundant micaceous minerals. The rocks consist primarily of quartz, feldspar and micaceous minerals (primarily biotite). These rocks are potentially susceptible to ASR.

4. Mafic rocks These rocks include intrusive igneous rocks such as diorite, metamorphosed igneous rocks such as amphibolite, and volcanic rocks such as andesite and basalt. These rocks are hard and competent. Amphibolite and diorite make up 1.7% of the stone and 1.0% of the sand. Andesite and basalt make up 1.3% of the stone and 0.1% of the sand. The diorite also consists primarily of plagioclase feldspar and amphibole but also contains pyroxene. This rock is fine to medium-grained and black and shows spherulitic and poikiloblastic textures (**Figure 9**). The amphibolite is medium-grained and also consists of plagioclase feldspar and amphibole, but the rock is strongly foliated (**Figure 10**). The andesite and basalt are black and fine-grained and consist primarily of plagioclase feldspar with phenocrysts of amphibole and pyroxene.

5. Other Other components present in trace amounts in the aggregate include the following. Rhyolite makes up 0.6% of the stone and 0.7% of the sand. This is a siliceous volcanic rock consisting of a fine grained matrix of feldspar and quartz with phenocrysts of quartz and occasionally biotite. Some of the rhyolites are lithic tuffs and contain fragments of rocks. Rhyolite is potentially susceptible to ASR. Other components observed in the sand include hematite (0.9%), mica (0.1%) and clay (0.2%).

5.0 CONCLUSIONS

The materials represented by the submitted samples are derived from a natural river deposit and are siliceous in composition. The materials consist primarily of granitic rocks with minor quartzites and mafic igneous and metamorphic rocks. The rocks are generally hard and competent and well-suited for the production of portland cement-based materials. Some of the particles are well-rounded, which can diminish the potential strength of paste-aggregate bonding. However, many aggregates with such properties are used routinely in the product of concrete without such adverse effects. No potentially deleterious materials, such as coal, lignite, friable particles, shale, claystone, ironstone or lightweight chert particles were observed. Clay was observed in the sand in trace amounts (0.2%).

The aggregate materials represented by the samples are rich in rock types that are known to be susceptible to ASR. However, in many regions such rocks are used routinely in the production of portland cement and show no record of deleterious expansions due to ASR while in service. **DRP** recommends that service records be referenced to assess the history of deleterious expansions due to ASR in concrete made with these materials and recommends comprehensive testing of these materials with appropriate ASTM tests to assess the potential for deleterious expansion due to ASR.

This concludes work performed on this project to date.

David Rothstein, Ph.D., P.G., FACI

Figures

(a)

(b)

Figure 1. (a) Photograph of #4 stone in as-received condition. (b) Photograph of #57/67 stone in as-received condition.

(c)

(d)

Figure 1 (cont'd). (c) Photograph of #467 stone derived from mixing the #4 stone and the #57/67 stone. (d) Photograph of fraction retained on the 38 mm (1 ½ in.) sieve.

(e)

(f)

Figure 1 (cont'd). Photographs of #467 stone showing fractions retained on the (e) 25 mm (1 in.) sieve and the (f) 19 mm (¾ in.) and 12.5 mm (½ in.) sieves.

(g)

Figure 1 (cont'd). (g) Photograph of #467 stone showing fractions retained on the 9.5 mm (⅜ in.) sieve and the 4.75 mm (#4) sieve.

(a)

Figure 2. Photograph of the concrete sand in as-received condition.

(b)

(c)

Figure 2 (cont'd). Photographs of concrete sand showing fractions retained on the (b) 4.75 mm (#4) sieve and the (c) 2.36 mm (#8) and 1.18 mm (#16) sieves.

(d)

(e)

Figure 2 (cont'd). Photographs of concrete sand showing fractions retained on the (d) 600 µm (#30) sieve and 300 µm (#50) sieve and the (e) 150 µm (#100) and 75 µm (#200) sieves.

(a)

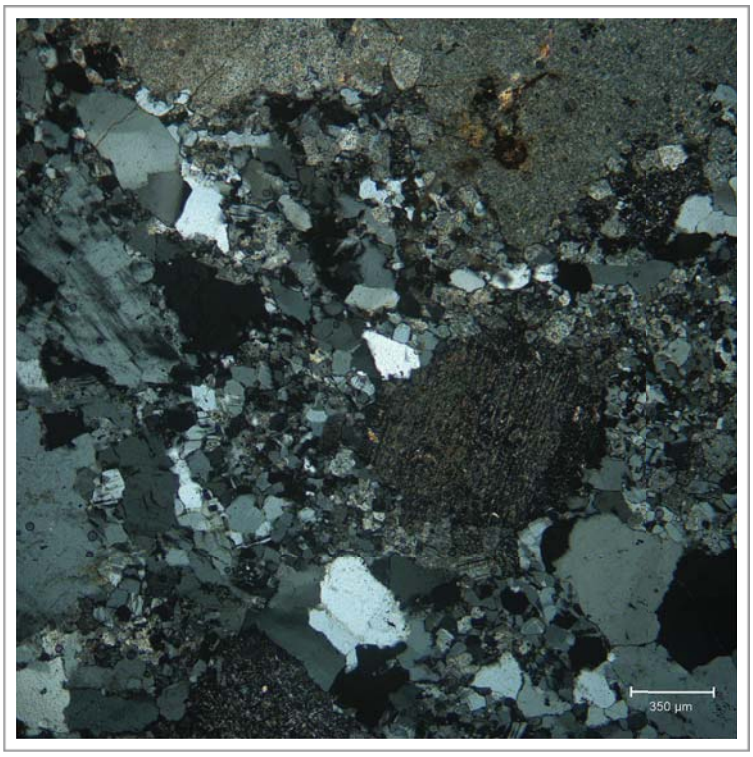

(b)

Figure 3. (a) Reflected light photomicrograph of polished surface of red granite particle. (b) Cross-polarized transmitted light photomicrograph of thin section of red granite particle.

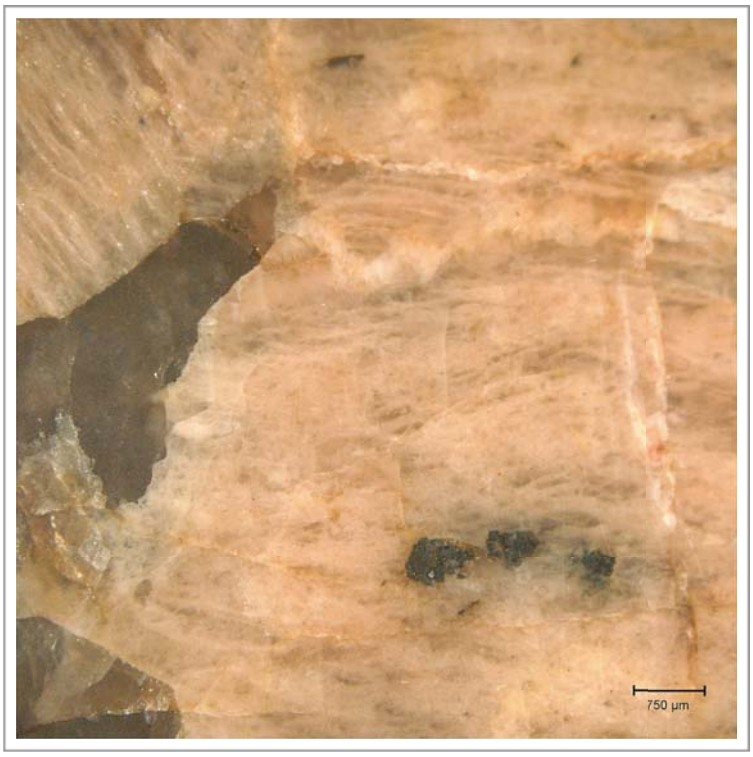

(a)

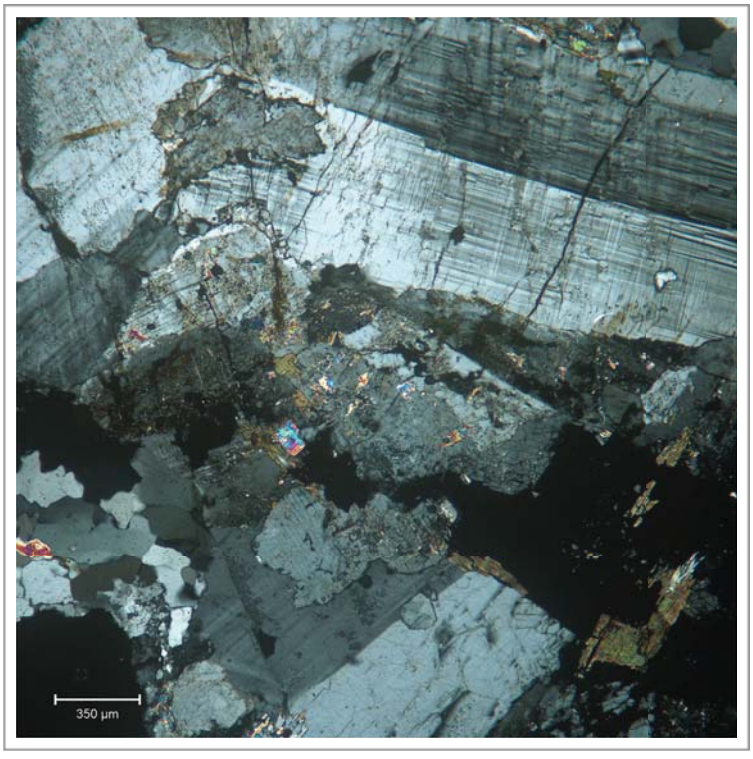

(b)

Figure 4. (a) Reflected light photomicrograph of polished surface of white granite particle. (b) Cross-polarized transmitted light photomicrograph of thin section of white granite particle.

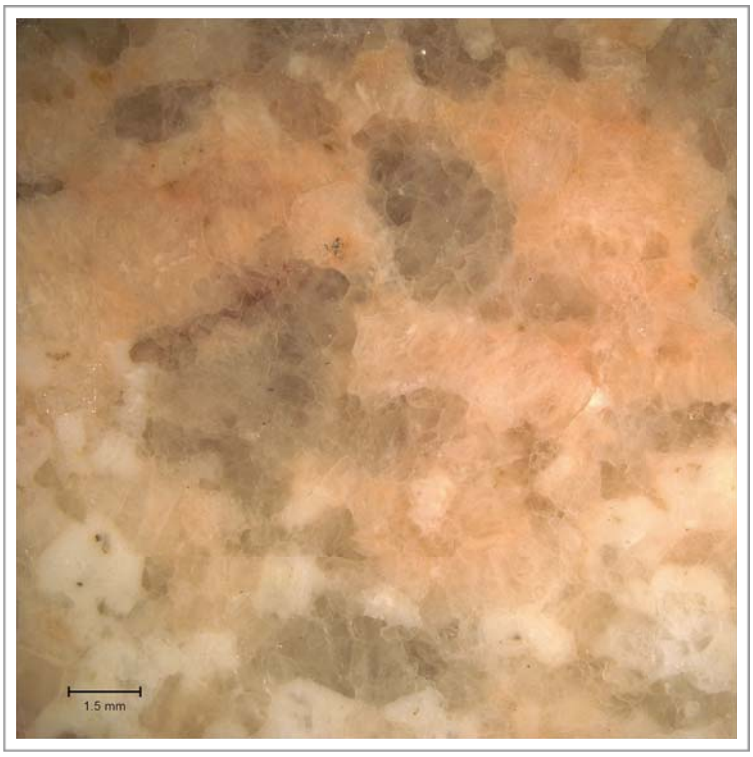

(a)

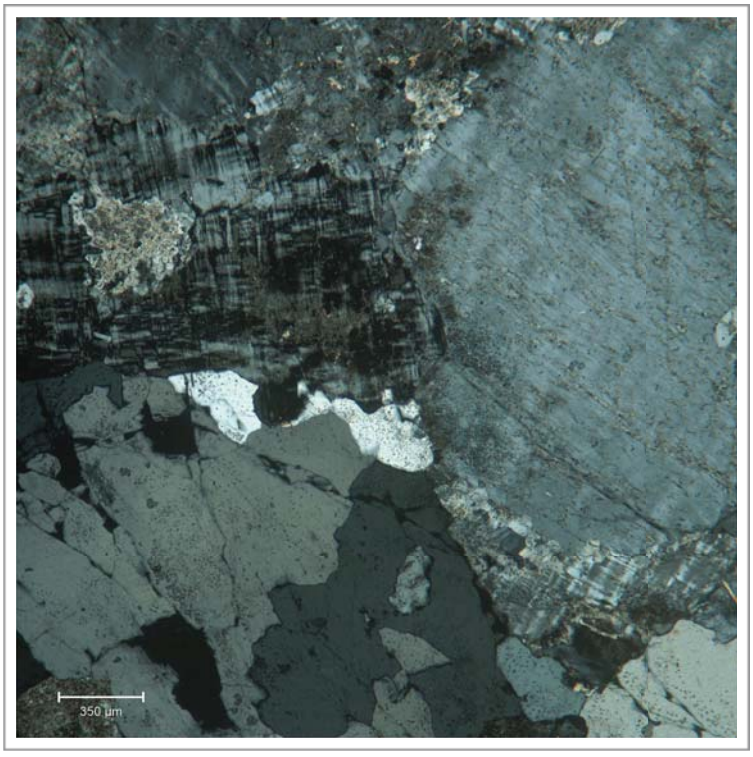

(b)

Figure 5. (a) Reflected light photomicrograph of polished surface of leucogranite particle. (b) Cross-polarized transmitted light photomicrograph of thin section of leucogranite particle.

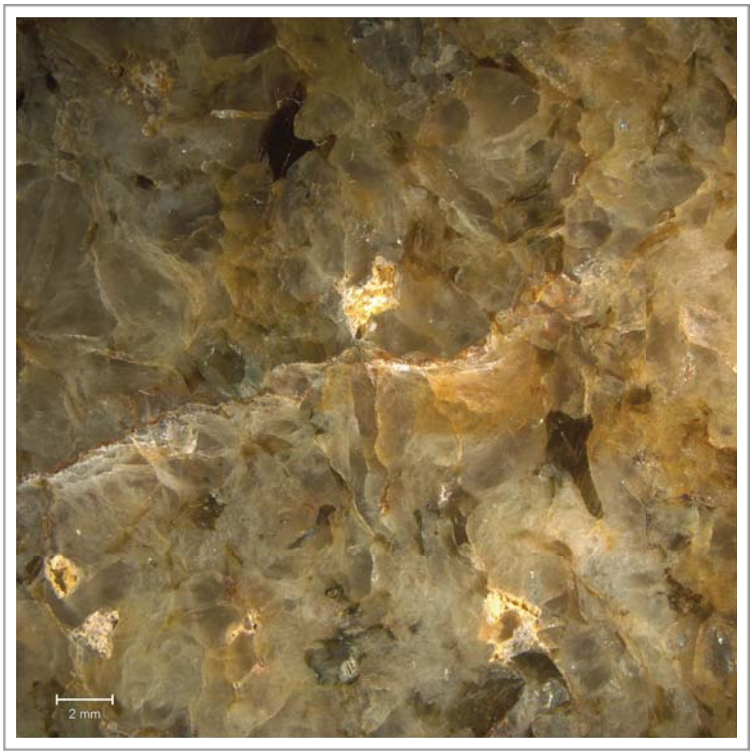

(a)

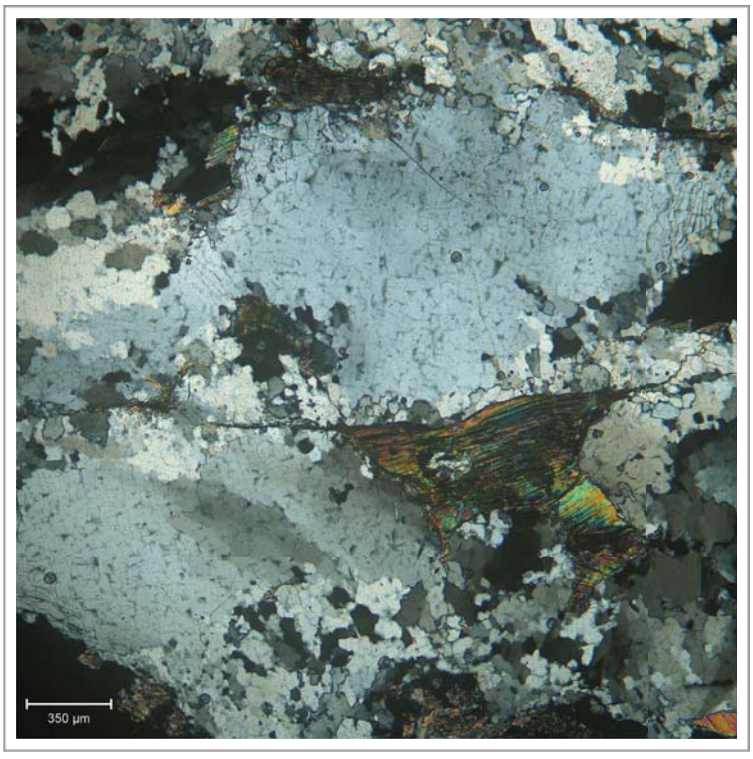

(b)

Figure 6. (a) Reflected light photomicrograph of polished surface of black granite particle. (b) Cross-polarized transmitted light photomicrograph of thin section of black granite particle.

(a)

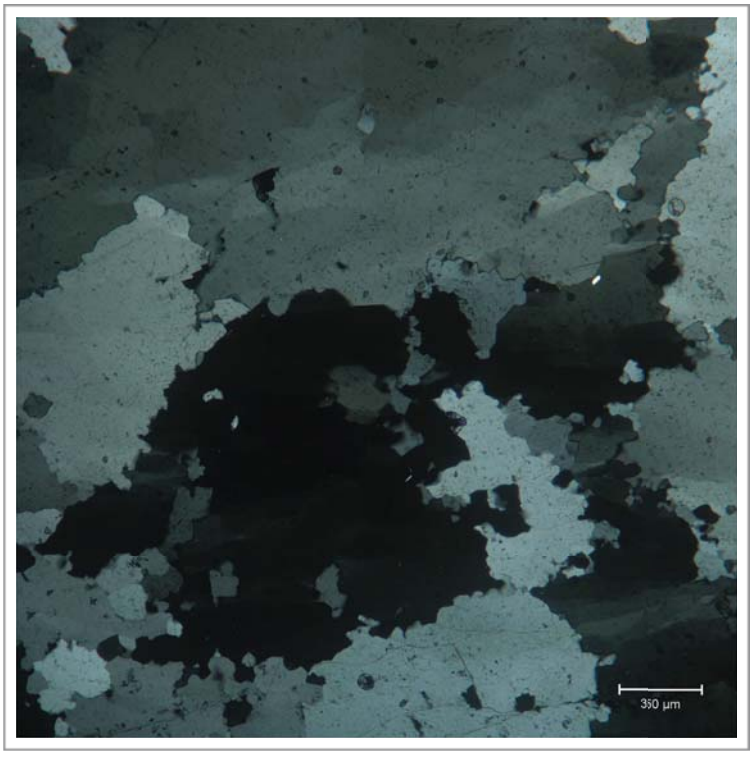

(b)

Figure 7. (a) Reflected light photomicrograph of polished surface of arenitic quartzite particle. (b) Cross-polarized transmitted light photomicrograph of thin section of arenitic quartzite particle.

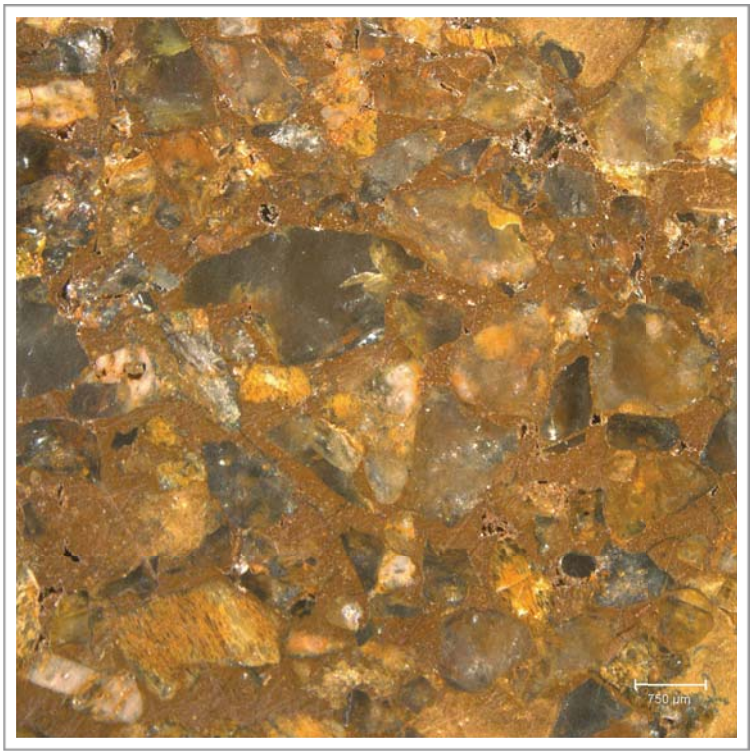

(a)

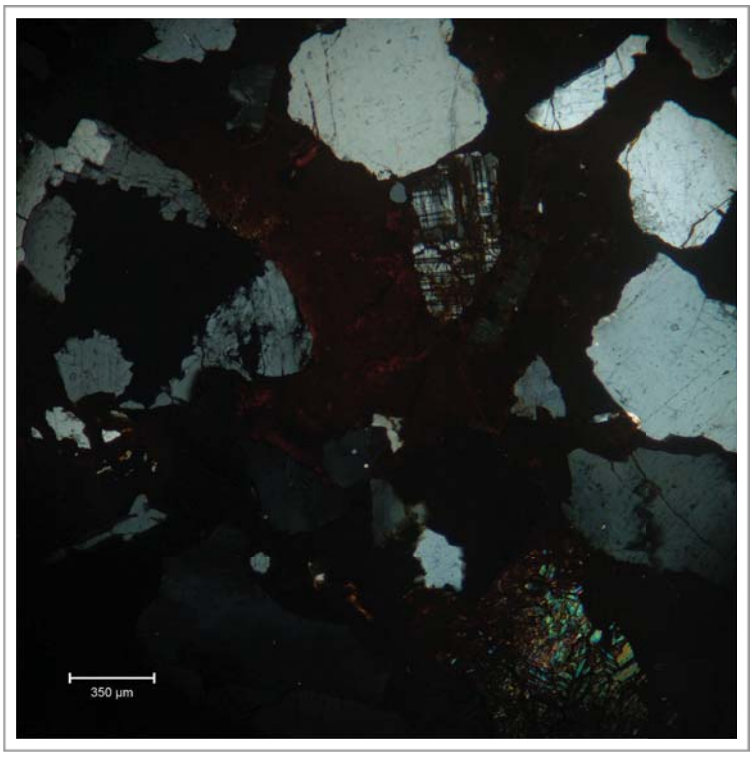

(b)

Figure 8. (a) Reflected light photomicrograph of polished surface of arkosic quartzite particle. (b) Cross-polarized transmitted light photomicrograph of thin section of arkosic quartzite particle.

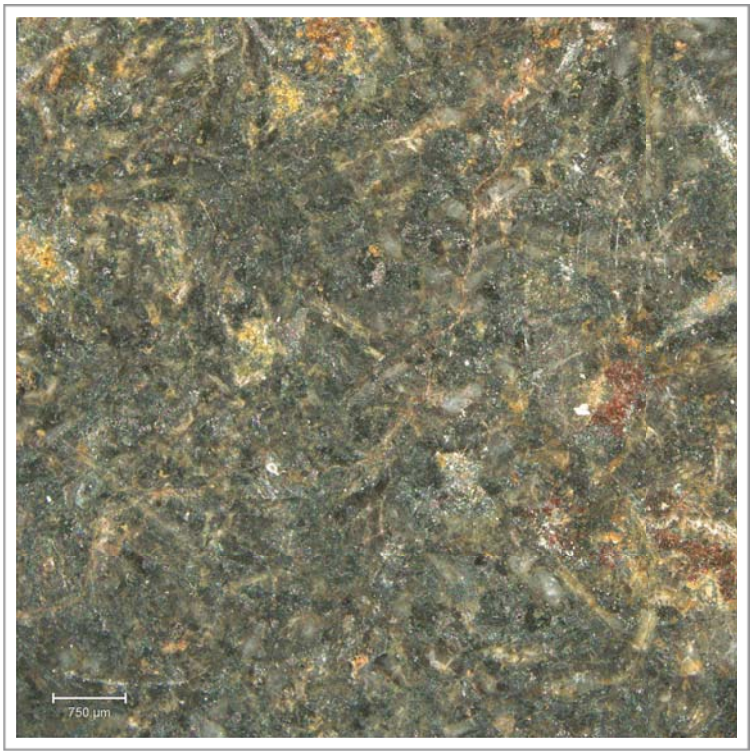

(a)

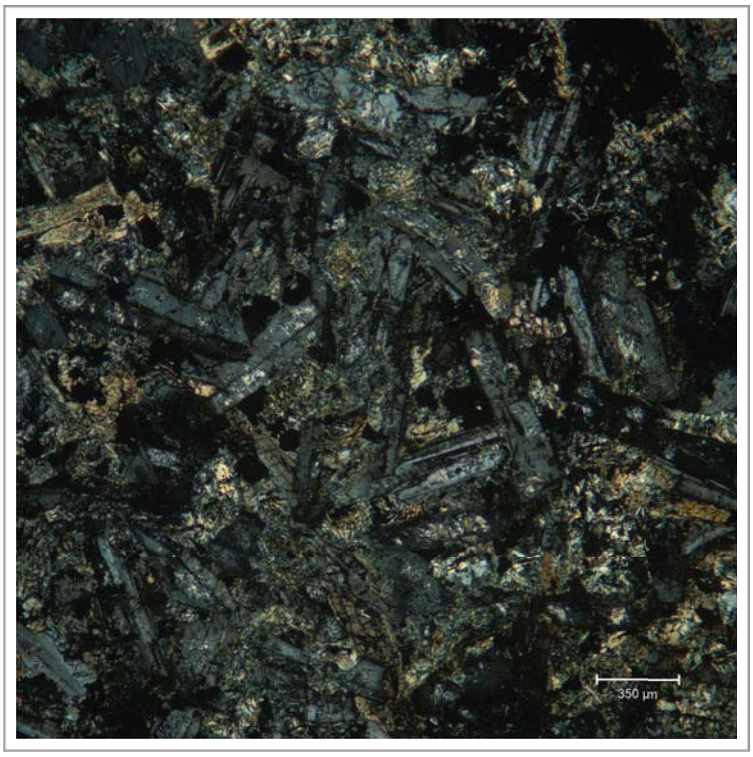

(b)

Figure 9. (a) Reflected light photomicrograph of polished surface of diorite particle. (b) Cross-polarized transmitted light photomicrograph of thin section of diorite particle.

(a)

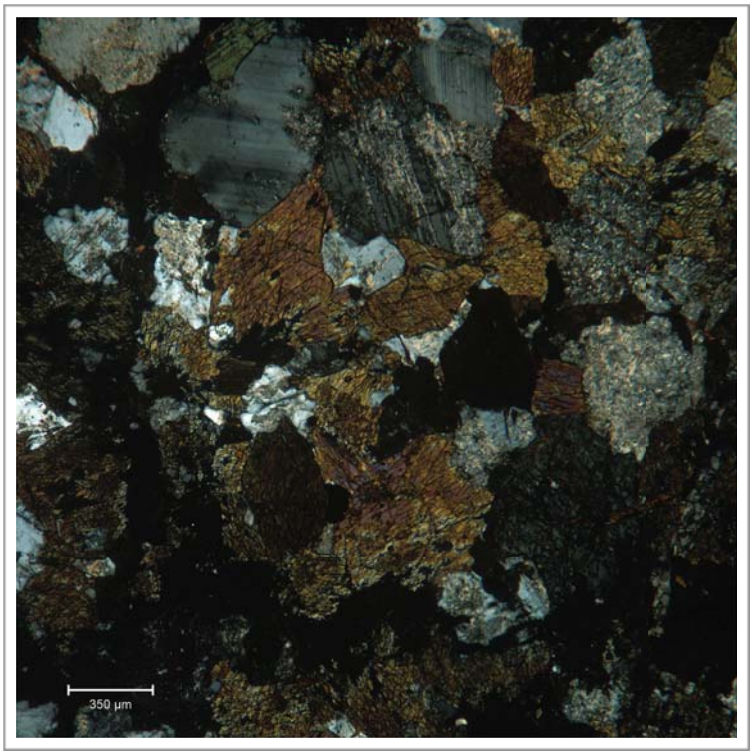

(b)

Figure 10. (a) Reflected light photomicrograph of polished surface of amphibolite particle. (b) Cross-polarized transmitted light photomicrograph of thin section of amphibolite particle.

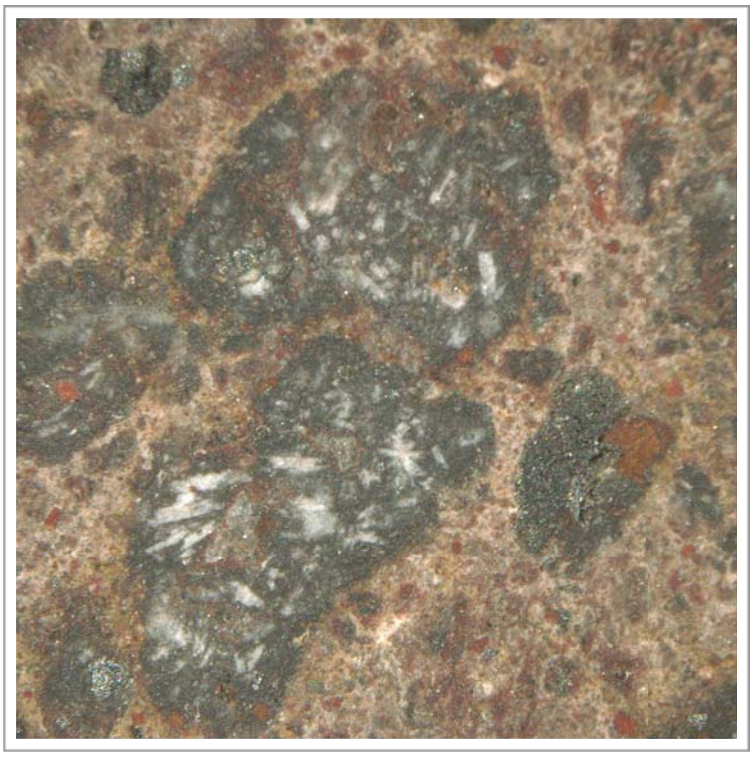

(a)

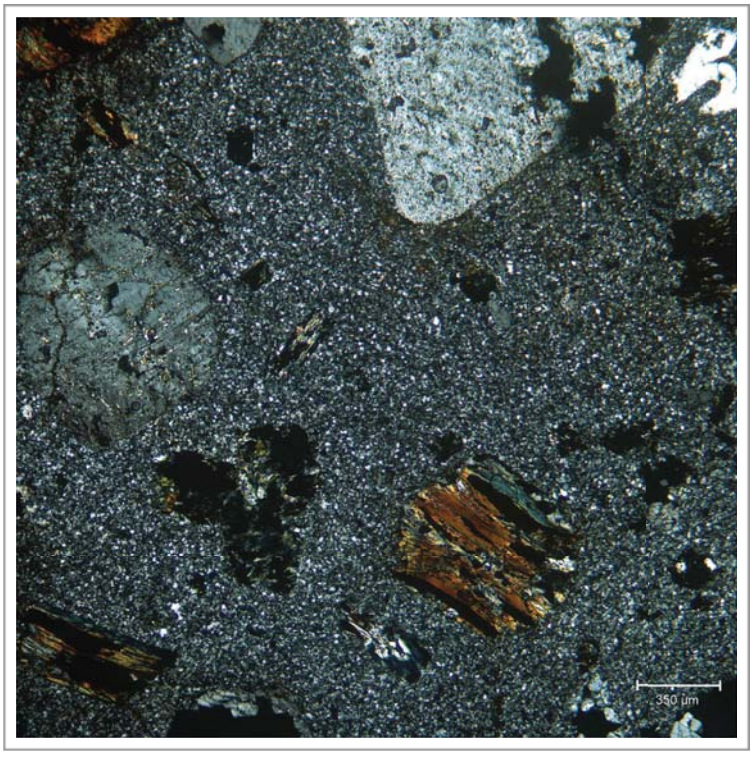

(b)

Figure 11. (a) Reflected light photomicrograph of polished surface of rhyolite particle. (b) Cross-polarized transmitted light photomicrograph of thin section of rhyolite particle.

Kumar Project 11.6.132 Aggregate Petrography

Appendices

Appendix A	**#467 Stone Petrography**
Appendix B	**Concrete Sand Petrography**

Table A1. Kumar 11.6.132 #467 Stone Sieve Analysis (ASTM C136)

Sieve	Wt (kg)	Wt (lb)	Retained	Cumulative	Passin
38 mm (1 ½ in.)	0.275	0.606	1.7%	1.7%	98.3%
25 mm (1 in.)					
19 mm (¾ in.)					
12.5 mm (½ in.)	5.115	11.273	32.0%	33.7%	66.3%
9.5 mm (⅜ in.)	4.405	9.709	27.5%	61.2%	38.8%
4.75 mm (No. 4)	5.910	13.026	36.9%	98.2%	
Fines	0.295	0.650	1.8%	100.0%	
Total	**16.000**	**35.264**	**100.0%**		

Table A2. Constituents of the Kumar 11.6.132 #467 Stone (by number of particles; ASTM C295)

	38 mm (1 ½ in.)		25 mm (1 in.)		19 mm (¾ in.)		12.5 mm (½ in.)		9.5 mm (
Stone Type	No.	%	No.	%	No.	%	No.	%	No.
Red Granite	16	29.6%	43	28.3%	79	48.2%	115	71.4%	156
Black Granite	15	27.8%	43	28.3%	36	22.0%	10	6.2%	4
Leucocratic Granite	5	9.3%	16	10.5%	10	6.1%	13	8.1%	4
White/Buff granite	0	0.0%	16	10.5%	21	12.8%	15	9.3%	21
Arenitic quartzite	8	14.8%	19	12.5%	5	3.0%	2	1.2%	1
Arkosic quartzite	0	0.0%	0	0.0%	5	3.0%	2	1.2%	1
Metagraywacke	8	14.8%	8	5.3%	1	0.6%	0	0.0%	1
Amphibolite/Diorite	2	3.7%	5	3.3%	4	2.4%	0	0.0%	0
Rhyolite	0	0.0%	0	0.0%	1	0.6%	1	0.6%	3
Andesite/Basalt	0	0.0%	2	1.3%	2	1.2%	3	1.9%	3
Total	**54**	**100%**	**152**	**100%**	**164**	**100%**	**161**	**100%**	**194**

Table A3. Constituents of the Kumar 11.6.132 #467 Stone (by normalized weighted percent; ASTM

Stone Type	38 mm (1 ½ in.)	25 mm (1 in.)	19 mm (¾ in.)	12.5 mm (½ in.)	9.5 mm (⅜ in.)	4.75 mm
Red Granite	4.0%	8.8%	3.2%	15.8%	13.8%	
Black Granite	3.8%	8.8%	1.4%	1.4%	0.4%	
Leucocratic Granite	1.3%	3.3%	0.4%	1.8%	0.4%	
White/Buff granite	0.0%	3.3%	0.8%	2.1%	1.9%	
Arenitic quartzite	2.0%	3.9%	0.2%	0.3%	0.1%	
Arkosic quartzite	0.0%	0.0%	0.2%	0.3%	0.1%	
Metagraywacke	2.0%	1.6%	0.0%	0.0%	0.1%	
Amphibolite/Diorite	0.5%	1.0%	0.2%	0.0%	0.0%	
Rhyolite	0.0%	0.0%	0.0%	0.1%	0.3%	
Andesite/Basalt	0.0%	0.4%	0.1%	0.4%	0.3%	
Total	**13.6%**	**31.1%**	**6.6%**	**22.1%**	**17.2%**	

Table B1. Kumar 11.6.132 Sand Sieve Analysis (ASTM C136)

Sieve	Wt (kg)	Wt (lb)	Retained	Cumulative	Passing
4.75 mm (# 4)	0.010	0.022	0.1%	0.1%	99.9%
2.36 mm (# 8)	0.965	2.127	9.7%	9.8%	90.2%
1.18 mm (# 16)	2.625	5.787	26.3%	36.0%	64.0%
600 µm (# 30)	2.765	6.096	27.7%	63.7%	36.3%
300 µm (# 50)	2.545	5.611	25.5%	89.1%	10.9%
150 µm (# 100)	0.880	1.940	8.8%	97.9%	2.1%
75 µm (#200)	0.160	0.353	1.6%	99.5%	0.5%
Pan Fines	0.045	0.099	0.5%	100.0%	0.0%
Total	**9.995**	**22.035**	**100.0%**		

Table B2. Constituents of the Kumar 11.6.132 Sand (by number of particles; ASTM C295)

	4.75 mm (#4)		2.36 mm (#8)		1.18 mm (#16)		600 µm (#30)		300 µm (#50)		150 µm
Rock Type	No.	%	No.	%	No.	%	No.	%	No.	%	No.
Granite	24	92.3%	104	62.7%	96	45.5%	52	32.9%	85	45.0%	56
Leucocratic Granite	1	3.8%	54	32.5%	107	50.7%	104	65.8%	95	50.3%	83
Foliated Granite	0	0.0%	2	1.2%	7	3.3%	1	0.6%	3	1.6%	0
Arenitic quartzite	1	3.8%	3	1.8%	0	0.0%	0	0.0%	0	0.0%	0
Amphibole/Diorite	0	0.0%	0	0.0%	0	0.0%	0	0.0%	5	2.6%	4
Rhyolite	0	0.0%	2	1.2%	1	0.5%	0	0.0%	1	0.5%	6
Andesite/Basalt	0	0.0%	1	0.6%	0	0.0%	0	0.0%	0	0.0%	0
Hematite	0	0.0%	0	0.0%	0	0.0%	0	0.0%	0	0.0%	14
Mica	0	0.0%	0	0.0%	0	0.0%	0	0.0%	0	0.0%	0
Clay	0	0.0%	0	0.0%	0	0.0%	1	0.6%	0	0.0%	1
Total	**26**	**100.0%**	**166**	**100.0%**	**211**	**100.0%**	**158**	**100.0%**	**189**	**100.0%**	**164**

Table B3. Constituents of the Kumar 11.6.132 Sand (by weighted percent; ASTM C2

Rock Type	4.75 mm (#4)	2.36 mm (#8)	1.18 mm (#16)	600 µm (#30)	300 µm (#50)	150 µm (#100)	75 µm (#200)
Granite	0.1%	6.1%	12.0%	9.1%	11.5%	3.0%	0.5%
Leucocratic Granite	0.0%	3.2%	13.4%	18.3%	12.9%	4.5%	0.8%
Foliated Granite	0.0%	0.1%	0.9%	0.2%	0.4%	0.0%	0.0%
Arenitic quartzite	0.0%	0.2%	0.0%	0.0%	0.0%	0.0%	0.0%
Amphibole/Diorite	0.0%	0.0%	0.0%	0.0%	0.7%	0.2%	0.1%
Rhyolite	0.0%	0.1%	0.1%	0.0%	0.1%	0.3%	0.0%
Andesite/Basalt	0.0%	0.1%	0.0%	0.0%	0.0%	0.0%	0.0%
Hematite	0.0%	0.0%	0.0%	0.0%	0.0%	0.8%	0.1%
Mica	0.0%	0.0%	0.0%	0.0%	0.0%	0.0%	0.1%
Clay	0.0%	0.0%	0.0%	0.2%	0.0%	0.1%	0.0%
Total	**0.1%**	**9.7%**	**26.4%**	**27.8%**	**25.6%**	**8.8%**	**1.6%**

APPENDIX B

Sand Castle Test Results

Crack Box Test #12 – Vaughan Filter Binder Test Results

Introduction

Samples were taken from the C-33 mix sand used for the Crack Box Test #12 and tested with the Vaughan Filter Binder Test to look for cementation. The sands tested were unused sand from the stock pile (Pre-Test 12)and sand that had been compacted into the crack box previously (Post-Test 12). The intention was to discern whether there was cementation possible of the sand, and also whether there was a significant difference in the potential for cementation after compaction.

Test Procedure and Test Materials

From the two sample sands, 8 specimens were prepared. All of the samples were compacted with a vibratory hammer according to ASTM D 7382 (wet-method, compacted at saturation) to determine the maximum density. The samples were oven dried until constant mass was reached (96 hours) and were allowed to cool for a period of 24 hours in ambient conditions before being tested. The moisture content and maximum density were recorded.

A water level of 1” above the base of the specimens was utilized for the first 20 minutes of the test. If failure did not occur during that time, the water level was raised to 2”. Failure was defined as the point where the sample disintegrates into the water. Two failure modes were observed for the tests run, splitting and toppling. Splitting failure occurs when the sample splits in half (or into sections) and falls off the test platform into the water. Splitting failure is considered an acceptable failure mode. The other failure mode is toppling; in this case, the sample leans over to one side and slowly disintegrates into the water. This is not considered a valid failure mode, and could possibly indicate either that the testing platform was not perfectly level or that there were significant internal variations in the compaction of the specimen.

The test is split into 4 time increments; T_1 through T_4. T_1 occurs after the specimen has been wetted, and is the time taken for the erosion of the sides of the sample reaches the water line (approximately 1 inch from the test plate and bottom of the sample). T_2 is defined as the time when the water is observed to have covered approximately 50% of the top of the specimen (full absorption). T_3 is the time when the disintegration of the sides of the specimen has reached half way up the sample (approximately 2.25 inches). T4 is the time of failure. The time is recorded as duration, in minutes and seconds, from the moment that the water reaches the 1 inch mark.

Crack Box Test #12 – Vaughan Filter Binder Test Results

Test Results

Table 1 provides a summary of results for the specimens. The outliers (T4 values significantly different that other tests for the same sample material) and the invalid failure modes are highlighted; those values were not used in the calculations.

				Time (sec)				
Sample	Plate	M%	γd (pcf)	T1	T2	T3	T4	Failure Mode
Post 12	J	12.3	112.9	18	162*		1208	Splitting
Post 12	I	12.4	114.1	20	124*		157	Splitting
Post 12	M	13.0	113.5	17			106	Splitting
Post 12	L	13.0	113.7	17	153*		204	Splitting
Pre 12	9	12.2	110.8	19	110		193	Splitting
Pre 12	I	12.5	109.7	18			92	Splitting
Pre 12	D	12.6	110.2	19			73	Toppling
Pre 12	13	13.3	108.8	14			62	Toppling

Table 1: Summary of Sand Castle Test Results

**indicates water level was raised to 2 inches during test*

Figure 1 shows the Pre-Test 12 and the Post-Test 12 material classification with respect to cementation potential according to the Modified Sand Castle Test method (Rinehart, August 2012). Both sample materials are Class 1, which means they have the lowest possible potential for cementation, respectively.

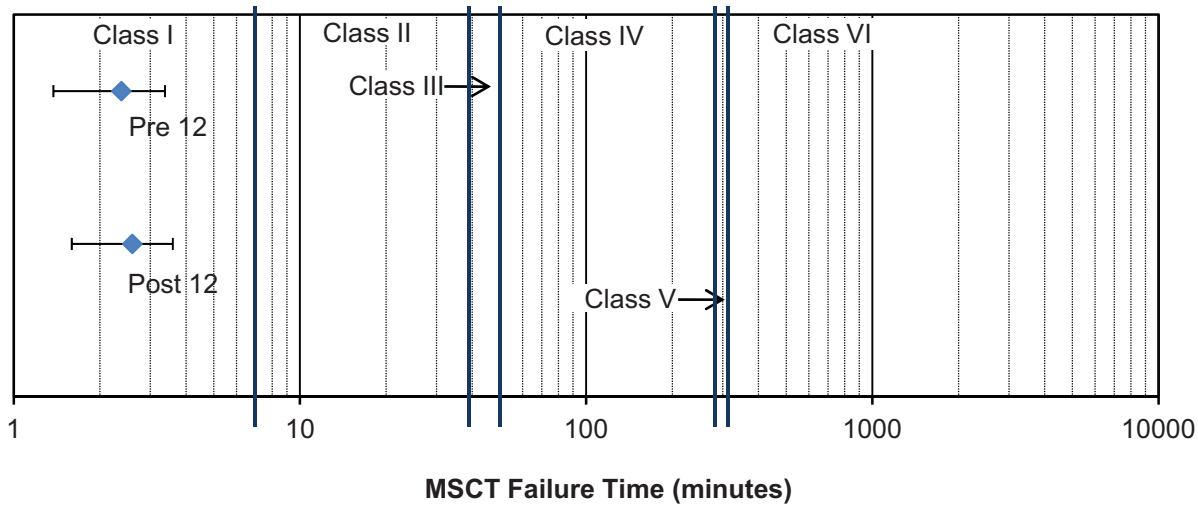

Figure 1: MSCT Failure times

Crack Box Test #12 – Vaughan Filter Binder Test Results

Figures 2 through 22 show the specimens at various stages of the Sand Castle Test. Due to the fast and sudden nature of the test stages and failures, it was not possible to capture all of the stages for each of the specimens.

The figures are shown in Appendix A. The data sheets used for the density testing and for the Sand Castle Tests are also included in Appendix A. A spreadsheet was used to calculate the average failure times for each of the samples; a copy of the calculation spreadsheet is in Appendix A.

References

Rinehart, R. V. (August 2012). *Development of a Test to Determine Cementation Potential of Embankment Dam Granular Filter Material – Results of Phase III Research.* Denver, CO: US Dept. of the Interior Technical Service Center.

Appendix A – Figures and Calculations

Sample	Plate	M%	γ_d (pcf)	Time (sec) T_1	T_2	T_3	T_4	Failure Mode
Post 12	J	12.3	112.9	18	162		1208	Splitting
Post 12	I	12.4	114.1	20	124		157	Splitting
Post 12	M	13.0	113.5	17			106	Splitting
Post 12	L	13.0	113.7	17	153		204	Splitting
Pre 12	9	12.2	110.8	19	110		193	Splitting
Pre 12	I	12.5	109.7	18			92	Splitting
Pre 12	D	12.6	110.2	19			73	Toppling
Pre 12	13	13.3	108.8	14			62	Toppling

Check % Diff	**Post 12**		γ_d (pcf)	**All**
112.9	114.1	max	114.1	max
114.1	112.9	min	108.8	min
113.5	1.1	% diff	4.6	% diff
113.7				

Check % Diff	**Pre 12**		M%	**All**
110.8	110.8	max	12.7	Average
109.7	108.8	min	0.4	std dev
110.2	1.8	% diff	3.1	COV
108.8				

Test Average Values

all tests

	T_4 (sec)	T_4 (min)	γ_d (pcf)
Post 12	418.8	7.0	113.6
Pre 12	105.0	1.8	109.9

Test Average Values

excluding invalid failures and outliers

	T_4 (sec)	T_4 (min)	γ_d (pcf)	
Post 12	155.7	2.6	113.8	1
Pre 12	142.5	2.4	110.3	2

	Avg	High	Low	+error	-error
Post 12	2.6	3.4	1.8	0.8	0.8
Pre 12	2.4	3.2	1.5	0.8	0.8

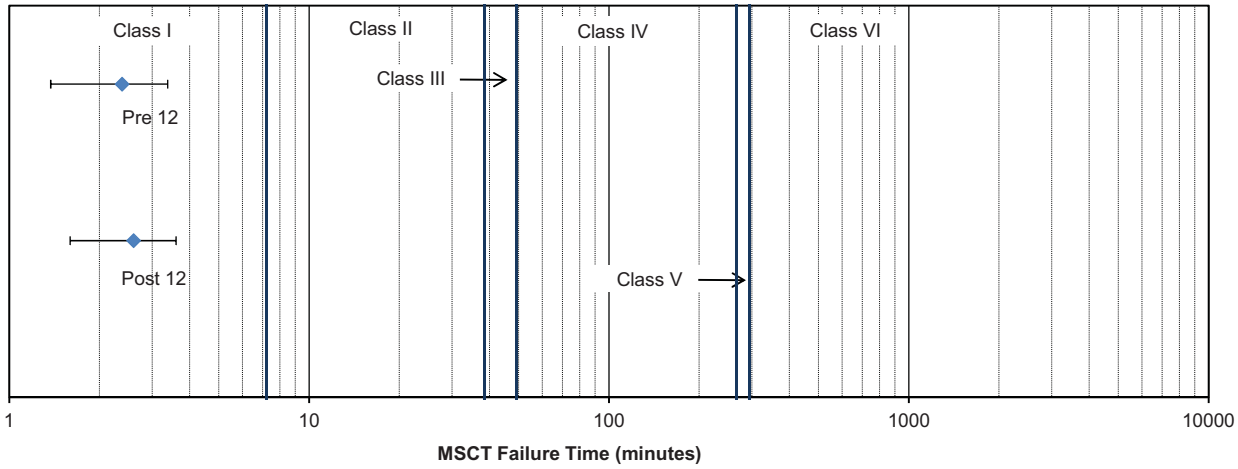

Appendix A – Figures and Calculations

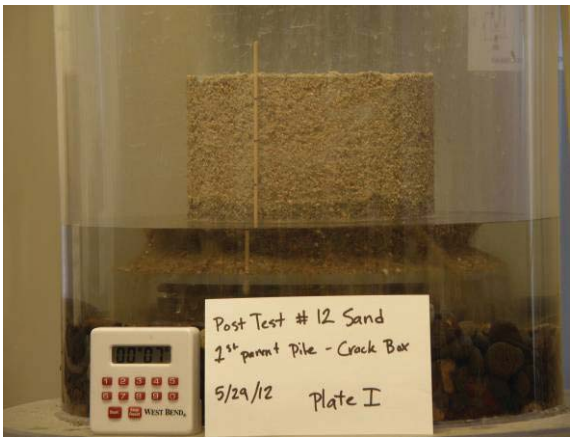

Figure 2: Post Test 12 Plate I T_0

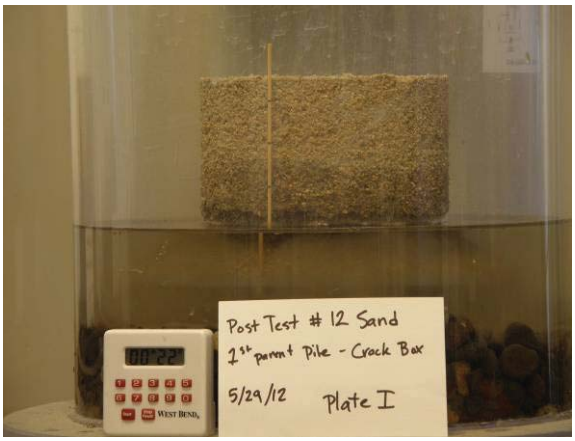

Figure 3: Post Test 12 Plate I T_1

Figure 4: Post Test 12 Plate I T_2

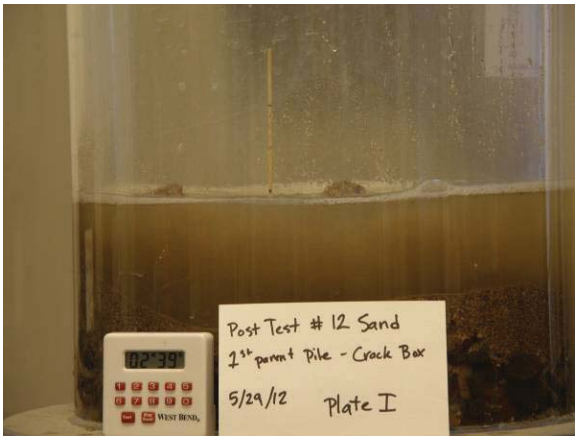

Figure 5: Post Test 12 Plate I T_4

Figure 6: Post Test 12 Plate J T_0

Figure 7: Post Test 12 Plate J T_4

Appendix A – Figures and Calculations

Figure 8: Post Test 12 Plate L T_0

Figure 9: Post Test 12 Plate L T_4

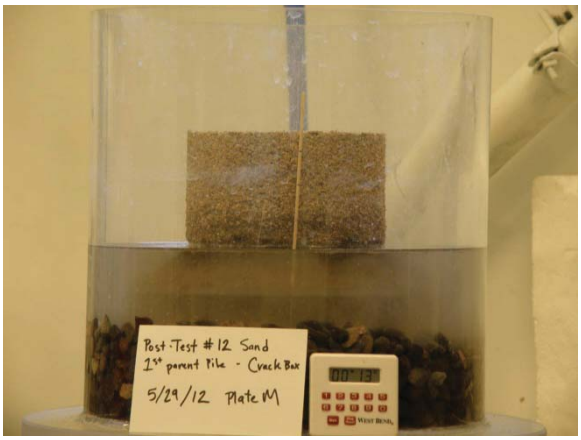

Figure 10: Post Test 12 Plate M T_1

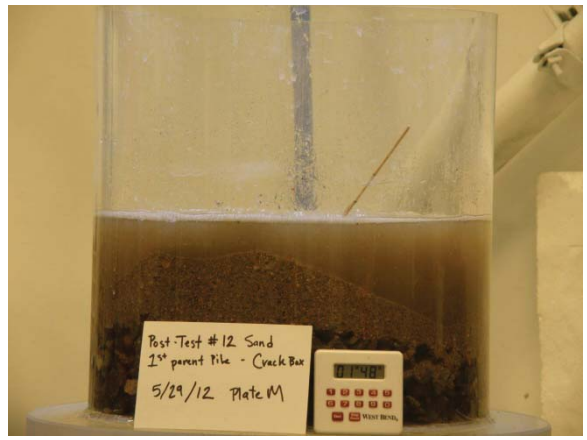

Figure 11: Post Test 12 Plate M T_4

Figure 12: Post Test 12 Plate 9 T_1

Figure 13: Post Test 12 Plate 9 T_2

Figure 14: Post Test 12 Plate 9 T_4

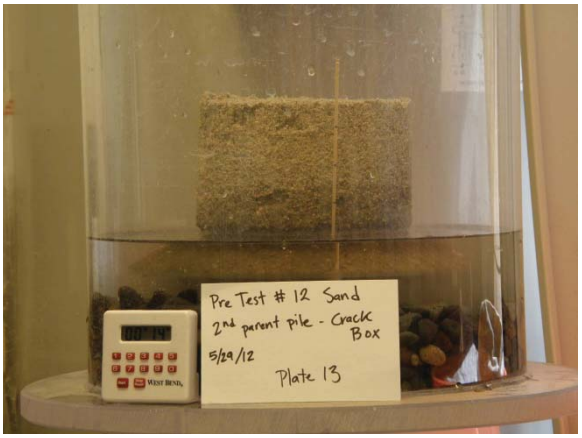

Figure 15: Post Test 12 Plate 13 T_1

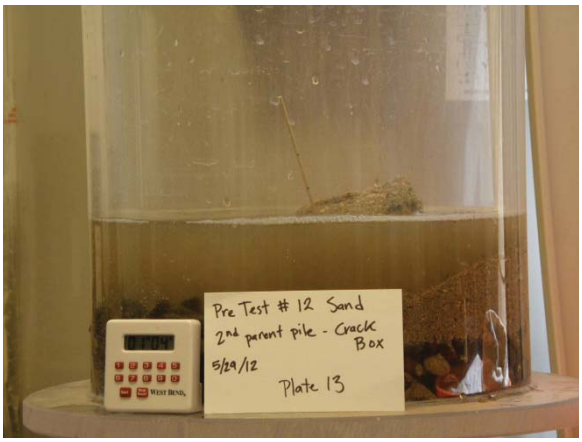

Figure 16: Post Test 12 Plate 13 T_4

Figure 17: Post Test 12 Plate D T_0

Figure 18: Post Test 12 Plate D T_1

Figure 19: Post Test 12 Plate D T_4

Appendix A – Figures and Calculations

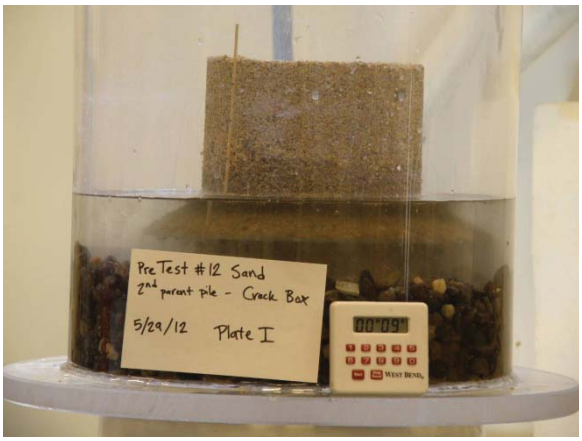

Figure 20: Post Test 12 Plate I T_0

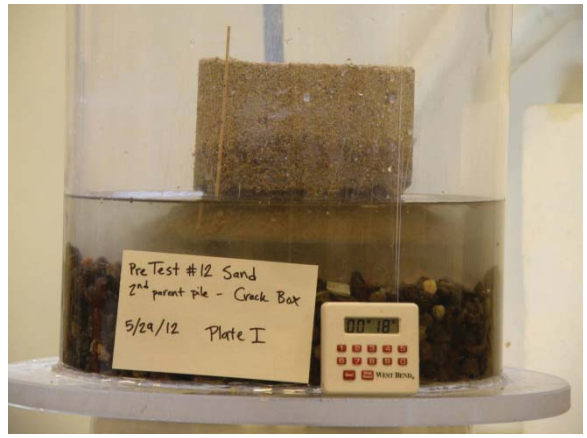

Figure 21: Post Test 12 Plate I T_1

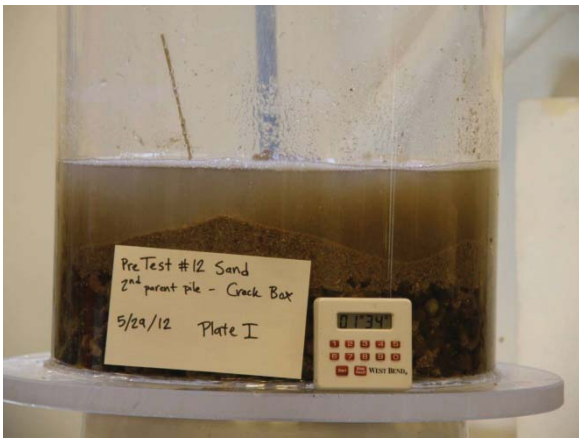

Figure 22: Post Test 12 Plate I T_4

VAUGHAN (SAND CASTLE) FILTER BINDER TEST

SAMPLE NO.	PROJECT	MATERIAL
Pre-Test #12 Sand	Crack - Box	2nd Parent Pile
TESTED BY / DATE	SPECIMEN DIMENSIONS in. / cm	

Specimen #	hr	min	sec	Remarks:
Plate I, R-8		2	43	Splitting failure prior to full absorption (90-)
Time to erosion line to reach water line[a]			18	
Time to full absorption[1]				
Time to 50% Disintegration[2]				
Time to 100% Disintegration		1	32	S_r = 58°, 56°, 56°
Plate D, H-22		2	48	Toppling failure
Time to erosion line reaching water line			19	
Time to full absorption[1]				
Time to 50% Disintegration[2]				
Time to 100% Disintegration		1	13	S_r = N/A
Plate 9, R-22				Splitting failure
Time to erosion line to reach water line			19	
Time to full absorption[1]	1		50	
Time to 50% Disintegration[2]				(90-)
Time to 100% Disintegration	3		13	S_r = 59°, 58°, 59°, 61°
Plate 13, R-1		2	59	Toppling failure
Time to erosion line to reach water line			14	
Time to full absorption[1]				
Time to 50% Disintegration[2]				
Time to 100% Disintegration	1		02	S_r = N/A

[1] Time when signs of water are visible over ~50% of top surface of specimen

[2] Time when the erosion line has progressed half way up specimen

a) initial = 1"

VAUGHAN (SAND CASTLE) FILTER BINDER TEST

SAMPLE NO.	PROJECT	MATERIAL
Post-Test #12 Sand	Crack-Box	1st Parent Pile
TESTED BY: BNJ — DATE: 5/29/12	SPECIMEN DIMENSIONS in. / cm	

Specimen # Plate M #14-5 →

	hr	min	sec
Time to erosion line to reach water line[a]		17	
Time to full absorption[1]	~~1~~	~~46~~	
Time to 50% Disintegration[2]			
Time to 100% Disintegration	1	46	

Remarks: Splitting failure before absorption, very near full absorption (90-) S_r = 56°, 62°, 60°, 56°

Specimen # Plate L A2 1:15

	hr	min	sec
Time to erosion line reaching water line		17	
Time to full absorption[1]	2	33	
Time to 50% Disintegration[2]			
Time to 100% Disintegration	3	24	

Remarks: Splitting failure (90-) S_r = 58°, 58°, 56°, 58°

Specimen # Plate J MD-2 1:21

	hr	min	sec
Time to erosion line to reach water line		18	
Time to full absorption[1]	2	42	
Time to 50% Disintegration[2]			
Time to 100% Disintegration	20	08	

Remarks: Splitting failure (90-) S_r = 59°, 60°, 58°, 58°

Specimen # Plate I A-1 1:45

	hr	min	sec
Time to erosion line to reach water line		20	
Time to full absorption[1]	2	04	
Time to 50% Disintegration[2]			
Time to 100% Disintegration	2	37	

Remarks: Splitting failure (90-) S_r = 60°, 56°, 54°, 58°

[1] Time when signs of water are visible over ~50% of top surface of specimen

[2] Time when the erosion line has progressed half way up specimen

a) initial = 1"

MAXIMUM INDEX UNIT WEIGHT VIA VIBRATING HAMMER (ASTM 7382)

SAMPLE NO.	PROJECT	FEATURE
Pre-Test #12 Sand	Crack-Box	2nd Parent Pile

% GRAVEL	%SAND	%FINES	MAX. PARTICLE SIZE

TESTED BY	DATE	COMPUTED BY	DATE	CHECKED BY	DATE
BNJ	5/24/12	BNJ	5/30/12	Rinehart	5/30/12

NOMINAL VOLUME OF MOLD [X] 0.075 ft^3 [ ] 0.5 ft^3

MAXIMUM INDEX UNIT WEIGHT DETERMINATION (ASTM D7382)

	Circle Units	DRY METHOD	WET METHOD
MOLD NO.			
SPECIMEN NO.			
(1) Mass of Mold and Soil	g / lbm		23.640
(2) Mass of Mold	g / lbm		14.384
(3) Mass of Dry Soil = (2)-(1)	g / lbm		
(4) Mass of Wet Soil = (1)-(1)	g / lbm		9.256 ✓
(5) Mass of Dry Soil = (4)/[1+(14)/100]	g / lbm		8.228 ✓
(6) Volume of Mold*	cm^3 / ft^3		0.075 (nominal)
(7) Soil Unit Weight = (3)/(4)**	g/cm^3 / lbf/ft^3		109.7 ✓

MOISTURE CONTENT DETERMINATION

(8) Container No.		R-8 / Plate I
(9) Mass of container + wet soil	g / lbm	12.148
(10) Mass of container + dry soil	g / lbm	11.126
(11) Mass of container	g / lbm	2.982
(12) Mass of water = (9)-(10)	g / lbm	1.022 ✓
(13) Mass of dry soil = (10)-(11)	g / lbm	8.144 ✓
(14) Moisture content = [(12)/(13)]x100	%	12.5 ✓

*Values obtained from Designation USBR 1010

** implies 1 lbm = 1 lbf

REMARKS: 5/28/12 11.122 lb
= 11.126 lb

MAXIMUM INDEX UNIT WEIGHT VIA VIBRATING HAMMER (ASTM 7382)

SAMPLE NO.	PROJECT	FEATURE
Pre-Test #12 Sand	Crack- Box	2nd parent Pile

% GRAVEL	%SAND	%FINES	MAX. PARTICLE SIZE

TESTED BY	DATE	COMPUTED BY	DATE	CHECKED BY	DATE
BNJ	5/24/12	BNJ	5/30/12	Rinehart	5/30/12

NOMINAL VOLUME OF MOLD ☒ 0.075 ft^3 ☐ 0.5 ft^3

MAXIMUM INDEX UNIT WEIGHT DETERMINATION (ASTM D7382)

	Circle Units	DRY METHOD	WET METHOD
MOLD NO.			
SPECIMEN NO.			
(1) Mass of Mold and Soil	g / lbm		23.690
(2) Mass of Mold	g / lbm		14.384
(3) Mass of Dry Soil = (2)-(1)	g / lbm		
(4) Mass of Wet Soil = (1)-(1)	g / lbm		9.306 ✓
(5) Mass of Dry Soil = (4)/[1+(14)/100]	g / lbm		8.265 ✓
(6) Volume of Mold*	cm^3 / ft^3		.075 (nominal)
(7) Soil Unit Weight = (3)/(4)**	g/cm^3 / lbf/ft^3		110.2 ✓

MOISTURE CONTENT DETERMINATION

(8) Container No.		H-22 / Plate D
(9) Mass of container + wet soil	g / lbm	12.158
(10) Mass of container + dry soil	g / lbm	11.126
(11) Mass of container	g / lbm	2.940
(12) Mass of water = (9)-(10)	g / lbm	1.032 ✓
(13) Mass of dry soil = (10)-(11)	g / lbm	8.186 ✓
(14) Moisture content = [(12)/(13)]x100	%	12.6 ✓

*Values obtained from Designation USBR 1010

** implies 1 lbm = 1 lbf

REMARKS: 5/28/12 = 11.122
= 11.126 lb

MAXIMUM INDEX UNIT WEIGHT VIA VIBRATING HAMMER (ASTM 7382)

SAMPLE NO.	PROJECT	FEATURE
Pre-Test #12 Sand	Crack - Box	2nd Parent Pile

% GRAVEL	%SAND	%FINES	MAX. PARTICLE SIZE

TESTED BY	DATE	COMPUTED BY	DATE	CHECKED BY	DATE
BNJ	5/24/12	BNJ	5/30/12	Kinehart	5/30/12

NOMINAL VOLUME OF MOLD ☒ 0.075 ft^3 ☐ 0.5 ft^3

MAXIMUM INDEX UNIT WEIGHT DETERMINATION (ASTM D7382)

	Circle Units	DRY METHOD	WET METHOD
MOLD NO.			
SPECIMEN NO.			
(1) Mass of Mold and Soil	g / lbm		23.704
(2) Mass of Mold	g / lbm		14.384
(3) Mass of Dry Soil = (2)-(1)	g / lbm		
(4) Mass of Wet Soil = (1)-(1)	g / lbm		9.320 ✓
(5) Mass of Dry Soil = (4)/[1+(14)/100]	g / lbm		8.307 ✓
(6) Volume of Mold*	cm^3 / ft^3		0.075 (nominal)
(7) Soil Unit Weight = (3)/(4)**	g/cm^3 / lbf/ft^3		110.8 ✓

MOISTURE CONTENT DETERMINATION

(8) Container No.		R-22 / Plate 9
(9) Mass of container + wet soil	g / lbm	12.160
(10) Mass of container + dry soil	g / lbm	11.158
(11) Mass of container	g / lbm	2.926
(12) Mass of water = (9)-(10)	g / lbm	1.002 ✓
(13) Mass of dry soil = (10)-(11)	g / lbm	8.232 ✓
(14) Moisture content = [(12)/(13)]x100	%	12.2 ✓

*Values obtained from Designation USBR 1010

** implies 1 lbm = 1 lbf

REMARKS: 5/28/12 = 11.154 lb
= 11.158 lb

MAXIMUM INDEX UNIT WEIGHT VIA VIBRATING HAMMER (ASTM 7382)

SAMPLE NO.	PROJECT	FEATURE
Pre-Test #12 Sand	Crack - Box	2nd parent pile

% GRAVEL	%SAND	%FINES	MAX. PARTICLE SIZE

TESTED BY	DATE	COMPUTED BY	DATE	CHECKED BY	DATE
BNJ	5/24/12	BNJ	5/30/12	Rinehart	5/30/12

NOMINAL VOLUME OF MOLD ☒ 0.075 ft^3 ☐ 0.5 ft^3

MAXIMUM INDEX UNIT WEIGHT DETERMINATION (ASTM D7382)

	Circle Units	DRY METHOD	WET METHOD
MOLD NO.			
SPECIMEN NO.			
(1) Mass of Mold and Soil	g / lbm		23.632
(2) Mass of Mold	g / lbm		14.384
(3) Mass of Dry Soil = (2)-(1)	g / lbm		
(4) Mass of Wet Soil = (1)-(1)	g / lbm		9.248 ✓
(5) Mass of Dry Soil = (4)/[1+(14)/100]	g / lbm		8.162 ✓
(6) Volume of Mold*	cm^3 / ft^3		0.075 (nominal)
(7) Soil Unit Weight = (3)/(4)**	g/cm^3 / lbf/ft^3		108.8 ✓

MOISTURE CONTENT DETERMINATION

(8) Container No.		R-1 / Plate 13
(9) Mass of container + wet soil	g / lbm	12.038
(10) Mass of container + dry soil	g / lbm	10.970
(11) Mass of container	g / lbm	2.962
(12) Mass of water = (9)-(10)	g / lbm	1.068 ✓
(13) Mass of dry soil = (10)-(11)	g / lbm	8.008 ✓
(14) Moisture content = [(12)/(13)]x100	%	13.3 ✓

*Values obtained from Designation USBR 1010

** implies 1 lbm = 1 lbf

REMARKS: 5/28/12 = 10.968
= 10.970

MAXIMUM INDEX UNIT WEIGHT VIA VIBRATING HAMMER (ASTM 7382)

SAMPLE NO.	PROJECT	FEATURE
Post-Test #12 Sand	Crack-Box	1st Parent Pile

% GRAVEL	%SAND	%FINES	MAX. PARTICLE SIZE

TESTED BY	DATE	COMPUTED BY	DATE	CHECKED BY	DATE
BNJ	5/24/12	BNJ	5/30/12	Rinehart	5/30/12

NOMINAL VOLUME OF MOLD ☒ 0.075 ft^3 ☐ 0.5 ft^3

MAXIMUM INDEX UNIT WEIGHT DETERMINATION (ASTM D7382)

	Circle Units	DRY METHOD	WET METHOD
MOLD NO.			
SPECIMEN NO.			
(1) Mass of Mold and Soil	g / lbm		24.000
(2) Mass of Mold	g / lbm		14.384
(3) Mass of Dry Soil = (2)-(1)	g / lbm		
(4) Mass of Wet Soil = (1)-(1)	g / lbm		9.616 ✓
(5) Mass of Dry Soil = (4)/[1+(14)/100]	g / lbm		8.510 ✓
(6) Volume of Mold*	cm^3 / ft^3		0.075 (nominal)
(7) Soil Unit Weight = (3)/(4)**	g/cm^3 / lbf/ft^3		113.5 ✓

MOISTURE CONTENT DETERMINATION

(8) Container No.		14.5 / Plate M
(9) Mass of container + wet soil	g / lbm	14.072
(10) Mass of container + dry soil	g / lbm	12.986
(11) Mass of container	g / lbm	4.610
(12) Mass of water = (9)-(10)	g / lbm	1.086 ✓
(13) Mass of dry soil = (10)-(11)	g / lbm	8.376 ✓
(14) Moisture content = [(12)/(13)]x100	%	13.0 ✓

*Values obtained from Designation USBR 1010

**implies 1 lbm = 1 lbf

REMARKS: 5/28/12 = 12.984
= 12.986

MAXIMUM INDEX UNIT WEIGHT VIA VIBRATING HAMMER (ASTM 7382)

SAMPLE NO.	PROJECT	FEATURE
Post-Test #12 Sand	Crack-Box	1st parent Pile

% GRAVEL	%SAND	%FINES	MAX. PARTICLE SIZE

TESTED BY	DATE	COMPUTED BY	DATE	CHECKED BY	DATE
BNJ	5/24/12	BNJ	5/30/12	Rinehart	5/30/12

NOMINAL VOLUME OF MOLD ☒ 0.075 ft^3 ☐ 0.5 ft^3

MAXIMUM INDEX UNIT WEIGHT DETERMINATION (ASTM D7382)

	Circle Units	DRY METHOD	WET METHOD
MOLD NO.			
SPECIMEN NO.			
(1) Mass of Mold and Soil	g / lbm		24.024
(2) Mass of Mold	g / lbm		14.384
(3) Mass of Dry Soil = (2)-(1)	g / lbm		
(4) Mass of Wet Soil = (1)-(1)	g / lbm		9.640 ✓
(5) Mass of Dry Soil = (4)/[1+(14)/100]	g / lbm		8.531 ✓
(6) Volume of Mold*	cm^3 / ft^3		.075 (nominal)
(7) Soil Unit Weight = (3)/(4)**	g/cm^3 / lbf/ft^3		113.7 ✓

MOISTURE CONTENT DETERMINATION

(8) Container No.		A2 / Plate L
(9) Mass of container + wet soil	g / lbm	14.048
(10) Mass of container + dry soil	g / lbm	12.954
(11) Mass of container	g / lbm	4.514
(12) Mass of water = (9)-(10)	g / lbm	1.094 ✓
(13) Mass of dry soil = (10)-(11)	g / lbm	8.440 ✓
(14) Moisture content = [(12)/(13)]x100	%	13.0 ✓

*Values obtained from Designation USBR 1010

** implies 1 lbm = 1 lbf

REMARKS: 5/28/12 = 12.950
= 12.954

MAXIMUM INDEX UNIT WEIGHT VIA VIBRATING HAMMER (ASTM 7382)

SAMPLE NO.	PROJECT	FEATURE
Post-test #12 Sand	Crack - Box	1st Parent Pile

% GRAVEL	%SAND	%FINES	MAX. PARTICLE SIZE

TESTED BY	DATE	COMPUTED BY	DATE	CHECKED BY	DATE
BNJ	5/24/12	BNJ	5/30/12	Rinehart	5/30/12

NOMINAL VOLUME OF MOLD ☒ 0.075 ft^3 ☐ 0.5 ft^3

MAXIMUM INDEX UNIT WEIGHT DETERMINATION (ASTM D7382)

	Circle Units	DRY METHOD	WET METHOD
MOLD NO.			
SPECIMEN NO.			
(1) Mass of Mold and Soil	g / lbm		23.892
(2) Mass of Mold	g / lbm		14.384
(3) Mass of Dry Soil = (2)-(1)	g / lbm		
(4) Mass of Wet Soil = (1)-(1)	g / lbm		9.508 ✓
(5) Mass of Dry Soil = (4)/[1+(14)/100]	g / lbm		8.467 ✓
(6) Volume of Mold*	cm^3 / ft^3		.075 (nominal)
(7) Soil Unit Weight = (3)/(4)**	g/cm^3 / lbf/ft^3		112.9 ✓

MOISTURE CONTENT DETERMINATION

(8) Container No.		MD-2 / Plate J
(9) Mass of container + wet soil	g / lbm	14.114
(10) Mass of container + dry soil	g / lbm	13.080
(11) Mass of container	g / lbm	4.704
(12) Mass of water = (9)-(10)	g / lbm	1.034 ✓
(13) Mass of dry soil = (10)-(11)	g / lbm	8.376 ✓
(14) Moisture content = [(12)/(13)]x100	%	12.3 ✓

*Values obtained from Designation USBR 1010

**implies 1 lbm = 1 lbf

REMARKS: 5/28/12 = 13.078
= 13.080

MAXIMUM INDEX UNIT WEIGHT VIA VIBRATING HAMMER (ASTM 7382)

SAMPLE NO.	PROJECT	FEATURE
Post-Test #12 Sand	Crack-Box	1st parent pile

% GRAVEL	%SAND	%FINES	MAX. PARTICLE SIZE

TESTED BY	DATE	COMPUTED BY	DATE	CHECKED BY	DATE
BNJ	5/24/12	BNJ	5/30/12	Rinehart	5/30/12

NOMINAL VOLUME OF MOLD ☒ 0.075 ft^3 ☐ 0.5 ft^3

MAXIMUM INDEX UNIT WEIGHT DETERMINATION (ASTM D7382)

	Circle Units	DRY METHOD	WET METHOD
MOLD NO.			
SPECIMEN NO.			
(1) Mass of Mold and Soil	g / lbm		24.006
(2) Mass of Mold	g / lbm		14.384
(3) Mass of Dry Soil = (2)-(1)	g / lbm		
(4) Mass of Wet Soil = (1)-(1)	g / lbm		9.622 ✓
(5) Mass of Dry Soil = (4)/[1+(14)/100]	g / lbm		8.560 ✓
(6) Volume of Mold*	cm^3 / ft^3		0.075 (nominal)
(7) Soil Unit Weight = (3)/(4)**	g/cm^3 / lbf/ft^3		114.1 ✓

MOISTURE CONTENT DETERMINATION

(8) Container No.		A1 / Rack F
(9) Mass of container + wet soil	g / lbm	14.260
(10) Mass of container + dry soil	g / lbm	13.204
(11) Mass of container	g / lbm	4.708
(12) Mass of water = (9)-(10)	g / lbm	1.056 ✓
(13) Mass of dry soil = (10)-(11)	g / lbm	8.496 ✓
(14) Moisture content = [(12)/(13)]x100	%	12.4 ✓

*Values obtained from Designation USBR 1010

**implies 1 lbm = 1 lbf

REMARKS: 5/28/12 = 13.200
= 13.204

APPENDIX C

Silt Physical Property Results

7-1391 (12-86)
Bureau of Reclamation

LABORATORY COMPACTION TEST

Designation USBR _____ - __ __

SAMPLE NO.	PROJECT	FEATURE
Crank Box Silt		
TESTED BY: BACA — DATE: 4/23/12	COMPUTED BY: BACA — DATE: 4/28/12	CHECKED BY — DATE

Blows per layer 25 No. of layers 3 Height of drop 18" in

Mass of tamping rod 5.5 lbm Volume of mold 0.0499 ft^3

Specimen No.								
Wet unit weight determinations								
Water added	(g or ml)	280	350	420	490	560	630	
Mass of mold + wet soil	(lbm)	12.924	13.214	13.328	13.444	13.280	13.044	
Mass of mold	(lbm)	7.166	7.166	7.166	7.166	7.166	7.166	
Mass of wet soil	(lbm)	5.758	6.048	6.162	6.278	6.114	5.878	
Wet unit weight	(lbf/ft^3)	115.4	121.2	123.5	125.8	122.5	117.8	
Penetration resistance determinations								
Needle No.		40	40	20	10	4	2	
Area of needle	(in^2)	1/40	1/40	1/20	1/10	1/4	1/2	
Penetrometer reading	(lbf) 1	89	71	70	60	44	30	
	(lbf) 2	81	74	65	63	52	33	
	(lbf) 3	94	69	68	65	55	30	
Average reading	(lbf)	88	71	68	63	36	31	
Penetration resistance	(lbf/in^2)	3520	2840	1360	630	144	62.	
Moisture content determinations								
Dish No.		414	K46	127	1600	155	X	
Mass of dish + wet soil	(g)	323.5	351.8	572.9	345.5	438.6	347.1	
Mass of dish + dry soil	(g)	307.8	329.7	521.3	314.2	357.6	311.4	
Mass of dish	(g)	145.9	148.6	153.6	118.7	170.6	133.3	
Mass of water	(g)	15.7	22.1	51.6	31.3	41.0	35.7	
Mass of dry soil	(g)	161.9	181.1	367.7	195.5	227.0	178.1	
Moisture content	(% of dry mass)	9.7	12.2	14.0	16.0	18.1	20.0	
Dry unit weight determinations								
Dry unit weight	(lbf/ft^3)	105.2	108.0	108.3	108.4	103.7	98.2	

Remarks:

Auxiliary tests:

USBR 5205 - __ __
USBR 5300 - __ __
USBR 5320 - __ __
USBR 5505 - __ __

GPO 849-889

7-1452 (9-86)
Bureau of Reclamation

MOISTURE CONTENT

Designation USBR 5300-

PROJECT: Crack box SiIT

FEATURE: Bonnie Dam

TESTED BY	DATE	COMPUTED BY	DATE	CHECKED BY	DATE

					UNITS
SAMPLE NUMBER					
CONTAINER NUMBER					
DATE PLACED IN OVEN	3/29/12				☐ g
MASS OF CONTAINER + WET SPECIMEN	1085.03				
MASS OF CONTAINER + DRY SPECIMEN	1070.31				☐ kg
MASS OF CONTAINER	890.67				
MASS OF WATER	14.72				☐ lbm
MASS OF DRY SPECIMEN	179.64				
MOISTURE CONTENT (%)	8.2				

TESTED BY	DATE	COMPUTED BY	DATE	CHECKED BY	DATE

					UNITS
SAMPLE NUMBER					
CONTAINER NUMBER					
DATE PLACED IN OVEN					☐ g
MASS OF CONTAINER + WET SPECIMEN					
MASS OF CONTAINER + DRY SPECIMEN					☐ kg
MASS OF CONTAINER					
MASS OF WATER					☐ lbm
MASS OF DRY SPECIMEN					
MOISTURE CONTENT (%)					

TESTED BY	DATE	COMPUTED BY	DATE	CHECKED BY	DATE

					UNITS
SAMPLE NUMBER					
CONTAINER NUMBER					
DATE PLACED IN OVEN					☐ g
MASS OF CONTAINER + WET SPECIMEN					
MASS OF CONTAINER + DRY SPECIMEN					☐ kg
MASS OF CONTAINER					
MASS OF WATER					☐ lbm
MASS OF DRY SPECIMEN					
MOISTURE CONTENT (%)					

7-1451 (9-86) Bureau of Reclamation	**GRADATION ANALYSIS**	Designation USBR 5325-____ Designation USBR 5330-____ Designation USBR 5335-____

SAMPLE NO.	PROJECT Crack box Silt	FEATURE
AREA	EXC. NO.	DEPTH

GRADATION OF GRAVEL SIZES

TESTED AND COMPUTED BY B. Baca	DATE 3/30/12	% MOISTURE CONTENT OF + NO. 4	WET MASS OF TOTAL SPECIMEN
CHECKED BY	DATE	% MOISTURE CONTENT OF – NO. 4	TOTAL DRY MASS OF SPECIMEN

SIEVE SIZE		3" (75 mm)	1-1/2" (37.5 mm)	3/4" (19.0 mm)	3/8" (9.5 mm)	NO. 4 (4.75 mm)	PAN
MASS OF CONTAINER AND RETAINED MATERIAL							
MASS OF CONTAINER							
WET MASS RETAINED							
DRY MASS RETAINED						0.0	
DRY MASS PASSING						54.7	☐ lbm ☐ kg ☒ g
% OF TOTAL PASSING						100.0	

GRADATION OF SAND SIZES

DRY MASS OF SPECIMEN 54.7 g	FACTOR = % TOTAL PASSING NO. 4 / DRY MASS OF SPECIMEN = 100.0 / 54.7 = 1.828
DISH NO. 121	DRY MASS OF SPECIMENT (SIEVED) 17.2
SIEVING TIME 15 min	DATE 4/4/12

SIEVE NO.	MASS RETAINED (g)	MASS PASSING (g)	FACTOR X MASS PASSING = % OF TOTAL PASSING	% OF TOTAL PASSING	PARTICLE DIAMETER	REMARKS
8	0.0	54.7		100.0	2.36 mm	MASS Dish + Soil - 210.1 172.6
16	0.0	54.7		100.0	1.18 cm	MASS Dish - 155.4 155.4
30	0.7	54.0		98.7	600 µm	MASS soil - 54.7 17.2
50	4.7	50.0		91.4	300 µm	
100	10.0	44.7		81.7	150 µm	
200	15.8	38.9		71.1	75 µm	
PAN	18.1					
TOTAL	0					

TESTED AND COMPUTED BY B. Baca	DATE 4/4/12	CHECKED BY	DATE

HYDROMETER ANALYSIS

HYDROMETER NO. 168655	DISPERSING AGENT Sodium Hexametaphosphate	
STARTING TIME 944	DATE 4/2/12	AMOUNT 4% 125 mL

TIME	TEMP °C	HYD READ	HYD CORR	CORR READ	FACTOR X CORRECT READ = % OF TOTAL PASSING	% OF TOTAL PASSING	PARTICLE DIAMETER	REMARKS
1 min	23.5	30.0	5.0	25.0		45.7	37 µm	
4 min	23.3	18.0	5.0	13.0		23.8	19 µm	
19 min	24.4	13.0	4.5	8.5		15.5	9 µm	
60 min	24.6	11.5	4.5	7.0		12.8	5 µm	AUXILIARY TESTS: USBR 5305- ___ USBR 5300- ___
7 h 15 min*							2 µm	
25 h 45 min*							1 µm	

TESTED AND COMPUTED BY B. Baca	DATE 4/2/12	CHECKED BY	DATE

*Not required for standard test.

7-1589 (10-86)
Bureau of Reclamation

SPECIFIC GRAVITY DETERMINATION
(VOLUME METHOD)

Designation USBR 5320-___

SAMPLE NO.	PROJECT	FEATURE
CRACK Box SILT		

SPECIMEN NO.	HOLE NO.	DEPTH ft ☐ m ☐

TESTED BY	DATE	COMPUTED BY	DATE	CHECKED BY	DATE
B. Baca	4/2/12		4/9/12		

	TRIAL NO. 1	TRIAL NO. 2
1. FLASK NO.	YMP 1	F2
2. MASS OF FLASK * (g)	101.42	103.68
3. VOLUME OF FLASK * (cm^3)	249.82	249.62
4. MASS OF SPECIMEN (g)	60.68	61.69
5. MASS OF FLASK + SPECIMEN + WATER (g)	388.29	391.05
6. TEMPERATURE OF WATER (°C)	19.6	19.4
7. MASS OF FLASK + WATER = (5) - (4) (g)	327.61	329.36
8. MASS OF WATER IN FLASK = (7) - (2) (g)	226.19	225.68
9. ABSOLUTE DENSITY OF WATER AT TEMP (6) (g/cm^3)	0.998285	0.998325
10. VOLUME OF WATER IN FLASK = (8) / (9) (cm^3)	226.58	226.06
11. VOLUME OF SOIL = (3) - (10) (cm^3)	23.24	23.56
12. SPECIFIC GRAVITY = (4) / (11) **	2.611	2.618
13. AVERAGE	2.61	

*Calibration data from USBR 1030
**Implies that for water 1 g = 1 mL = 1 cm^3

7-1702 (11-85) Bureau of Reclamation	SOIL CONSISTENCY TEST ONE-POINT LIQUID LIMIT METHOD	Designation: USBR _____ - ____ ___

SAMPLE NO.	FEATURE	PROJECT
Crack Box Silt		

Air dried	☒	Tested by B. Rice	Date 4/9/12
Oven dried	☐	Computed by _____	Date _____
Natural	☐	Checked by _____	Date _____

		PLASTIC LIMIT	
Trial No.		1	2
Dish No.			
No. of blows (N)			
Mass of dish + wet soil	(g)		
Mass of dish + dry soil	(g)	N/P	
Mass of dish	(g)		
Mass of water	(g)		
Mass of dry soil	(g)		
Moisture	%		
Average Plastic Limit			

	LIQUID LIMIIT	
	1	2
W_n =		
F_n =		
Liquid Limit		

SHRINKAGE LIMIT

1. Shrinkage Dish No.			
2. Mass of dish + wet soil	(g)		
3. Mass of dish + dry soil	(g)		
4. Mass of dish	(g)		
5. Mass of water (2-3)	(g)		
6. Mass of dry soil (W_o)(3-4)	(g)		
7. % Moisture (5/6 x 100)			
8. Vol. Shrinkage Dish (V)			
9. Vol. Dry Soil (V_o)			
10. $V - V_o$ = (8-9)			
11. $\frac{V - V_o}{W_o} \times 100 = \frac{(10 \times 100)}{6}$			
12. Shrinkage Limit (7-11)			
13. Shrinkage Ratio (6/9)			

$$LL = Wn \left(\frac{N}{25}\right)^{0.120}$$

$$F_n = \left(\frac{N}{25}\right)^{0.120}$$

$$LL = (F_n)(W_n)$$

N	F_n
20	0.974
21	0.979
22	0.985
23	0.990
24	0.995
25	1.000
26	1.005
27	1.009
28	1.014
29	1.018
30	1.022

PI = LL – PL

PLASTICITY INDEX:

PI = _____ - ____ = ____

LIQUID LIMIT (LL) = _____

PLASTIC LIMIT (PL) = _____

PLASTICITY INDEX (PI) = _____

SHRINKAGE LIMIT (SL) = _____

Auxiliary tests:

USBR 5205 - ___ ___

USBR 5300 - ___ ___

USBR 5350 - ___ ___

USBR 5350 - ___ ___

USBR 5365 - ___ ___

Remarks: Could not Roll a Thread.

Sample is non-Plastic !!

APPENDIX D

Geophysics Paper

ICSE6-103

Preliminary Implementation of Geophysical Techniques to Monitor Embankment Dam Filter Cracking at the Laboratory Scale

Robert V. RINEHART[1], Minal L. PAREKH[2], Justin B. RITTGERS[3], Michael A. MOONEY[4], and Andre REVIL[5]

[1]Civil Engineer, Materials Engineering & Research Laboratory, Bureau of Reclamation
PO Box 25007, Denver, CO 80225; e-mail: rrinehart@usbr.gov

[2]Graduate Student, SmartGeo Program, Colorado School of Mines
1500 Illinois Street, Golden, CO 80401; e-mail: mparekh@mines.edu

[3] Graduate Student, SmartGeo Program, Colorado School of Mines
1500 Illinois Street, Golden, CO 80401; e-mail: jrittger@mines.edu

[4]Professor, Civil & Environmental Engineering Department, Colorado School of Mines
1500 Illinois Street, Golden, CO 80401; e-mail: mooney@mines.edu

[5] Professor, Geophysics Department, Colorado School of Mines
1500 Illinois Street, Golden, CO 80401; e-mail: arevil@mines.edu

Internal erosion presents a significant hazard to water retaining structures and is most often identified in its progressive stages through visual inspections or observations. Acoustic or ultrasonic methods in combination with electrical geophysical methods can be used as a tool for detection and continuous monitoring of subsurface internal erosion initiation in its early stages. This research investigates passive acoustic emission, self potential, and cross-hole tomography for suitability as long-term, remote and continuous monitoring techniques for internal erosion and cracking of embankment dams. Geophysical data from the three techniques have been collected during manually imposed cracking of granular filter materials. Specifically, data has been collected during both self-healing (i.e., desirable filter behavior) and during continuing erosion (i.e., undesirable filter behavior). The data is compared to baseline, pre-crack data. This proof-of-concept research provides evidence of these geophysical techniques for effective monitoring of embankment cracking as a precursor to internal erosion. This paper presents the details of the instrumentation systems, data acquisition parameters, and early findings from the research. 2D seismic velocity tomograms, passive acoustic and passive electrical signatures associated with cracking and suffusion are discussed.

Key Words

geophysics, cross hole tomography, self potential, passive acoustic emission, internal erosion, embankment dam filters, continuous remote monitoring

I INTRODUCTION

Internal erosion in earthen embankments (dams, levees) occurs when a critical combination of hydraulic gradient, in-situ stress conditions, soil porosity and intrinsic permeability, and material properties results in increased and uncontrolled seepage. This leads to the transport and migration of soil particles in a localized area, often at a crack in the soil (e.g., from desiccation, settlement, or seismic activity). Internal erosion presents a significant hazard to embankment dams, dikes, levees, abutments, spillways, and foundations, and a review of historical dam failures shows that about half of all embankment dam failures are related to internal erosion [Foster, 1998; Schmertmann, 2000]. This critical failure mode is difficult to detect in early stages, and typically is not identified until it has progressed to a full piping situation [Foster, 2008]. Further, a broad search of the literature indicates that acceptable means of determining the factor of safety against internal erosion have not been determined. It is also recognized that it is dangerous to place undue

[1] Corresponding author

confidence in a structure based on years of successful performance as internal erosion incidents can manifest after decades of satisfactory performance – underscoring the need for continuous monitoring.

Signs of active internal erosion, including sink holes, sand boils, and muddy seepage, are often discovered by local residents or during periodic visual safety inspections. Alternatively, identifying the onset and progression of internal erosion by continuously and remotely monitoring for subsurface changes would be preferred, allowing for early intervention and risk reduction. Several geophysical techniques are believed to hold potential as monitoring tools, including passive Acoustic Emission (AE), Self Potential (SP), and cross-hole direct-transmission sonic tomography (CT) are further discussed below.

Internal erosion can be mitigated by incorporating granular filter zones into the embankment, to filter or retain embankment soils and prevent particle migration. The Bureau of Reclamation, in partnership with the U.S. Army Corps of Engineers has been conducting large scale embankment filter research for several years to gain a better understanding of: cracked filter performance, conditions which cause a crack within a filter, ability of a filter to heal under flow conditions, and effectiveness of a filter to stop or control flow [Redlinger, 2012]. A laboratory model referred to as the soil crack box was constructed (Figure 1). The box allows for the compaction of filter material in various configurations, subsequent cracking of the filter (i.e., to simulate differential settlement, desiccation, or seismically induced cracking), and impingement of reservoir water upon the cracked filter.

The present work includes SP electrodes installed near the surface of the granular filter within the crack box, CT logging tubes (one transmitter, one receiver) installed through the full height of the filter on both sides of the crack zone, and AE monitoring using periodic passive recording from the CT receivers (geophones). Data have been collected via the three methods before filter cracking, during cracking, and during active water flow through the cracked filter. This paper presents the test set-up, geophysical instrumentation, and promising preliminary results.

II LABORATORY SETUP

II.1 Laboratory Embankment Filter Model

The geometry of the laboratory filter model (soil crack box) simulates field geometric conditions, and performs similarly to a granular embankment dam filter. The observed seepage is constant head, and the induced cracks are similar to those that occur in earthen embankments. The resulting design, shown in Figure 1, includes several components: a 2000 liter reservoir large enough to provide near-constant water supply, a 7 m^3 zone to contain embankment and filter materials, and a 2.75 m long channel through which water passes from the reservoir to the embankment material. The box is constructed in two identical halves and hinged at the bottom centerline. Once full of material (Figure 1d), hydraulic jacks force the box to pivot at the hinge, inducing a crack (2.5 cm, typical) within the material (Figure 1e). The size of the box allows placement and compaction using vibratory methods similar to those used in the field. Potential seepage paths through the apparatus (i.e. hinges, joints) were thoroughly sealed with silicone caulk to minimize leaking. Sandpaper was installed along the walls confining the filter material to provide friction intended to simulate shear resistance provided by confinement. A drain was installed on each side of the floor of the material box to allow drainage below the filter material (simulating a drain below a filter zone). Drainage can be measured through outlet pipes. The drains can also be closed to

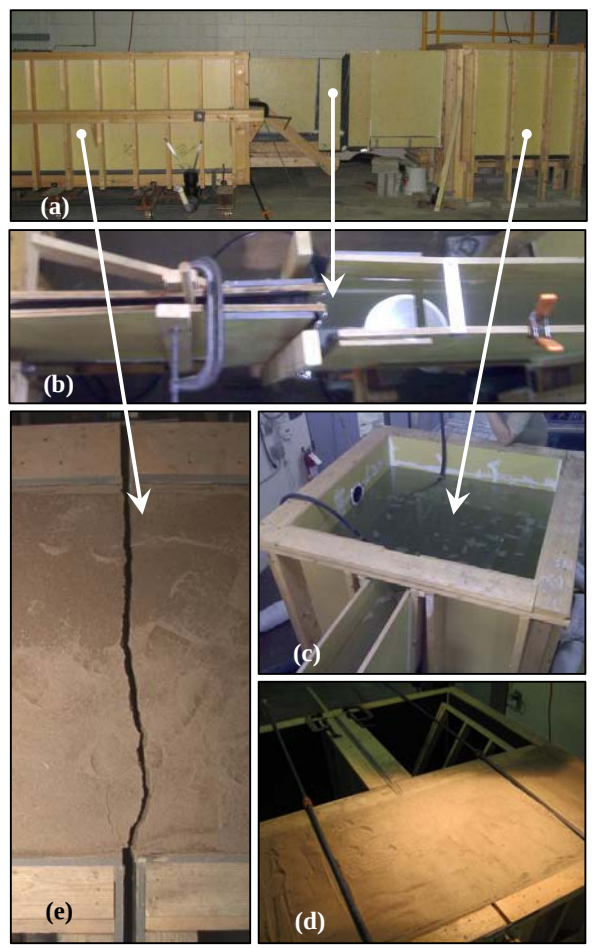

Figure 1: Laboratory layout of filter model showing: (a) assembled model, (b) upstream channel, (c) constant head reservoir, (d) uncracked filter, and (e) cracked filter (2.5 cm)

prevent drainage (simulating a filter that is isolated, or a drain that is clogged).

During a typical test the reservoir is released by removing a solid gate between the upstream channel and the reservoir. Water flows into and through the filter material in the box. Filter performance is observed and judged qualitatively by the material's ability to sustain a crack, heal a crack under flow conditions, and stop or control flow through cracks. For more detail please refer to [Redlinger, 2012].

II.2 Geophysical Techniques

One means to continuously monitor for concentrated seepage and internal erosion is passive Acoustic Emission (AE) monitoring. AE monitoring involves using acoustic transducers (e.g., geophones or accelerometers) to passively "listen" for acoustic energy that is released from internal sources including earthquakes, impact or gradual loading forces, and impulsive sources (e.g., collapse events). Research regarding AE in soils has been ongoing since the 1970s [Koerner, 1976, 1981; Buck, 1986; Hung, 2009] and recent work by the United States Department of Agriculture and Ole Miss University has shown that AE exists due to internal erosion [Lu, 2004; Hickey, 2010]. In cases where data from several seismic monitoring stations are available, AE source localization can be performed through triangulation or a variety of more complex techniques. Research has shown that sudden or gradual increases in the rate or magnitude of AE events can be linked to cracking or internal erosion [Talwani, 1984, 1997].

A second potential means to continuously monitor for internal erosion is through the implementation of compressional seismic wave (p-wave) or shear wave (s-wave) cross-hole tomography (CT). Similar to AE monitoring, this technique utilizes acoustic transducers, only in the case of CT, recorded energy is from 'active' or intentionally generated vibrational or impact-type sources. The transmitters and receivers are accurately time-synchronized, and similar to CAT scan medical imaging technology, CT is performed using a multitude of transmitter-receiver pair geometries, helping to illuminate the materials between borehole pairs (e.g., see Figure 2). This geophysical technique allows for reconstruction of the spatial distribution of seismic velocity, related to the material's density and elastic properties including the bulk and shear moduli. By repeating the data acquisition over time, this imaging could prove useful in tracking the evolution of subsurface features (i.e., time-lapse geophysics).

A third promising means to continuously monitor for internal erosion and concentrated seepage is through the use of the Self Potential (SP) method. The SP technique involves the measurement of the variation of the electrical potential distributions across the ground surface (or within boreholes) with respect to both space and time. These electrical potentials are associated with very small subsurface electric fields created by a variety of sources, including fluid flow through porous media (i.e., streaming potential). SP can help to quickly map the lateral location and geometry of preferential flow paths in the X-Y plane [Crespy, 2008]. The addition of other information about the electrical conductivity and material properties allows for the SP data to be inversely modeled to retrieve more useful quantitative parameters such as depth to the phreatic surface and groundwater flow velocity distributions [Sheffer, 2007]. Inverse analysis of SP data may prove useful, in that 3D fluid flow velocity distributions can be solved for within the first order, offering information on the severity and geometry of open transverse cracks, internal erosion and related concentrated seepage pathways within earth embankment structures.

II.3 Instrumented Tests

Geophysical instrumentation was included in two filter experiments: a two stage filter comprised of poorly graded sand upstream of poorly graded gravel (designated T11, Figure 3), and a single stage filter comprised of poorly graded sand (designated T12, Figure 4). The sand material met the requirements (including gradation) for fine aggregate in ASTM C33. Generally, C33 fine aggregate (commonly referred to as concrete sand) is considered a good all-purpose filter material, capable of filtering a wide

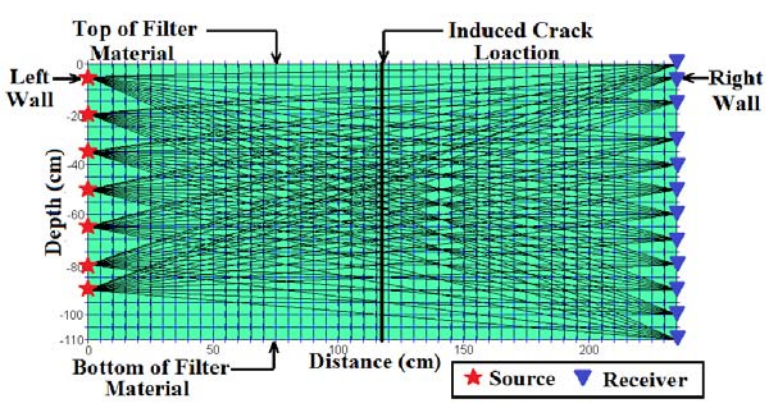

Figure 2. Approximate CT raypath coverage between source (left edge) and receiver (right edge) locations for T11 and T12 (boxes represent discretization for tomography modeling)

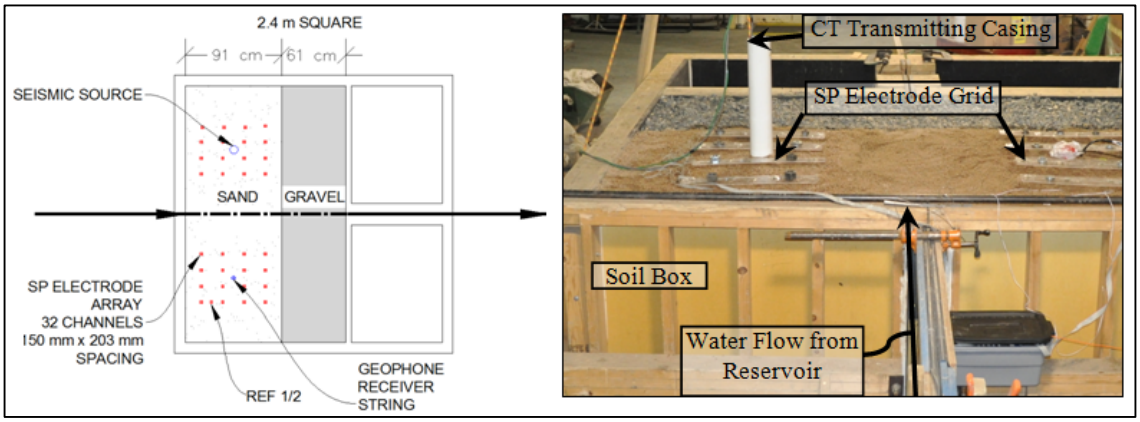

Figure 3. Schematic (left) and pre-crack photograph (right) of filter geometry and instrumentation for T11 – two stage filter

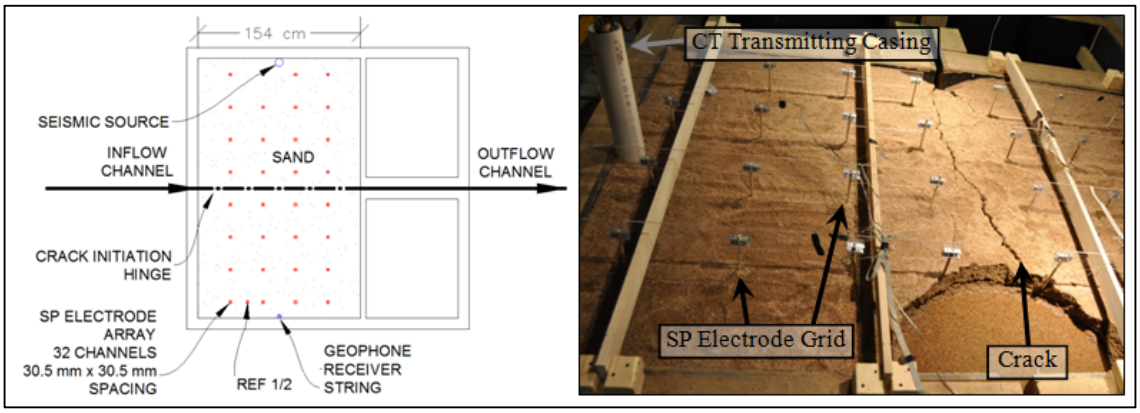

Figure 4. Schematic (left) and post-crack photograph (right) of filter geometry and instrumentation for T12 – single stage filter

range of embankment materials. The gradation of the gravel, which had a maximum particle size of 19 mm, was filter-compatible with the gradation of the sand. Both the sand and gravel materials contained less than 2% fines at the time of compaction.

Filter materials were compacted in the box using a vibratory plate. In-situ moisture and density were determined using the sand cone test (ASTM D1556). Average dry unit weights for the sand material were 16.9 kN/m^3 and 17.4 kN/m^3 for tests T11 and T12, respectively. Moisture content for the sand material was 5.0% for both tests. The gravel material was not tested, but received the same compactive effort (i.e., number of passes with the vibratory plate) as the sand.

Figures 3 and 4 show schematics and photographs of the geophysical instrument layout for tests T11 and T12, respectively. For both tests, SP electrodes were placed in contact with the surface of the poorly graded sand material on a grid spacing within the crack box. A harness, configured to minimize impact to the crack zone, prohibited electrode movement. For T11, electrodes were mounted to the underside of acrylic sheeting with the electrode grids offset 38 cm from the crack alignment. For T12, electrodes were mounted to rods suspended from a frame located approximately 15 cm above the soil surface to allow the electrodes to be in firm contact with the soil, but to also allow the soil to move freely beneath them. SP data were collected on 32 channels using a BioSemi EEG multi-channel, high resolution electrical potential measurement system. Specifications for geophysical applications using a BioSemi system can be found in [Crespy, 2008]. Electrical potentials were measured with respect to a reference electrode ("REF1/2" on Figures 3 and 4).

Casings for CT transmitting and receiving (76 mm inside diameter PVC pipe) were installed through the full height of the sand, offset 1.2 m from the crack alignment on both sides for T11 (Figure 3) and placed along the inside wall of the box for T12 (Figure 4). The seismic source, an Olson Instruments P-SV triaxial impact source triggered through Olson's Freedom Data PC system, is a down-hole source capable of

generating shear and compressional waves by directly impacting the inside of the casing at a set depth. For these tests, the source depth ranged from 5 cm to 90 cm below the surface, generally at 15 cm intervals (Figure 2). The receiver array was comprised of twelve 10 Hz center-frequency geophone transducers and was also used to collect passive AE data. A Geometrics Geode seismic recorder acquired signals from the geophone receiver string. Tomographic data waveforms were acquired using a sample interval of 0.25 ms over a duration of 0.20 s to 0.25 s. The Geode also acquired AE waveforms at sample intervals of 0.20 to 0.25 ms over a 4 to 30 s duration.

The study included collecting data via the three geophysical methods before filter cracking (i.e., after compaction), during and after cracking, and while the crack in the filter material was subjected to focused water flow. For test T11, a 2.5 cm wide crack was opened and subjected to focused water flow with the drains in the bottom of the box open. The crack healed and did not result in flow to the downstream collection reservoir. The 2.5 cm wide crack was subjected to flow overnight without erosion or flow to the downstream collection reservoir. The following morning, the crack was opened to approximately 15 cm. The crack healed and did not result in flow to the downstream collection reservoir.

For test T12, a 2.5 cm wide crack was opened and subjected to focused water flow, with the drains in the bottom of the box open. The crack healed and did not result in flow to the downstream collection reservoir. The 2.5 cm crack was subjected to flow overnight without erosion or flow to the downstream collection reservoir. The following morning, the drains in the bottom of the box were closed and the crack was again subjected to water overnight. The crack healed and did not result in flow to the downstream collection reservoir. The following day, the crack was opened incrementally (approximately 1.25 cm/6 min) to approximately 15 cm with the drains closed. The crack collapsed and healed several times, until the filter failed and allowed uncontrolled flow to continue to the downstream collection reservoir.

Digital video cameras positioned at the upstream reservoir, two angles downstream of the filter material, and directly overhead of the crack captured video during the cracking and flow events and provided a visual reference for the timing of erosion and healing events.

III PRELIMINARY RESULTS

III.1 Passive Acoustic Emission

AE data were recorded for several hours and on various days throughout each test using repeated 4, 10 or 30 s records. The recorded frequencies ranged from approximately 5 to 250 Hz, which allowed for identification of unique spectral signatures at various stages of internal erosion, overtopping flow, collapse events and self-healing phenomena that occurred throughout the filter tests. Preliminary results of this portion of the study are shown in the spectrograms presented in Figure 5. Here, the power spectrums of AE data are plotted as a function of time for three representative, 30-second time periods. The color scale of the three panels represents normalized power at a given frequency and record time (power spectra averaged for each second of recorded data). Warmer colors (i.e., reds and yellows) represent higher energy levels and more activity, while cooler colors (i.e., blues and greens) represent lower energy levels and less activity at a given frequency. Within the recorded spectra, bands of high power noise at relatively low-frequencies (e.g., 10-50 Hz) associated with the laboratory utility duct-work and nearby machinery dominate the signal. Electrical power-grid noise is also apparent in the data as high-energy bands (red) at 60 Hz and its harmonics (120 Hz and 180 Hz).

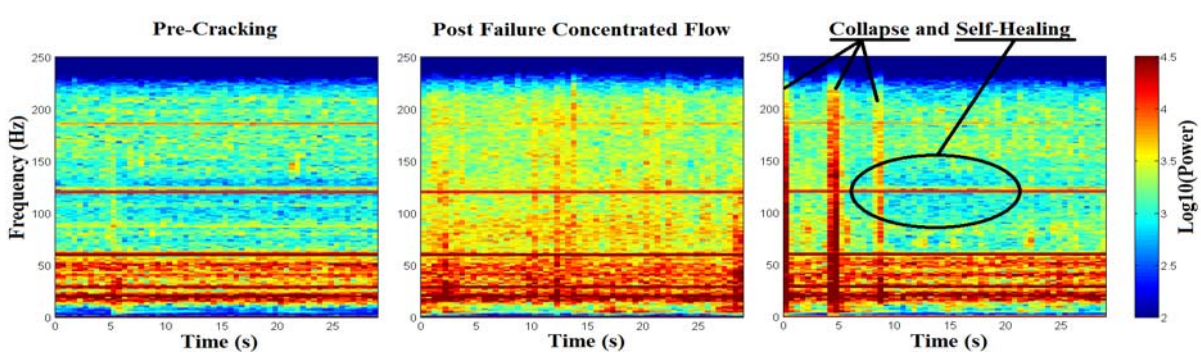

Figure 5. AE signatures during three stages of T12: Pre-cracking baseline (left), post filter cracking during concentrated flow (center), and subsequent sidewall-collapse and self-healing events (right)

Comparison of the pre-cracking baseline data and data collected during concentrated flow (left and center panels of Figure 5, respectively) shows a spectral distinction between the two stages of the test. The right-hand panel of Figure 5 shows broad-band events representing a collapse event, where the sidewalls of the induced crack collapsed into the open fracture. The relatively high energy observed at higher frequencies during concentrated flow (center panel) disappears after the collapse events, indicating cessation concentrated flow due to self-healing of the filter material. These preliminary results show important and noticeable relationships between AE signatures and erosion phenomena. As seen in Figure 5, unique AE signatures of filter collapse and self-healing were observed during these experiments, showing promise for the successful use of the AE method in monitoring applications for full-scale embankment structures.

III.2 Cross-hole Tomography

Preliminary results of the cross-hole p-wave tomography data are presented in Figures 6 and 7. Figure 6 shows the change in p-wave arrival time with travel distance between source-receiver pairs (note that an increase in arrival time with similar offset indicates lower velocity). The data contain trends that suggest an overall decrease in p-wave velocities with cracking, relative to the pre-crack data set from T12. The progressive slowing of the material velocity likely reflects a decrease in the stress field due to the cracking, increase in water content, and/or loosening of the compacted filter materials.

Figure 7 depicts velocity tomograms calculated for each time step during T12 (pre-crack, 2hrs and 24hrs after cracking and initiation of flow). CT data acquisition was achieved by integrating two separate seismic systems: one system generated the seismic source, and the other system recorded the data at the receivers. Interfacing these two systems resulted in a timing mismatch between the source (time-zero) and the beginning of each seismic CT record, and while the absolute time synchronization discrepancy is unknown, it was consistent for all data recorded. As a result, all calculated velocities presented here are considered relative and not absolute seismic velocities. Velocities presented in the tomograms shown on Figure 7 are slower than expected true velocities of the filter material, however the relative changes between time steps represent true or absolute decreases in p-wave velocity.

A progressive overall decrease in the p-wave velocity distribution can be seen in each subsequent tomogram moving left to right in Figure 7. More noticeable changes occur between the two and 24-hour tomograms than between the zero and two hour tomograms. This may be due to the infiltration of moisture into the materials surrounding the crack and throughout the filter material, helping to homogenize the velocity distribution within the filter model. Still, a noticeable decrease in velocity is captured using the tomography

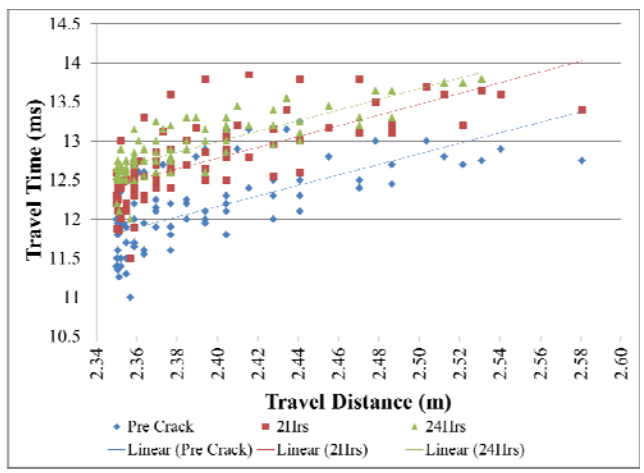

Figure 6. Scatter plots of p-wave travel time versus source-receiver separation for T12 data. Trend lines have been added to depict the overall relative decrease in calculated velocities over the course of T12.

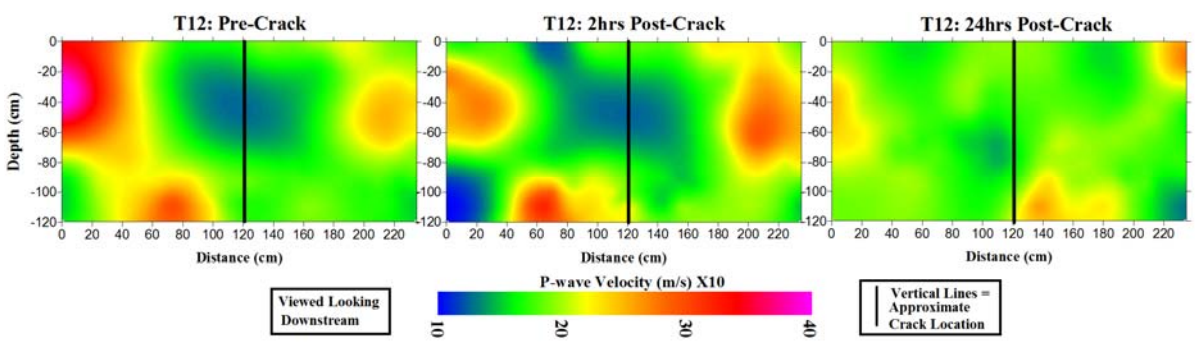

Figure 7. P-wave tomograms for T12 data collected pre-crack (left panel), and 2hrs and 24hrs after cracking of filter material and subjection to concentrated flow (center panel and right panel respectively)

method. Unfortunately, failure of the filter material happened too quickly after collecting the 24hr post-crack data set, preventing collection of post-failure data sets. We expect that further internal erosion and sloughing of materials leading up to and during the failure events of T12 would have further decreased the stress field and hence the p-wave velocities within the filter materials. These results show promise for the applicability of seismic tomography techniques for successfully detection and imaging of filter material cracking and failure phenomena within earthen embankment structures.

III.3 Self Potential

Preliminary SP results are shown in Figure 8, where contour plots of SP data are presented for select times during T11. Figure 8 depicts a sequence of snapshots of the electrical potential distribution across the top surface of the filter material (plan view) where the SP electrodes were installed. These contour images depict the development of a positive SP anomaly typically associated with the flow of fluid through porous media. Here, water is flowing from right to left, and the resultant SP anomaly is seen to develop in a progressive fashion in the downstream direction. The SP anomaly is located above the majority of concentrated fluid flow within the filter material, near the crack alignment. The physical mechanism that causes the SP anomaly seen in Figure 8 is proportional to the velocity of fluid flow through the filter material. Therefore, the observed SP anomaly is expected to develop in the vicinity of concentrated flow through the filter material, and is expected to subside in the advent of self-healing phenomena that decrease or stop flow entirely. This observed and expected relationship between SP data and the state of the filter material offers promise in the applicability of the SP technique towards full-scale embankment time-lapse monitoring efforts.

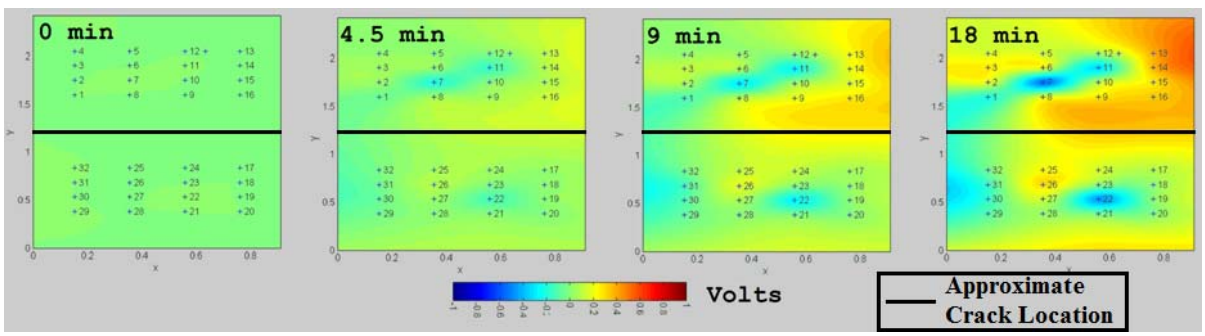

Figure 8. Plan view contour plots of electric potential distributions (SP data) at select time-steps after initial cracking of filter material and subjection to fluid flow during T11.

IV CONCLUSIONS AND APPLICATIONS

The threat of embankment failure from uncontrolled flow through a crack is exacerbated not only by the lack of understanding of the parameters contributing to cracking, healing, and flow control, but also by the absence of early detection and monitoring methods capable of identifying the process in its early stages. Applications using time-lapse geophysics hold promise for detecting spatial and temporal changes in the subsurface conditions through continuous monitoring. This paper describes some promising signatures in geophysical signals associated with cracking, concentrated flow, and collapsing and healing. While the laboratory is a controlled environment, a large amount of man-made ambient noise exists with respect to seismic and electrical signals. Despite this challenging data acquisition environment, we have demonstrated that precursory internal erosion phenomena, collapse and subsequent healing events are evident and well above the spectral noise floors of the SP and AE data presented herein. CT-measured changes in the seismic velocity distributions as a result of crack formation, concentrated flow and fluid infiltration are quite evident. The time lapse SP signatures clearly indicate water flowing through the partially saturated soil concentrated along the induced crack.

These various patterns can be used to develop data analysis algorithms for automated detection of cracking and self-healing events, and early notification of these potential risks within earthen embankment structures. A time-lapse monitoring system can be used to describe baseline signals and to set thresholds for notification. Work remains to further understand the link between identifiable cracking, healing, and flow events, as well as the risk of filter failure, in order to provide a complete picture for dam safety decision making. Our research in the cracked filter box is ongoing; however, this study serves as a preliminary proof

of concept. For a full scale earth dam, direct application in the form of buried geophones, surface geophones or other types of seismic transducers and/or surface SP electrodes can augment conventional instrumentation to enable a higher resolution (in time and in space) response that might otherwise go unnoticed by traditional instrumentation and visual methods.

V ACKNOWLEDGEMENTS

The authors are grateful for financial assistance provided by the Bureau of Reclamation Science & Technology Program, U.S. Army Corps of Engineers Risk Management Center, National Science Foundation (NSF IGERT Program: DGE-0801692), and the Hydroresearch Foundation. The authors are indebted to Olson Engineering, Inc. for the generous loan of their cross-hole tomography equipment.

VI REFERENCES

Buck, C. J., and Watters, R. J., (1986). "Acoustic Emission Generation From Water Flow Through Granular Soils." In *Proceedings of the 22nd Symposium on Engineering Geology and Soils Engineering*, 138–154. Boise, Idaho.

Crespy, A., Revil, A., Linde, N., Byrdina, S., Jardani, A., Bolève, A., and Henry, P., (2008), Detection and localization of hydromechanical disturbances in a sandbox using the self-potential method, *Journal of Geophysical Research*, *113*, B01205, doi: 10.1029/2007JB005042.

Foster, M., Fell, R., Vroman, N., Cyganiewicz, J., Sills, G., and Davidson, R., (2008). "Seepage and Piping Toolbox--Continuation, Progression, Intervention, and Breach." In *28th Annual United States Society on Dams Conference: The Sustainability of Experience--Investing in the Human Factor*, 1049–1064. Portland, Oregon.

Foster, M.A., Fell, R., and Spannagle, M. (1998). Analysis of Embankment Dam Incidents, *UNICIV Report No. R-374*, University of New South Wales, Sydney, Australia.

Hickey, C., Ekimov, A., Hanson, G., and Sabatier, J., (2010). "Time-Lapse Seismic Measurements on a Small Earthen Embankment During an Internal Erosion Experiment." In *SAGEEP 2009 Proceedings*. Keystone, Colorado.

Hung, M-H., Lauchle, G. C., and Wang, M C., (2009). "Seepage-Induced Acoustic Emission in Granular Soils." *Journal of Geotechnical and Geoenvironmental Engineering ASCE*, Vol. 135, No. 4, pp. 566–572.

Koerner, R. M., Lord, A. E., McCabe, W. M., and Curran, J. W., (1976). "Acoustic Emission Behavior of Granular Soils." *Journal of the Geotechnical Engineering Division, ASCE* Vol. 102, No. GT7, pp 761–773.

Koerner, R. M., McCabe, W. M., and Lord, A. E., (1981). "Acoustic Emission Behavior and Monitoring of Soils." In *Acoustic Emissions in Geotechnical Engineering Practice, A Symposium Sponsored by ASTM Committee D-18 on Soil and Rock for Engineering Purposes*, ed. V. P. Drnevich and R. E. Gray, pp 93–141. ASTM Publication Code Number 04-750000-38. Baltimore, MD: American Society for Testing and Materials.

Lu, Z., Hickey, C., and Sabatier, J., (2004). "Effects of Compaction on the Acoustic Velocity in Soils." *Soil Science Society of America Journal* 68 (February): pp 7–16.

Redlinger, C., Rudkin, C., Hanneman, D., and Engemoen, W. (2012). "Lessons Learned from Large-Scale Filter Testing," Manuscript Submitted March 2012 to 6th International Conference on Scour and Erosion, Paris, France, August 27-31, 2012.

Schmertmann, J. H. (2000). "The No-Filter Factor of Safety against Piping Through Sands," Geotechnical Special Publication No. 11 Judgement and Innovation, The Heritage and Future of the Geotechnical Engineering Profession, pp. 65-132.

Sheffer, M., (2007), Forward modeling and inversion of streaming potential for the interpretation of hydraulic conditions from self-potential data, 2007 *Ph.D. Thesis, The university of British Columbia*, pp 6-8.

Talwani, P., (1997). "Seismotectonics of Koyna-Warna Region." *Pure Applied Geophysics.*

Talwani, P., (1984). "Pore Pressure Diffusion and the Mechanism of Reservoir-Induced Seismicity." *Pure Applied Geophysics*, 122: pp 122,947-965.

APPENDIX E

Maximum Density Tests

Relative Density Determination Using Vibratory Hammer

Sample No.	Project	Feature
1	Denver	Crack Box Soil

% Gravel	% Sand	% Fines	Max. Particle Size	Tested By	Date
			#4	Tparent YUMA LAB	3/10/2010

Minimum Unit Index Unit Weight

	Measure No.			
	Specimen No.			
1.	Wt. of Soil + Measure.	lbs.	20.44	20.42
2.	Wt. Measure.	lbs.	13.3	13.3
3.	Wt. of Soil. [(1.) - (2.)]	lbs.	7.14	7.12
4.	Volume of Measure.	ft³	0.0752	0.0752
5.	Dry Unit Weight. [(3.) / (4.)]	lbs./ft³	94.9	94.7
6.	Minimum Index Unit Weight	lbs./ft³	*	

Moisture Content Determination

			Field	Maximum
	Pan No.			
7.	Wt. Pan + Wet Soil.	lbs.		
8.	Wt. Pan + Dry Soil.	lbs.		
9.	Wt. of Pan.	lbs.		
10.	Wt. Water. [(7.) - (8.)]	lbs.		
11.	Wt. Dry Soil. [(8.) - (9.)]	lbs.		
12.	Moisture Content [((10.)/(11)) x 100]	%		

Maximum Index Unit Weight Determination Using Vibratory Hammer Method ASTM 7382

			Dry Method	Wet Method
	Specimen No.			
13.	Wt. of Soil + Measure.	lbs.	22.17 23.244	23.178
14.	Wt. Measure.	lbs.	13.32 14.336	14.336
15.	Wt. of Dry Soil. [(13.) - (14.)]	lbs.	8.85	
16.	Wt. of Wet Soil. [(13.) - (14.)]	lbs.		
17.	Wt. of Dry Soil. [(16.) / {1+((12.)/100)}]	ft³		
18.	Volume of Measure.	ft³	.0752	
19.	Dry Unit Weight [(15.) / (18.)] or [(17.) / (18.)]	lbs./ft³	117.7	
20.	Maximum Index Unit Weight	lbs./ft³	117.7	

Percent Relative Density

21.	In-place unit weight.	
22.	Maximum Index Unit Weight. (20.)	
23.	Minimum Index Unit Weight. (6.)	
24	(22.) x [(21.) - (23.)]	
25	(21.) x [(22.) - (23.)]	
	Percent Relative Density. [(24.) / (25.)] x 100	%

Percent Relative Compaction. [(21.) / (20.)] x 100

_____ %

* smaller mold sizes than standard

.0751 8

#1

MAX

Relative Density Determination Using Vibratory Hammer

Sample No.			Project	Feature	
% Gravel	% Sand	% Fines	Max Particle Size	Tested By	Date

Minimum Unit Index Weight

Measure No.			
Specimen No.			
1. Wt of Soil + Measure	lbs.		
2. Wt of Measure	lbs.		
3. Wt of Soil. [(1)-(2)]	lbs.		
4.Volume of Measure	ft^3		
5. Dry Unit Wt [(3)/(4)]	lbs/ft^3		
6. Min. Index Unit Wt	lbs/ft^3		

Moisture Content Determination

		Field	Max
Pan No.			
7. Wt of Pan + Wet Soil	lbs.		
8. Wt of Pan + Dry Soil	lbs.		
9. Wt of Pan	lbs.		
10. Wt. of Water [(7)-(8)]	lbs.		
11. Wt. of Dry Soil [(8)-(9)]	lbs.		
12. Moisture Content [(10)/(11) x 100]	%		

Maximum Index Unit Weight Determination Using Vibratory Hammer Method ASTM 7382

		Dry Method		Wet Method
Speciment No.				
13. Wt. of Soil + Measure	lbs.	23.244	23.178	
14. Wt. of Measure	lbs.	14.366	14.366	
15. Wt. of Dry Soil [(13)-(14)]	lbs.	8.878	8.812	
16. Wt. of Wet Soil [(13)-(14)]	lbs.			
17. Wt. of Dry Soil [(16) / 1+ (12) / 100)]	ft^3			
18. Volume of Measure	ft^3	0.0752	0.0752	
19. Dry Unit Wt. [(15)/(18)] or [(17)/(18)]	lbs/ft^3	118.1	117.2	
20. Maximum Index Unit Wt.	lbs/ft^3	118.1		

Percent Relative Density and Compaction

21. In-place unit wt.	lbs/ft^3	
22. Max Index Unit wt. (20)	lbs/ft^3	
23. Min Index Unit wt. (6)	lbs/ft^3	
24. (22)x[(21)-(23)]		
25. (21)x[(22)-(23)]		
Percent Relative Density [(24)/(25)] x 100	%	
Percent Relative Compaction [(21)/(20)] x 100	%	

Relative Density Determination Using Vibratory Hammer

Sample No. CB3 pile	Project Crack Box	Feature

% Gravel	% Sand	% Fines	Max Particle Size	Tested By	Date
0	97.4	2.6	2.36 mm	T. Howard	10/28/11

Minimum Unit Index Weight

Measure No.		5	5
Specimen No.		1	2
1. Wt of Soil + Measure	lbs.	17.422	17.414
2. Wt of Measure	lbs.	7.392	7.392
3. Wt of Soil. [(1)-(2)]	lbs.	10.030	10.022
4.Volume of Measure	ft^3	0.1013	0.1013
5. Dry Unit Wt [(3)/(4)]	lbs/ft^3	99.01	98.93
6. Min. Index Unit Wt	lbs/ft^3	99.0	

Moisture Content Determination

		Field	Max
Pan No.		R-7	
7. Wt of Pan + Wet Soil	g ~~lbs.~~	991	
8. Wt of Pan + Dry Soil	g ~~lbs.~~	990.2	
9. Wt of Pan	g ~~lbs.~~	188	
10. Wt. of Water [(7)-(8)]	g ~~lbs.~~	0.8	
11. Wt. of Dry Soil [(8)-(9)]	g ~~lbs.~~	802.2	
12. Moisture Content [(10)/(11) x 100]	%	.10%	

Maximum Index Unit Weight Determination Using Vibratory Hammer Method ASTM 7382

		Dry Method	Wet Method
Speciment No.		1 / 2	
13. Wt. of Soil + Measure	lbs.	23.322 / 23.358	
14. Wt. of Measure	lbs.	14.346 / 14.346	
15. Wt. of Dry Soil [(13)-(14)]	lbs.	8.976 / 9.012	
16. Wt. of Wet Soil [(13)-(14)]	lbs.		
17. Wt. of Dry Soil [(16) / 1+ (12) / 100)]	ft^3		
18. Volume of Measure	ft^3	.07518 / 0.07518	
19. Dry Unit Wt. [(15)/(18)] or [(17)/(18)]	lbs/ft^3	119.39 / 119.87	
20. Maximum Index Unit Wt.	lbs/ft^3	119.6	

Percent Relative Density and Compaction

21. In-place unit wt.	lbs/ft^3	
22. Max Index Unit wt. (20)	lbs/ft^3	
23. Min Index Unit wt. (6)	lbs/ft^3	
24. (22)x[(21)-(23)]		
25. (21)x[(22)-(23)]		
Percent Relative Density [(24)/(25)] x 100	%	
Percent Relative Compaction [(21)/(20)] x 100	%	

Relative Density Determination Using Vibratory Hammer

Sample No. L33-59-89 - A			Project Crack Box	Feature	
% Gravel	% Sand	% Fines	Max Particle Size 1"	Tested By A.L.M.	Date 06-29-2011

Minimum Unit Index Weight

Measure No.			
Specimen No.			
1. Wt of Soil + Measure	lbs.		
2. Wt of Measure	lbs.		
3. Wt of Soil. [(1)-(2)]	lbs.		
4.Volume of Measure	ft^3		
5. Dry Unit Wt [(3)/(4)]	lbs/ft^3		
6. Min. Index Unit Wt	lbs/ft^3		

Moisture Content Determination

		Field	Max
Pan No.			
7. Wt of Pan + Wet Soil	lbs.		
8. Wt of Pan + Dry Soil	lbs.		
9. Wt of Pan	lbs.		
10. Wt. of Water [(7)-(8)]	lbs.		
11. Wt. of Dry Soil [(8)-(9)]	lbs.		
12. Moisture Content [(10)/(11) x 100]	%		

Maximum Index Unit Weight Determination Using Vibratory Hammer Method ASTM 7382

		Dry Method	Wet Method
Speciment No.			
13. Wt. of Soil + Measure	lbs.	125.0 lbs	
14. Wt. of Measure	lbs.	56.3 lbs	
15. Wt. of Dry Soil [(13)-(14)]	lbs.	68.7 lbs	
16. Wt. of Wet Soil [(13)-(14)]	lbs.	Dry	
17. Wt. of Dry Soil [(16) / 1+ (12) / 100)]	ft^3	N/A	
18. Volume of Measure	ft^3	0.4992 ft^3	
19. Dry Unit Wt. [(15)/(18)] or [(17)/(18)]	lbs/ft^3	137.62 pcf	
20. Maximum Index Unit Wt.	lbs/ft^3		

Percent Relative Density and Compaction

21. In-place unit wt.	lbs/ft^3	
22. Max Index Unit wt. (20)	lbs/ft^3	
23. Min Index Unit wt. (6)	lbs/ft^3	
24. (22)x[(21)-(23)]		
25. (21)x[(22)-(23)]		
Percent Relative Density [(24)/(25)] x 100	%	
Percent Relative Compaction [(21)/(20)] x 100	%	

Relative Density Determination Using Vibratory Hammer

Sample No. 4-Oven dry	Project Crackbox	Feature

% Gravel	% Sand	% Fines	Max Particle Size	Tested By Casey Dowling	Date 7/1/2011

Minimum Unit Index Weight

Measure No.			
Specimen No.			
1. Wt of Soil + Measure	lbs.		
2. Wt of Measure	lbs.		
3. Wt of Soil. [(1)-(2)]	lbs.		
4.Volume of Measure	ft^3		
5. Dry Unit Wt [(3)/(4)]	lbs/ft^3		
6. Min. Index Unit Wt	lbs/ft^3		

Moisture Content Determination

		Field	Max
Pan No.			
7. Wt of Pan + Wet Soil	lbs.		
8. Wt of Pan + Dry Soil	lbs.		
9. Wt of Pan	lbs.		
10. Wt. of Water [(7)-(8)]	lbs.		
11. Wt. of Dry Soil [(8)-(9)]	lbs.		
12. Moisture Content [(10)/(11) x 100]	%		

Maximum Index Unit Weight Determination Using Vibratory Hammer Method ASTM 7382

		Dry Method	Wet Method
Speciment No.		4-Oven Dry	
13. Wt. of Soil + Measure	lbs.	125.6	
14. Wt. of Measure	lbs.	56.3	
15. Wt. of Dry Soil [(13)-(14)]	lbs.	69.3	
16. Wt. of Wet Soil [(13)-(14)]	lbs.		
17. Wt. of Dry Soil [(16) / 1+ (12) / 100)]	ft^3		
18. Volume of Measure	ft^3	0.4992	
19. Dry Unit Wt. [(15)/(18)] or [(17)/(18)]	lbs/ft^3	138.82	
20. Maximum Index Unit Wt.	lbs/ft^3		

Percent Relative Density and Compaction

21. In-place unit wt.	lbs/ft^3	
22. Max Index Unit wt. (20)	lbs/ft^3	
23. Min Index Unit wt. (6)	lbs/ft^3	
24. (22)x[(21)-(23)]		
25. (21)x[(22)-(23)]		
Percent Relative Density [(24)/(25)] x 100	%	
Percent Relative Compaction [(21)/(20)] x 100	%	

Trail 1 material for Test #9

Relative Density Determination Using Vibratory Hammer

Sample No.	Project	Feature
Crack Box Part 2		

% Gravel	% Sand	% Fines	Max Particle Size	Tested By	Date
			1.0"	P. Jiny	8/10/2011

Minimum Unit Index Weight

Measure No.			
Specimen No.			
1. Wt of Soil + Measure	lbs.		
2. Wt of Measure	lbs.		
3. Wt of Soil. [(1)-(2)]	lbs.		
4.Volume of Measure	ft^3		
5. Dry Unit Wt [(3)/(4)]	lbs/ft^3		
6. Min. Index Unit Wt	lbs/ft^3		

Moisture Content Determination

		Field	Max
Pan No.			
7. Wt of Pan + Wet Soil	lbs.		81.30
8. Wt of Pan + Dry Soil	lbs.		77.55
9. Wt of Pan	lbs.		8.60
10. Wt. of Water [(7)-(8)]	lbs.		3.75
11. Wt. of Dry Soil [(8)-(9)]	lbs.		68.95
12. Moisture Content [(10)/(11) x 100]	%		5.4%

Maximum Index Unit Weight Determination Using Vibratory Hammer Method ASTM 7382

		Dry Method	Wet Method
Speciment No.			Trail I
13. Wt. of Soil + Measure	lbs.		129.15 lbs
14. Wt. of Measure	lbs.		56.25 lbs
15. Wt. of Dry Soil [(13)-(14)]	lbs.		69.2 lbs
16. Wt. of Wet Soil [(13)-(14)]	lbs.		72.90 lbs
17. Wt. of Dry Soil [(16) / 1+ (12) / 100)]	ft^3		
18. Volume of Measure	ft^3		0.4992
19. Dry Unit Wt. [(15)/(18)] or [(17)/(18)]	lbs/ft^3		138.6
20. Maximum Index Unit Wt.	lbs/ft^3		138.2

Percent Relative Density and Compaction

21. In-place unit wt.	lbs/ft^3	
22. Max Index Unit wt. (20)	lbs/ft^3	
23. Min Index Unit wt. (6)	lbs/ft^3	
24. (22)x[(21)-(23)]		
25. (21)x[(22)-(23)]		
Percent Relative Density [(24)/(25)] x 100	%	
Percent Relative Compaction [(21)/(20)] x 100	%	

Trail 2 material for Test #9

Relative Density Determination Using Vibratory Hammer

Sample No.	Project	Feature
Crack box Part 2		

% Gravel	% Sand	% Fines	Max Particle Size	Tested By	Date
			1.0"	D. Ing	8/10/2011

Minimum Unit Index Weight

Measure No.			
Specimen No.			
1. Wt of Soil + Measure	lbs.		
2. Wt of Measure	lbs.		
3. Wt of Soil. [(1)-(2)]	lbs.		
4.Volume of Measure	ft^3		
5. Dry Unit Wt [(3)/(4)]	lbs/ft^3		
6. Min. Index Unit Wt	lbs/ft^3		

Moisture Content Determination

		Field	Max
Pan No.			~~79.90~~
7. Wt of Pan + Wet Soil	lbs.		79.900
8. Wt of Pan + Dry Soil	lbs.		76.338
9. Wt of Pan	lbs.		7.814
10. Wt. of Water [(7)-(8)]	lbs.		3.562
11. Wt. of Dry Soil [(8)-(9)]	lbs.		68.524
12. Moisture Content [(10)/(11) x 100]	%	5.2%	

Maximum Index Unit Weight Determination Using Vibratory Hammer Method ASTM 7382

		Dry Method	Wet Method
Speciment No.			Trail 2
13. Wt. of Soil + Measure	lbs.		128.55 lbs
14. Wt. of Measure	lbs.		56.25 lbs
15. Wt. of Dry Soil [(13)-(14)]	lbs.		
16. Wt. of Wet Soil [(13)-(14)]	lbs.		72.30 lbs
17. Wt. of Dry Soil [(16) / 1+ (12) / 100)]	ft^3		68.726 lbs
18. Volume of Measure	ft^3		0.4992 lbs
19. Dry Unit Wt. [(15)/(18)] or [(17)/(18)]	lbs/ft^3		137.7 pcf
20. Maximum Index Unit Wt.	lbs/ft^3		138.2

Percent Relative Density and Compaction

21. In-place unit wt.	lbs/ft^3	
22. Max Index Unit wt. (20)	lbs/ft^3	
23. Min Index Unit wt. (6)	lbs/ft^3	
24. (22)x[(21)-(23)]		
25. (21)x[(22)-(23)]		
Percent Relative Density [(24)/(25)] x 100	%	
Percent Relative Compaction [(21)/(20)] x 100	%	